الجمهورية الجزائرية الديمقراطية الشعبية

Democratic and Popular Republic of Algeria

وزارة التعليم العالي والبحث العلمي

Ministry of Higher Education and Scientific Research

جامعة العربي التبسي – تبسة

Larbi Tébessi University – Tébessa –

Faculty of Science and Technology

Civil Engineering Department

A thesis submitted in partial fulfilment of the requirements for the degree of Master Research in

Civil Engineering ‘’Structures’’

By : ABO DHIS Alaa Fadl

Study and Modelling of the Behavior of Metal Connectors in Steel-Concrete Mixed Beams

Thesis defended on 29st June 2020

Thesis committee

Chair : Dr. SOLTANI. M. R

Supervisor: Dr. BOUTAGOUGA Djamel

Examiner : Mr. LABED Abderrahim

Academic Year: 2019/2020

Acknowledgment

First and foremost praise to almighty God, this thesis was completed after hard daily continuous work, I dedicate this humble work to my family whom I will always be indebtedness to endure the bitterness of separation, and they were always backing me up with strength and hope, thanks also must be presented to all my brothers how to escort me in the long way of study life, and all of my colleagues.

l would like to express my sincere thanks to my supervisor, Dr. BOUTAGOUGA Djamel, for his patience, encouragement, kindness, and generosity at all stages of my research work. He always found time to share his vast and deep knowledge in a highly intelligible manner with me. Great thanks to all working staff in the department of civil engineering for the support and help in all the courses.

ABO DHIS Alaa Fadl

ABSTRACT:

In this work, a range of experimental data is collected from the literature and used to validate a finite element model established using ABAQUS software to simulate the push-out tests on a shear connector of I-shape and channel. The simulation is based on the concrete damaged plasticity model, plasticity the steel. The prediction accuracy of the studied model is compared with experimental results that are obtained by other researchers. The comparison indicates that the model is sufficiently accurate to be used in modeling the specimen's push-out tests. The specimens were designed to study the effect of the following parameters on the ultimate load capacity: the height of the connector, the length of the connector, the compressive strength of concrete, the load capacity, the modes of failure were presented and discussed.

RESUME:

Dans ce travail, une gamme de données expérimentales est collectée à partir de la littérature et utilisée pour valider un modèle d'éléments finis établi à l'aide du logiciel ABAQUS pour simuler les tests de poussée sur un connecteur de cisaillement de forme en I et de canal. La simulation est basée sur le modèle de plasticité du béton endommagé, la plasticité de l'acier. La précision de prédiction du modèle étudié est comparée aux résultats expérimentaux obtenus par d'autres chercheurs. La comparaison indique que le modèle est suffisamment précis pour être utilisé dans la modélisation des tests d'extraction de l'échantillon. Les éprouvettes ont été conçues pour étudier l'effet des paramètres suivants sur la capacité de charge ultime: la hauteur du connecteur, la longueur du connecteur, la résistance à la compression du baton la capacité de charge, les modes de défaillance ont été présentés et discutés.

ملخص

في هذا العمل، يتم جمع مجموعة من البيانات التجريبية من الأدبيات واستخدامها للتحقق من صحة نموذج العناصر المحدودة التي تم إنشاؤها باستخدام برنامج ABAQUS لمحاكاة اختبارات الدفع على موصل القص للشكل I والقناة. تعتمد المحاكاة على نموذج اللدونة التالفة للخرسانة، اللدونة على الفولاذ. تتم مقارنة دقة التنبؤ بالنموذج المدروس مع النتائج التجريبية التي حصل عليها باحثون آخرون. تشير المقارنة إلى أن النموذج دقيق بما فيه الكفاية لاستخدامه في نمذجة اختبارات دفع العينة. تم تصميم العينات لدراسة تأثير المعلمات التالية على سعة الحمولة القصوى: ارتفاع الموصل، وطول الموصل، وقوة ضغط الخرسانة، تم عرض ومناقشة سعة الحمولة، وأنماط الفشل.

Key words:

Push-out test, Steel, concrete, I-shape shear connector, Channel shear connector, F.E.M, Composite beam, ABAQUS.

Nowadays, steel-concrete mixed structures are widely used in the field of civil engineering in many structural applications, especially in long-span mixed bridges (50-80 meters), or in the building sector with the common use of floors with mixed slabs. In general, a structural element is defined as mixed "steel-concrete" if it combines the two materials so as to extract the most of this association.

Owing to their association, the strength of composite beams and the resistance to bending, shear and torsion are significantly increased. Therefore, composite beams can efficiently offer, high strength, high stiffness, high resistance to seismic and cyclic loading, increasing load capacity, better fire resistance, reduction in construction depth and saving in weight of steel.

In mixed "steel-concrete" beams, the connection between the two different materials is generally not obtained by adhesion (as in the case of reinforced concrete), but by means of connecting members, called shear connectors, which are used to transfer longitudinal shear forces across the steel-concrete interface. It is this third component of mixed constructions, which ensures the composite action of a section made of two materials steel and concrete. The major role of the connection is to prevent, or at least to limit, the sliding tending to occur at the steel-concrete interface under the effect of external actions and to transmit the forces between the steel part and the concrete part of the mixed section. In other words, a mixed section tends to behave like a monolithic section.

The shear strength of the connector and the resistance of the concrete slab against longitudinal cracking are the main factors affecting the shear stiffness and strength of the shear connection. Therefore, the design of shear connectors is a vital aspect in the design of composite beams. Shear connectors are of many types in the terms of shape and type of manufacturing material. According to the distribution of shear forces and functional dependency between strength and deformation, they are often categorized as rigid or flexible. For rigid shear connectors, shear forces are resisted through the front side by shearing, and in the proximity of ultimate strength its deformation is insignificant. Stronger concentrated stress in the surrounding concrete is produced by this type of connector, which results in either failure of the concrete or failure of the weld. Whereas, for flexible shear connectors, shear forces are resisted by bending, tension or shearing at the root, at the connection point of the steel beam, a point where upon reaching the ultimate strength values, such connectors are subjected to plastic deformation.

Calculation of the structural behavior of composite beams depends on how much slip is assumed to occur at the interface between concrete and steel. The nonlinear behaviour of "concrete-

connector" is attributed to the process of damage and plasticity. The process of damage can be attributed to micro-cracking, coalescence, and decohesion, etc. The plasticity behaviour can be characterized by several phenomena such as strain softening, progressive deterioration, and volumetric expansion, etc. Experimental push-off tests are the traditional source of knowledge about the load-slip behavior and the shear capacity of the shear stud in composite beams.

The main idea of this master's thesis is to numerically investigate the nonlinear load slip behaviour of shear connectors by using the finite element software ABAQUS. The concrete damage plasticity model was adopted in order to numerically model the nonlinear behaviour of concrete. Several shear connector specimens are studied. The obtained results are compared to experimental works issued from literature.

Methodology followed in this thesis:

This Thesis contains a general introduction, five chapters and a conclusion.

The introduction involves brief information about the work conducted in this study and the objectives of the study.

Chapter 1: an overview of composite structures and composite action in mixed beams is presented in this chapter.

Chapter 2: in this chapter, an introduction on shear connectors, type of shear connectors, advantages and disadvantages of each type of connectors is presented.

Chapter 3: The concepts of modelling of steel and concrete behavior are investigated.

Chapter 4: This chapter gives information about the finite element software ABAQUS. Moreover, the modelling details of 3D models for push out test of specimens are given.

Chapter 5: In this chapter we presented and discussed the obtained results of the push-out test modelling.

Finally, the conclusion: presents a brief summary of the study undertaken within the scope of this work and relevant remarks and comments.

CHAPTER I: COMPOSITE STRUCTEURES

1. Generalities

Composite structures provide a method of using two materials together so as to utilize each material to its best advantage. The most important and most frequently encountered combination of construction materials is that of steel and concrete, with applications in multi-story commercial buildings and factories, as well as in bridges. The interconnection to obtain the single unit action is by combinations of mechanical shear connectors.

The principle of composite action underpins the use of composite materials in construction. It relates to the interaction of two or more separate elements acting together and contributing together rather than separately. By physically connecting them, the strength of the beams and the resistance to bending, shear and torsion are significantly increased. In composite beam design, shear connectors are commonly used to transfer longitudinal shear forces across the steel-concrete interface. The shear strength of the connector and the resistance of the concrete slab against longitudinal cracking are the main factors affecting the shear stiffness and strength of the shear connection [1].

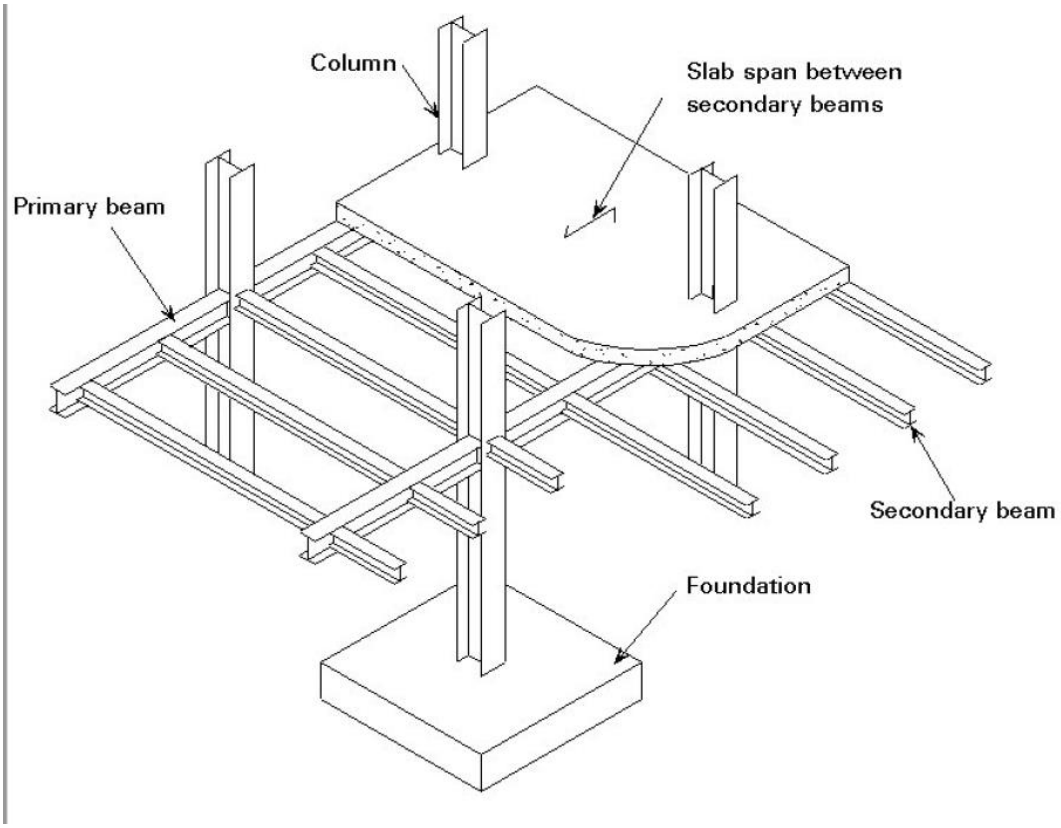

Figure 1.1 Typical Structure

2. Mixed Structural Systems

In multi-story buildings, structural steel is typically used together with concrete; for example, steel beams with concrete floor slabs. The same applies to road bridges, where concrete decks are normally preferred. It is a fact, however, that engineers are increasingly designing composite and mixed building systems of structural steel and reinforced concrete to produce more efficient structures when compared to designs using either material alone.

A further important consideration is that the use of rolled steel sections, profiled metal decking and/or prefabricated composite members speeds up execution. For maximum efficiency and economy, the joints should be cheap to fabricate and straightforward to erect on site.

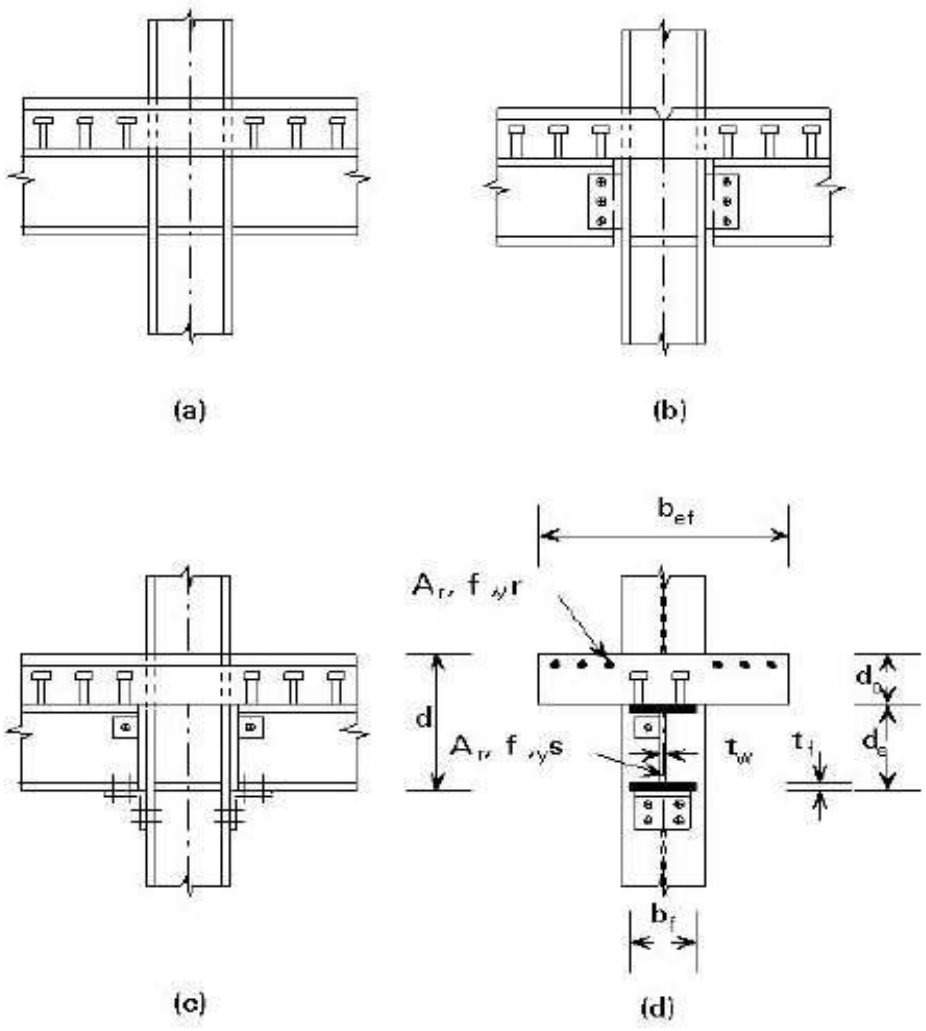

Figure 1.2 Composite Joints

3. Composite Beams

In many buildings and bridges, it is common to have a concrete slab supported by steel beams. If the steel beams are connected to the concrete slab in such as a way that the two acts as one unit, the beam is called as composite beam.

Composite beams are similar to concrete T-beams where the flange of the T-beam is made of concrete slab and the web of the T-beam is made of the steel section.

Composite beam has the advantage that the concrete in the slab takes all or most of the compression (for which it is best suited), while the steel beam takes all tension in the overall system.

Instead of an in situ concrete slab, precast concrete floor or deck units can be used, see Figure 1.3. Careful detailing and construction practice are needed to ensure adequate containment for the connectors. Figure 1.3a shows a system using large prefabricated deck elements with longitudinal joints. The gaps between the units would be filled with mortar in the final structure, thereby giving composite action with the beams. Figure 1.3b shows thin prefabricated concrete elements, supported by the steel beam flange. These elements act as permanent formwork when casting the in-situ concrete. The transverse distances between the stud shanks and the edge of the prefabricated concrete element may be small however, making it difficult to ensure adequate containment for the connectors. The main reason for the use of these thin plate elements (usually 4-5 *cm* thick) is that they are easy to handle, and almost as convenient to handle as metal decking. Figure 1.3b also shows a partly encased composite beam, the voids of which are filled with concrete. This type of composite section is often used in parts of Europe today, in order to enhance the fire resistance rating without additional protection measures. The lower steel flange remains unprotected.

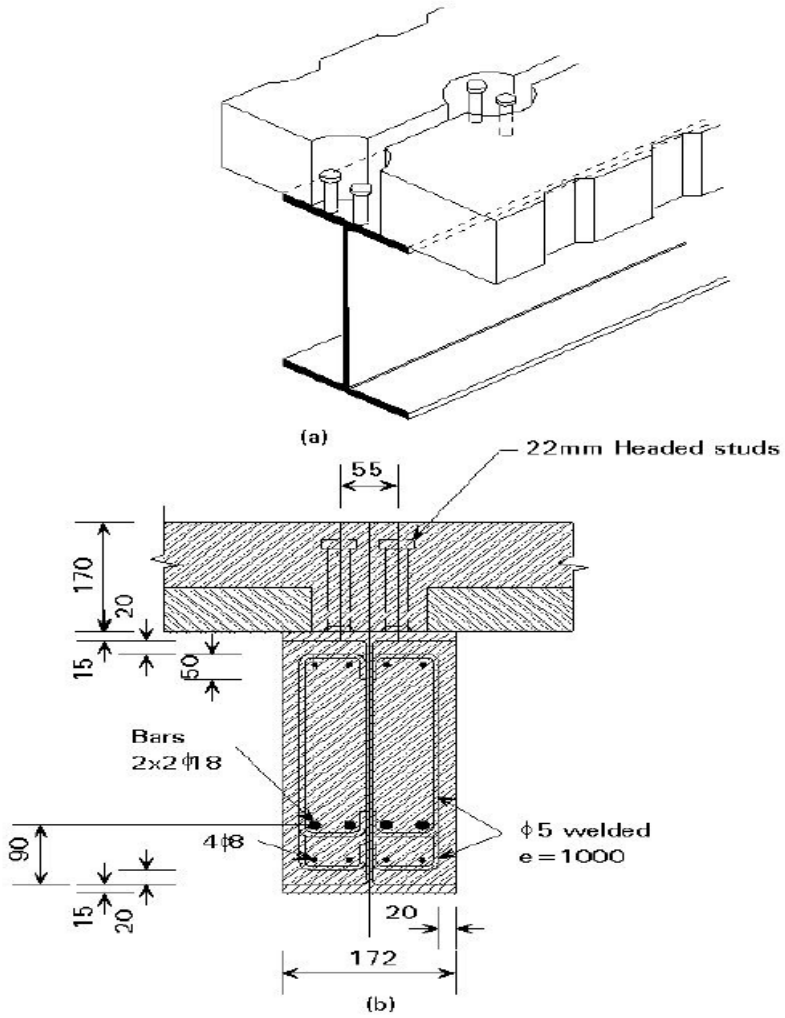

Figure 1.3 Use of Precast Concrete Floor Units

The usual practice however, in the case of commercial and industrial buildings (see Figure 1.6), is to construct the floors using metal decking which incorporates additional embossments or indentations to provide composite action. This is a very economical way to speed up construction, and is an important part of modern structural systems. The deck supports the loads developed before and during concreting and later acts compositely with the in-situ concrete. Steel decking with re-entrant and trapezoidal profiles are typically used, see Figures 1.4 and 1.5.

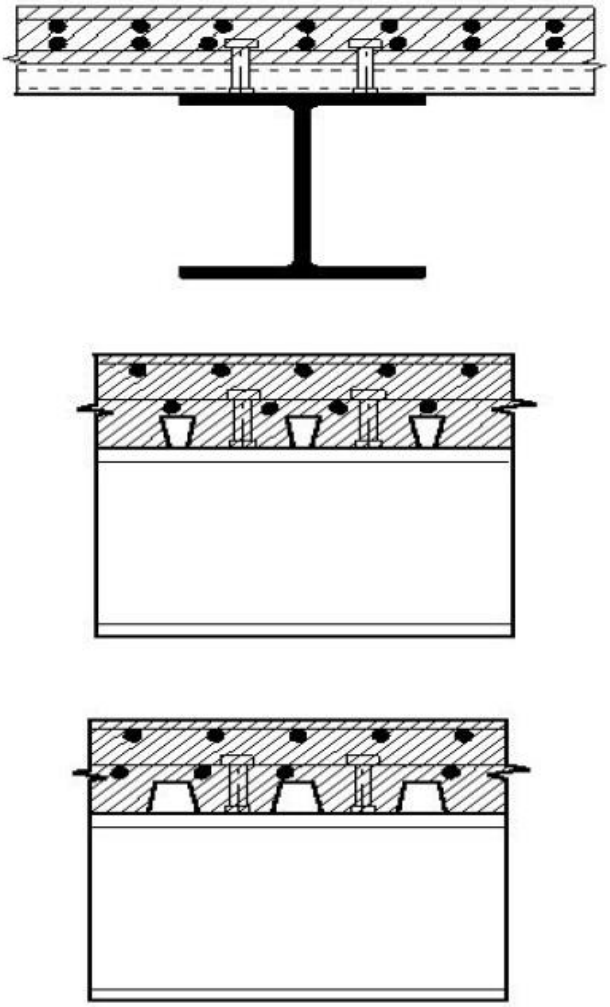

Figure 1.4 The Use of Metal Decking of Different Shapes

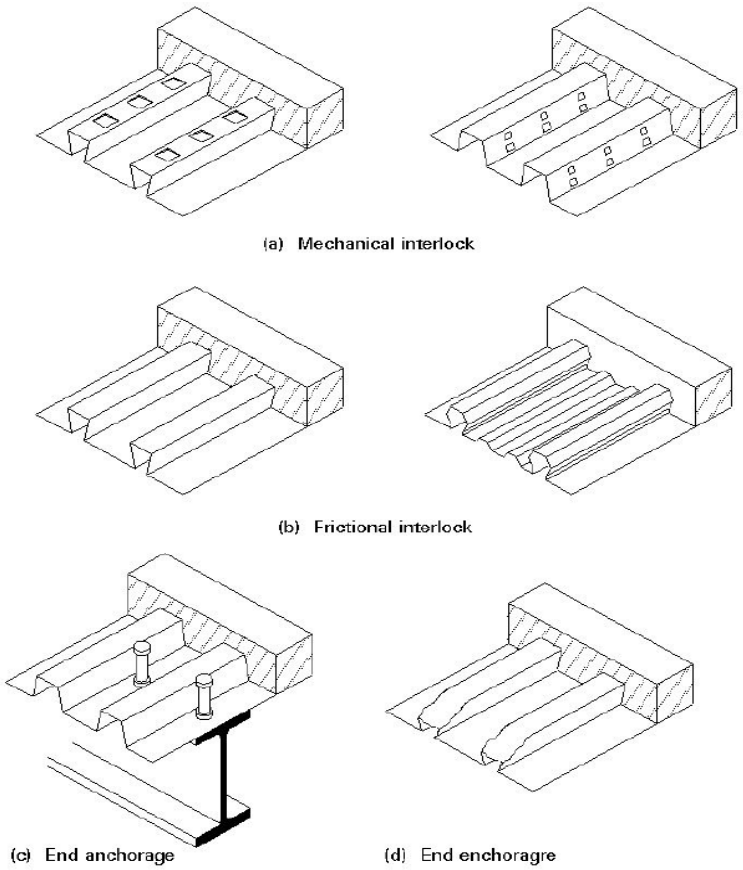

Figure 1.5 Typical Forms of Interlock in Composite Slabs

Figure 1. 6: The Usual Practice for Commercial and Industrial Buildings Is to Construct the Floors Using Metal Decking Which Is Embossed to Provide Composite Action.

3.1. Composite Action in Beams

Composite beams, subject mainly to bending, consist of a steel section acting compositely with one (or two) flanges of reinforced concrete. The two materials are interconnected by means of mechanical shear connectors. It is current European practice to achieve this connection by means of headed studs, semi-automatically welded to the steel flange, see Figure 1.7.

Figure 1.7 Welding the Shear Studs to the Steel Flange

Figure 1.8 shows several composite beam cross-sections in which the wet concrete has been cast in situ on timber shuttering. For single span beams, sagging bending moments, due to applied vertical loads, cause tensile forces in the steel section and compression in the concrete deck thereby making optimum use of each material. Therefore, composite beams, even with small steel sections, have high stiffness and can carry heavy loads on long spans.

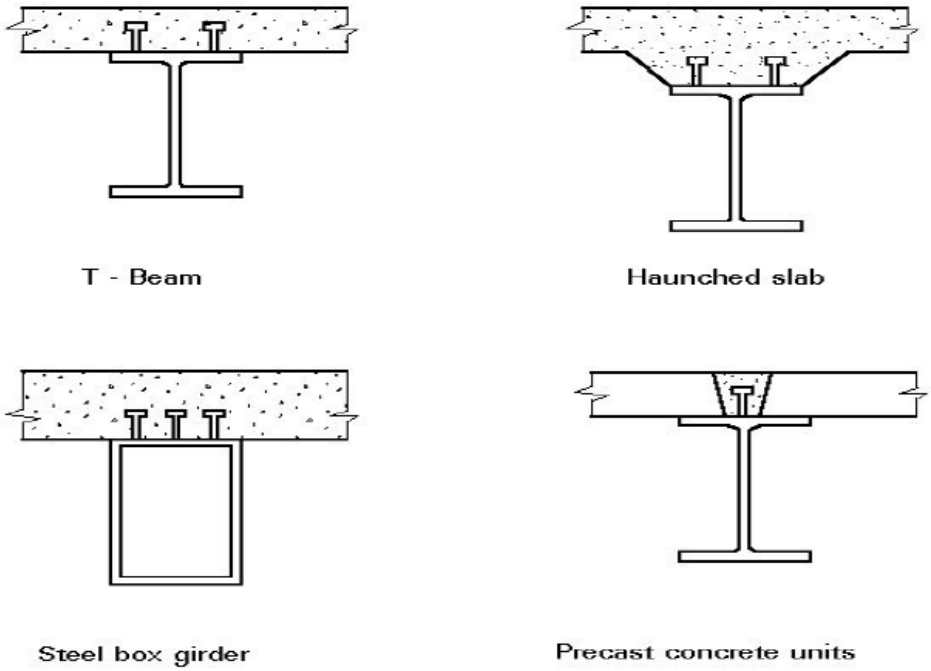

Figure 1.8 Typical Beam Cross Sections

If slip is free to occur at the interface between the steel section and the concrete slab, each component will act independently, as shown in Figure 1.9. If slip at the interface is eliminated, or at least reduced, the slab and the steel member will act together as a composite unit. The resulting increase in resistance will depend on the extent to which slip is prevented. It should be noted that Figure 1.9 refers to the use of headed stud shear connectors. The degree of interaction depends mainly on the degree of shear connection used [2].

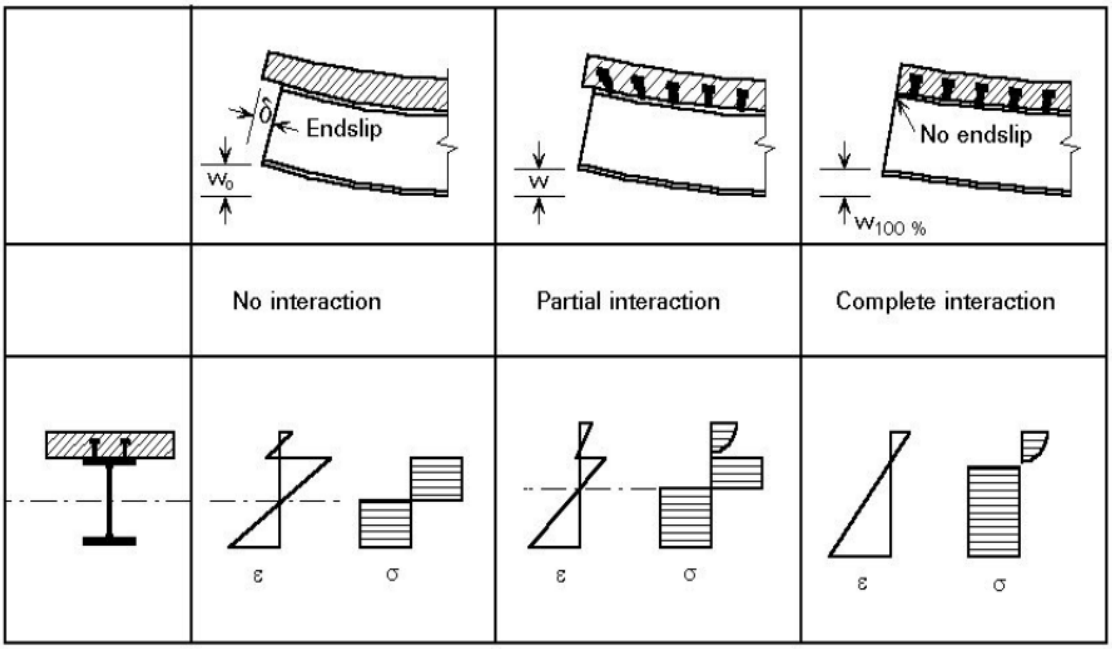

Figure 1.9 Composite Steel Beam-Concrete Slab Interaction

3.2. Types of Communication Composite Beam

Steel-concrete composite beams have been used for a considerable time in bridge and building construction. A composite beam consists of a steel section and a reinforced concrete slab interconnected by shear connectors, as shown in Fig. 1.10. It is common knowledge that concrete is strong in compression but weak when subjected to tension, while steel is strong in tension but slender steel members are susceptible to buckling while under compressive forces. The fact that each material is used to take advantage of its positive attributes makes composite steel-concrete construction very efficient and economical.

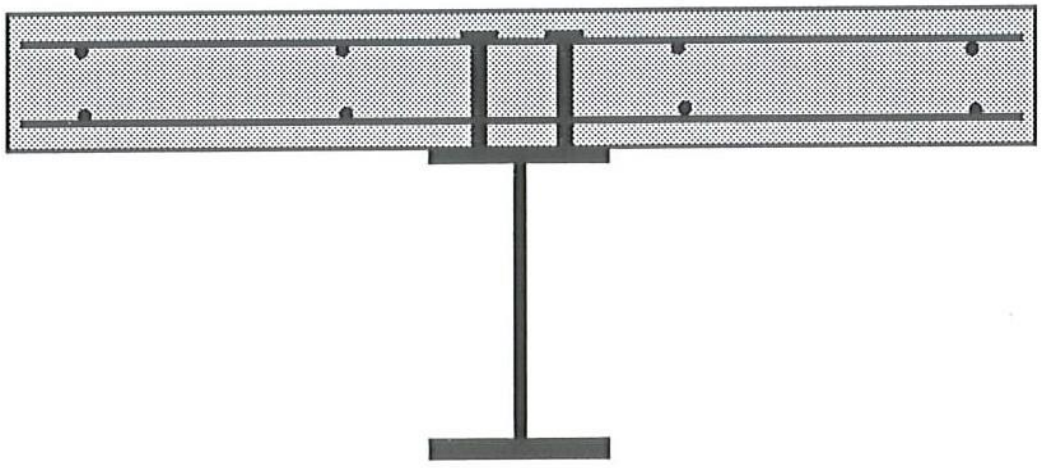

Figure 1.10 Composite Beam with Solid Slab

Composite beams with solid concrete slabs are frequently used in bridge construction. In recent years, the development of an effective composite flooring deck system has greatly enhanced the competitiveness and effectiveness of steel-framed construction for high-rise building.

In today's building industry, composite beams invariably incorporate a formed metal deck as shown in Figure 1.11. This type of composite flooring system consists of a cold-formed, profiled steel sheet which acts not only as the permanent formwork for an in-situ cast concrete slab, but also acts as tensile reinforcement for the slab. The metal deck can be oriented parallel to the beam (Figure 1.11). or perpendicular to the beam (Figure 1.12).

Figure 1.11 Composite Beam with Ribbed Metal Deck

Composite beams offer several advantages over non-composite sections. Since the load is carried jointly by the concrete slab and the steel beam, the size of the steel section is smaller than otherwise would be required. This reduces the overall height of the building and the steel tonnage required, thus resulting in a direct cost reduction. A composite beam is also stiffer than a non-composite beam of the same size and thus experiences less deflection and floor vibrations.

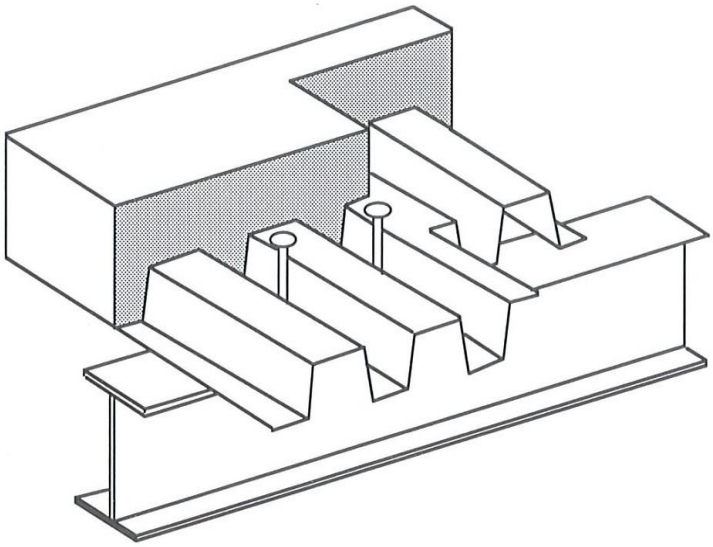

Figure 1.12 Composite beam with ribbed metal deck (oriented perpendicular to the beam).

An essential component of a composite beam is the shear connection between the steel section and the concrete slab. This connection is provided by mechanical shear connectors, which allow the transfer of forces in the concrete to the steel and vice versa and also resist vertical uplift forces at the steel-concrete interface. The shear connectors are installed on the top flange of the steel beam, usually by means of welding, before the slab is cast. These connectors ensure that the two different materials that constitute the composite section act as a single unit [3].

3.3. Description of a Composite Beam on Simple Supports

3.3.1. Behavior of a Non-Composite Beam

For non-mixed constructions, the steel sections are sized to support only the loads acting on the floor plus the self-weight of the slab as is presented in figure 1.13. The section will be symmetrical concerning the axis located halfway up and the axis neutral will pass through this point. The section will deform relative to this neutral axis and the stresses of the stretched outer fiber and the compressed outer fiber will be identical. The stresses (σt) in tension and (σc) in compression of the steel section can be.

determined using simple bending theory:

$$\sigma = \frac{M_S}{W_{sa}} = \frac{M_S \cdot \frac{h}{2}}{I_{sa}} \qquad (1.1)$$

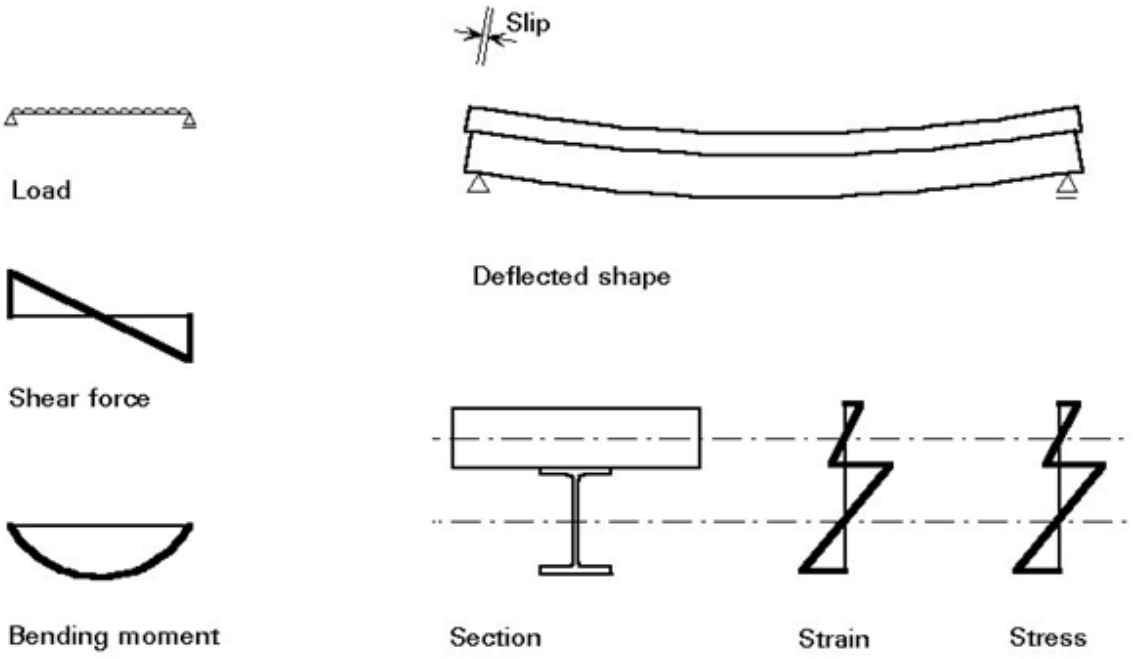

Figure 1.13 Non-Composite Beam.

The concrete slab is not connected to the steel section and will therefore behave independently. As it is generally very flexible in longitudinal bending, it will deform along the curvature of the steel section and have its neutral axis. The face bottom of the concrete slab can slide on the upper face of the steel section and it will produce a significant slip between the two faces. The flexural strength of the slab is often very weak and is overlooked.

3.3.2. Behavior of a Composite Beam

On the other hand, if the concrete slab is connected to the steel section, the two elements act jointly to support the service charges as presented on the figure 1.14. Slipping between the slab and the steel section will now be prevented and the connection will withstand horizontal shear forces which are similar in distribution to vertical sheer forces (shear forces) as shown in Figure 1.13.

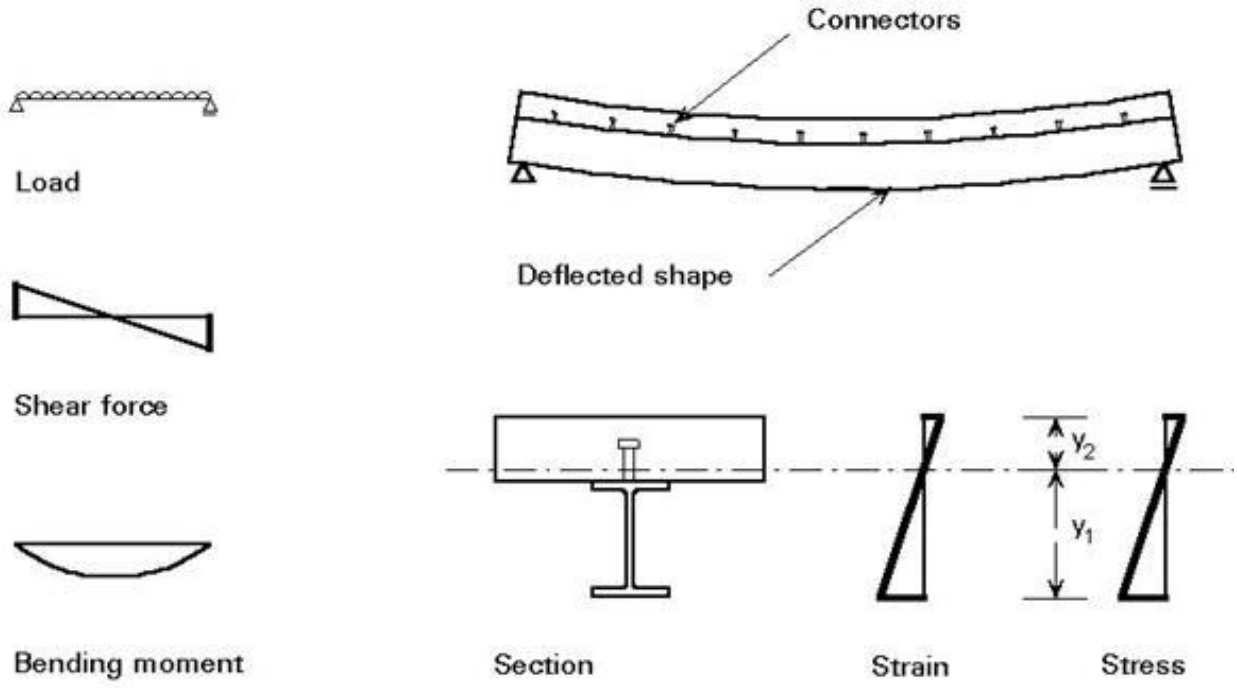

Figure 1.14 Composite Beam.

The mixed section is non-symmetrical and will have a single neutral axis often located near the face upper section of steel. Tensile and compressive stresses on fibers
external will therefore be dependent on the moment of inertia (Ism) of the entire mixed section and their distances from this neutral axis (in the case of a perfect connection).

Assuming that the loading will induce elastic deformations, the stresses created in the section will be determined using the theory of bending. Constraints for the state service limit (ELS) can be obtained from relationships:

$$\sigma_t = \frac{M_S \cdot y_1}{I_{sm}}; \quad \sigma_c = \frac{M_S \cdot y_2}{I_{sm}} \tag{1.2}$$

The value of the moment of inertia (Ism) of the mixed section is generally several times that of the steel section. We will notice that for similar loads the constraints in the extreme fibers generated in the mixed section will be much weaker than those generated in the non-mixed section.

The transverse stresses that develop in the slab when it is wearing transversely along the beam are assumed not to influence the behavior longitudinal for the dimensioning of the composite beam they are generally ignored. However, the span of the beam often dictates the level at which the slab can intervene in longitudinal bending. This will be covered in more detail in the next lesson

and we assume here that half of the lateral span, half of each side of the cross-section steel is effective in resuming longitudinal compression.

3.4. Structural Behavior

The way in which the composite beam behaves under stresses of low values, average values then to ruin, is described in what follows in stages. The load, the moment bending and shear stress,

Step 1 - Figure 1.14

For very low loads, steel and concrete will behave in a way approximately linear. The connection between the two materials will support constraints very low shear and it is unlikely that appreciable longitudinal shifts will happen. The beam will deform in such a way that the distribution of the deformations at the mid-span will be linear as shown in Figure 1.14 and the resulting stresses will be also, linear.

One can notice from the deformation diagram that in the present case, the slab is thick because the neutral axis is located inside the concrete section. As a result, part of the concrete is stretched. We assume that the tensioned concrete is cracked and that it does not take up the tensile stresses. If the slab thickness was small, it would be likely that the neutral axis is in the steel section and the section above the neutral axis is in compression.

Step 2 - Figure 1.15

When the loads increase, the shear stresses between the slab and the section in steel will cause the deformation of the connection. These deformations are known as the sliding name and will contribute to the general deformation of the beam. Figure 1.15 shows the effects of sliding on the distribution of strains and stresses. For many composite beams, the slip is very weak and can be neglected. This step corresponds to the service charges for the mixed section classes that have been sized for partial connection. We will describe it in more detail and details in the connector section.

Step 3 - Figures 1.15 and 1.16

The charge will eventually be sufficient to induce plastic stresses in one or many of the materials.

Step 3a

In the case where the plasticization is located in the steel section, the plasticity will extend to the whole section and rectangular stress diagrams will develop as presented in Figure 1.16. It is generally assumed that for the ultimate limit state, the diagrams plastic stresses develop in such a way that the entire steel section reaches the elastic limit.

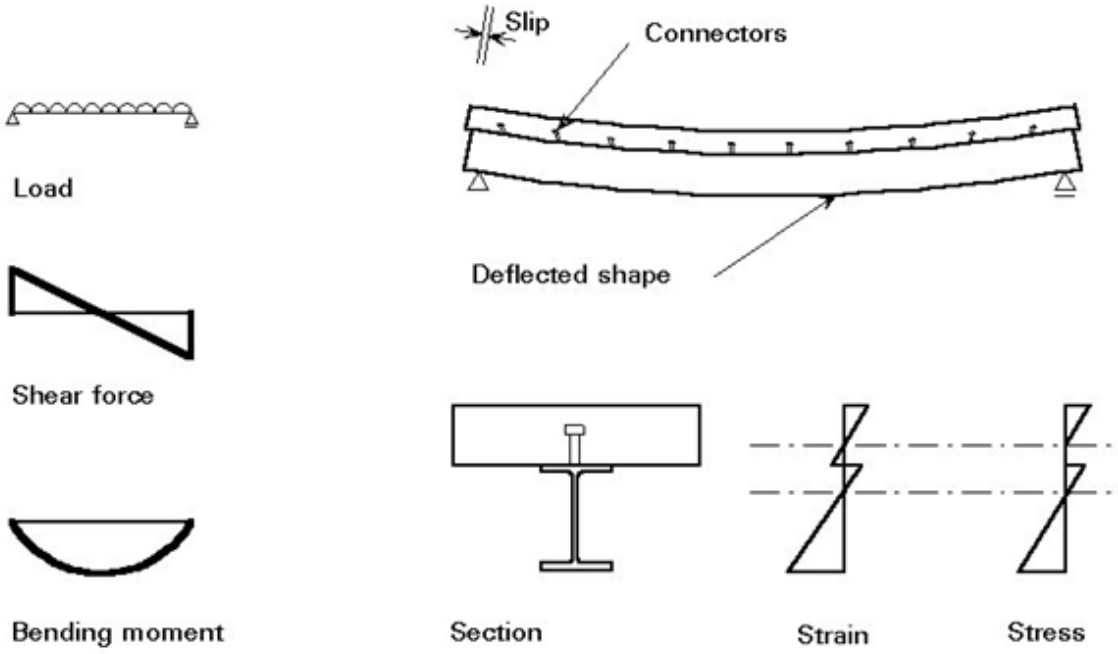

Figure 1.15 Composite Beam Step 2.

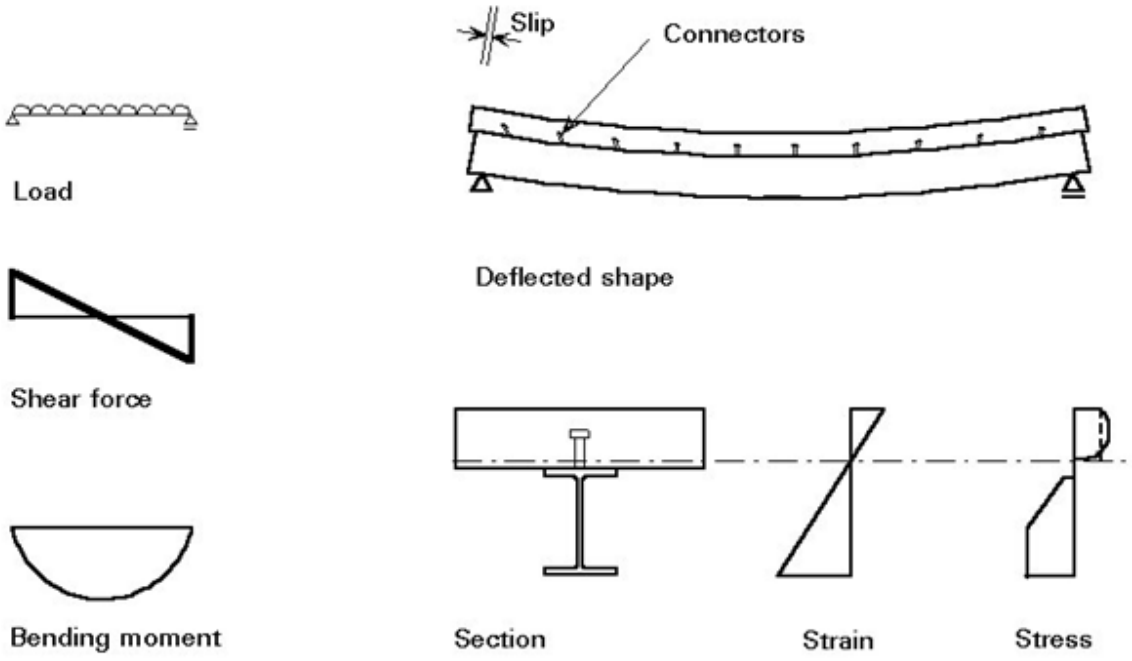

Figure 1.16 Composite Beam Step 3.

Step 3b

Concrete is not a ductile material and if the stresses which occur there are sufficiently large to cause overloading a sudden (explosive) rupture brittle slab may occur. This rupture is similar to the fragile rupture as it can be provided in over-stressed reinforced concrete beams. The volume of concrete used in most conventional slabs makes this unlikely to happen inconveniently. With the increase in compression stresses created by the increase in deformations, the stress diagram in concrete turns into a triangular shape shown in Figure 1.15 to a shape shown in Figure 1.16. Sizing this form is difficult to model mathematically and we use approximations. For mixed beams, the most common approximation is the rectangular distribution of constraints shown by the curve in dotted lines in Figure 1.16.

Step 3c

Other components of the composite beam may rupture before the steel plasticizes or the concrete doesn't crash, it's the connectors. As the loading level increases, shear strains and therefore shear stresses at the interface between the steel section and the concrete will also increase proportionally. For a beam mixed on simple supports uniformly charged which one supposes to deform so elastic, the longitudinal shear force (T) expressed per meter of beam occurring between the slab and the steel section can be obtained by the following relationship:

$$T = \frac{V \cdot \hat{S}}{I} \tag{1.3}$$

Where: S is the static moment of the section.

As the longitudinal shear force is directly proportional to the shear force, the greatest effort will be placed on the end connectors. For charges of low values, the force acting on a connector will produce elastic deformations, and one notes that the slip between the slab and the steel section will be the greatest at the end of the beam. For this loading step, the longitudinal shear and the deformation of a conventional composite beam is shown in Figure 1.18a.

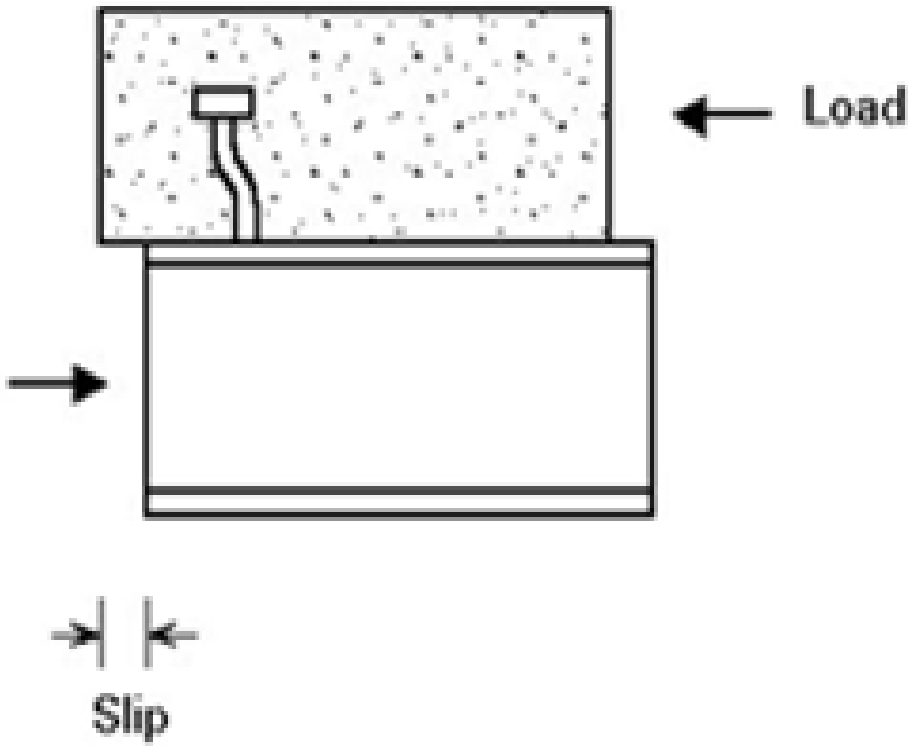

Figure 1.17 Effect on The Shear Connector.

If the load increases, the longitudinal shear force increases. The effort on the end connector may very well cause plastic deformation. A typical relationship between the load and the slip for a connector is presented in figure 1.18. The ductility of the connectors mean that the connectors are capable of plastic deformation while resisting the longitudinal shear force. Figure 1.18b shows the situation when the two end connectors are plastically deformed.

The increase in applied loads will produce an increase in horizontal shear and deformation of the connectors. As a result, the connectors located near the center of symmetry of the beam will also successively begin to deform plastically. The failure will occur once all connectors have reached their ultimate strength as this is shown in Figure 1.18c. This sequence of shearing and stressing of connectors is presented in an amplified manner in figures. 1.18a, 1.18b, and 1.18c. This sequence depends on the ability of the connectors to deform the plastic. The connector's ends must be able to deform considerably before those located near the axis of symmetry of the beam also reach their ultimate capacity to resistance.

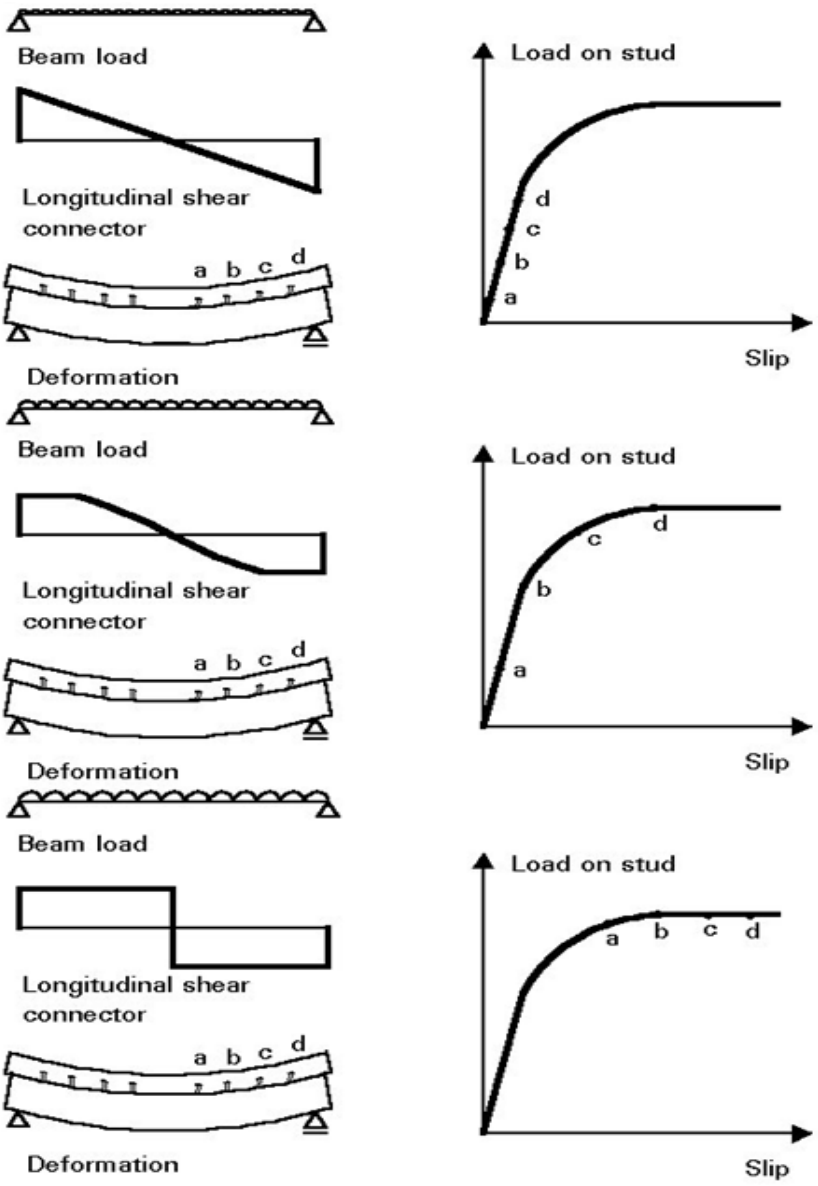

Figure 1.18 The Behavior of Connectors in Shear.

CHAPTER II: *SHEAR CONNECTOR*

1. Introduction

Over the years, the construction industry has taken advantage of the enormous global strides made in technology to witness a creative and innovative advancement of construction materials and material properties. Without a doubt, there has been a progressive widespread of composite construction given to the fact that it provides improvement to the mechanical properties of structural members. The use of composite action between steel and concrete achieved through shear connectors is a well-established cost-effective arrangement for floor systems in multi-story steel frame building structures as well as in bridge deck construction. A composite flexural member will have higher strength and stiffness compared to a bare steel member, resulting in reduced deflection and floor vibration in the structure. Composite flexural members can be used as girders in bridges or primary and secondary beams in building systems. Mechanical connectors for shear transfer must be used in these members to achieve the desired composite behavior.

The shear connectors are commonly used to ensure composite action in a steel–concrete composite beam and they are responsible for transferring the horizontal shear forces that are formed due to flexural action. The need for mechanical shear connectors also arises to transfer earthquake forces between concrete slab and steel beams that are part of the lateral load resisting system of the structure. Besides, these elements function under axial loads to resist vertical upward forces and prevent the premature separation of steel beams and concrete slab in the vertical direction [4].

Many types of shear connectors have been developed and used in the past. The most widely used shear connector in practice is the welded stud (Figure2.1(a)) with a suitable head that contributes to the shear transfer and prevents the uplift. Nevertheless, due to the small load carrying capacity of stud connectors and also due to the fatigue problems caused by live loads on composite bridges, some other alternative shear connectors are proposed such as the angle connector with anti-uplift bar (Figure2.1(b)) and the channel connector (Figure2.1(c)) which are frequently used in Algeria and in some other countries.

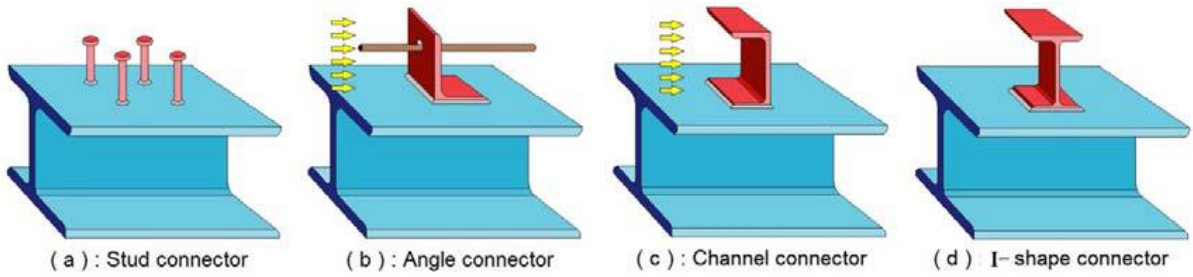

Figure 2.1 Types of Shear Connectors

The economic considerations continue to motivate the development of new systems to ensure the load transfer between steel and concrete components in composite structures. Recently, several authors have proposed new types of shear connectors, such as Y-type perfobond rib connector, J-hook connector, Bolted connector, Rubber-sleeved stud, V-shaped angle and I-shape connectors. As shown in Figure 1(d), the I-shape connector is appropriate to resist shear forces and prevent vertical separation between the steel beam and the concrete slab. In addition, angle and channel connectors are limited to shear transfer in the recommended direction only, while the I-shape connector can resist and transfer shear in the two directions with same quantity, making it the more useful shear connector in composite beams subjected to seismic loading. Moreover, the facility of producing the I-shape connectors by their cutting from the ordinary laminated I profiles is another advantage. The welding task has the same characteristics as referred for angle and channel connectors [5]. C-shaped connectors and I-shape Shear Connectors include the fact that it does not require an expensive machine to install. The installation procedure would be similar to that used for beam stiffeners and connection components. Thus, adopting this option eliminates one trade on the job site, the shear connector installation crew, resulting in further savings in construction costs. Inspection procedures such as bending tests required for headed studs may not be necessary for channel and angel connectors and I-shape Shear Connectors. It is robust and can take rough handling.

2.1. Headed Studs

To resist horizontal shear and vertical uplift forces in composite steel-concrete structures, the most commonly used type of shear connector is the head stud. Also referred to as the Nelson stud (Figure 2.2), this type of connector contributes to the shear transfer and prevents uplift, as it is designed to work as an arc welding electrode, and, simultaneously, after the welding, acts as the resisting connector with a suitable head. As a result of the high degree of automation in the workshop or on site, this type of connector is commonly used worldwide. However, in structures submitted to fatigue, the use of this type of connector has some restrictions, the requirement for specific welding equipment and a high-power generator on site for its use limits the utilization of such connectors. Another drawback is that the strength for concrete grades higher than C30/37 is normally governed by the strength of the steel cross section of the stud. Hence, higher concrete grades will not be advantageous for this connector device. Furthermore, it is practically impossible to automate the welding of headed studs (Zingoni, 2001) [6].

Much research has been carried out on headed stud shear connectors and various equations have been proposed to estimate the strength of studs (Viest, 1956a; Ollgaard et al., 1971; Gelfi and

Marini, 2002; Lee et al., 2005). Viest carried out the initial studies on stud shear connectors, where full-scale push out specimens were tested with various sizes and spacing of the studs. The push-out and composite beam tests were used in studies on stud shear connectors to evaluate shear capacities. In order to investigate the behaviour of headed shear stud connectors in solid slabs, an accurate nonlinear finite element model was developed by Ellobody (2002) and Lam and Ellobody (2005). Validation against test results and comparison with data specified in the current codes of practice, such as BS5950 (Standard, 1994) and AISC (AISC, 2005a), were carried out using the effective numerical model (Lam and EI-Lobody, 2001). The results of the experiment conducted by these authors are comparable with the results obtained from the finite element analysis. The finite element model offered accurate predictions on the capacity of the shear connection, the load slip behavior of the headed studs and the failure modes.

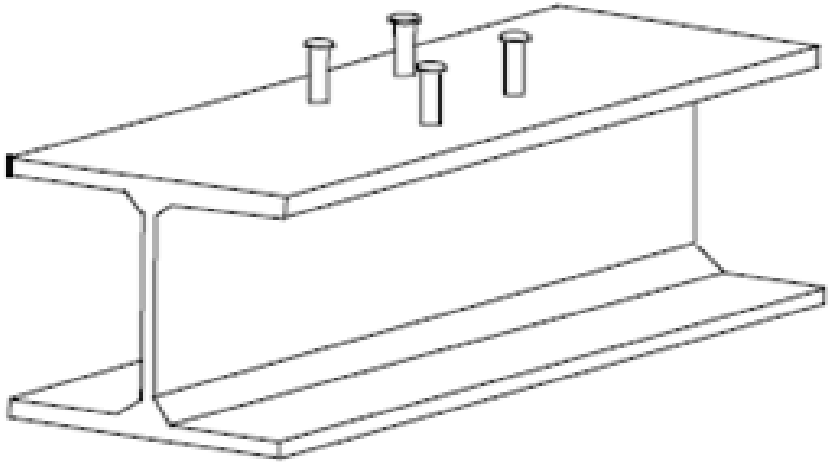

Figure 2.2 Head Stud Shear Connector

Presently, the headed stud is the most widely used shear connector in composite construction. The advantages of headed stud connectors can be summarized as follows: fast welding, good anchor in concrete, the arrangement of reinforcement through the slab is easy, production of large scale size is easy, the standard dimensioned head is a resistance factor for slab uplift and bending and shearing load-bearing capacity in the lower area of the connector shaft, tensile force in the connector shaft and the friction forces in the composite interface. There are almost no tensile forces acting on the shank in high strength concrete. Nonetheless, due to the small load carrying capacity of stud connectors, they have to be installed in large numbers. This usually produces a cluttering effect and an unsafe working place. Therefor other forms of types of connectors such as C-shaped connectors (angle and channel) and I-shape Shear Connectors, were developed. A few channel and angel connectors and I-shape Shear Connectors will replace a large

number of headed studs. This would avoid the clutter usually produced by studs which creates an unsafe workplace during construction [7].

2.2. T-Rib Connector

In the scope of a study on perfobond connectors, Vianna et al. (2009) presented an alternative connector for headed studs, called the T-perfobond (Figure 2.3). The author also provided a comparative study between the behaviour of these connectors and a limited number of T-perfobond connectors. By adding a flange to the plate, which acts as a block, the derivation of this connector from the perfobond connector was created. The need to combine the large strength of a block type connector with some ductility and uplift resistance arising from the holes at the perfobond connector web is a motivating factor for the development of this T-perfobond connector. In order to prevent a premature loss of stiffness in the connection, the T-rib connector detail should minimize the prying action effect (Ferreira, 2000). As leftover rolled sections can be used to produce the T-rib connectors, it could reduce cost and minimize welding work. The four steps involved in the fabrication process of the T-rib connectors: (i) initial profile, (ii) web holes, (iii) flange holes, (iv) opposite flange saw cut are as shown in Figure 2.3. For similar longitudinal plate geometries, the resistance and stiffness of T-perfobond connectors are higher than that of perfobond connectors. In addition to this advantage, the use of T-perfobondc onnectors offers benefits in terms of saving material and labour, as they are produced with ordinary laminated I or H sections.

Figure 2.3 T-RIB Shear Connector

2.3. Channel Connectors

Channel connectors might not need inspection procedures, such as bending test of headed studs, due to the highly reliable conventional welding system used in the welding of these connectors. The load carrying capacity of a channel shear connector is higher than that of a stud shear connector. This enables replacement of a large number of headed studs with a few channel connectors (Maleki and Bagheri, 2008a). Viest et al. (1952) reported on the test results of full size and push-out specimens. The focus of this preliminary study was to understand the channel shear connectors' behaviour and to evaluate whether the use of channels as shear connectors is feasible (Figure 2.4). Slutter and Driscoll (1962) reported the results of another experimental study carried out at the Lehigh University concerning shear connectors. The results of 41 push-out specimens tested by the mentioned research constituted the basis from which the equations included in the American Institute of Steel Construction specification (AISC, 2005) (AISC, 2005b) and the Canadian standard (CSA, 2001) for the strength of channel shear connectors embedded in a solid concrete slab were derived.

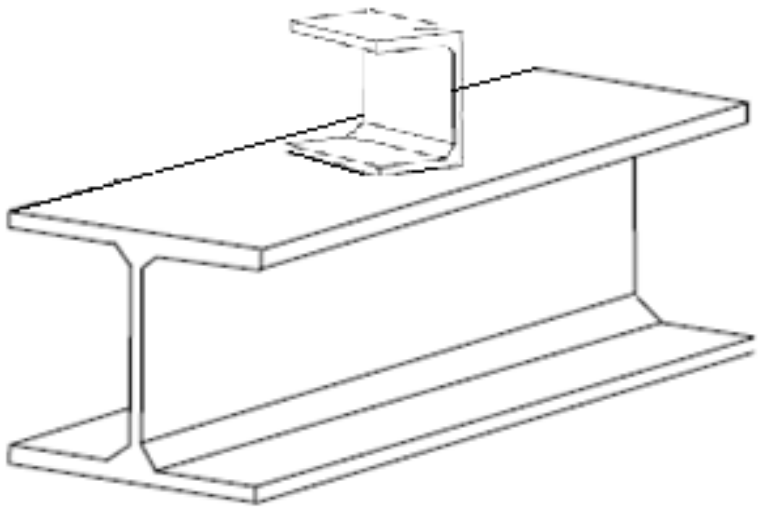

Figure 2.4 Channel Shear Connector

2.4. I-shape Shear Connectors

Various reasons like monetary contemplations and strength aspects has persuaded in development of I-shape shear connector. Due to its symmetry in both the axes, it offers more resisting in bending. Similar to channel connector, connection is established by welding one flange of rolled I section to flange of steel beam.

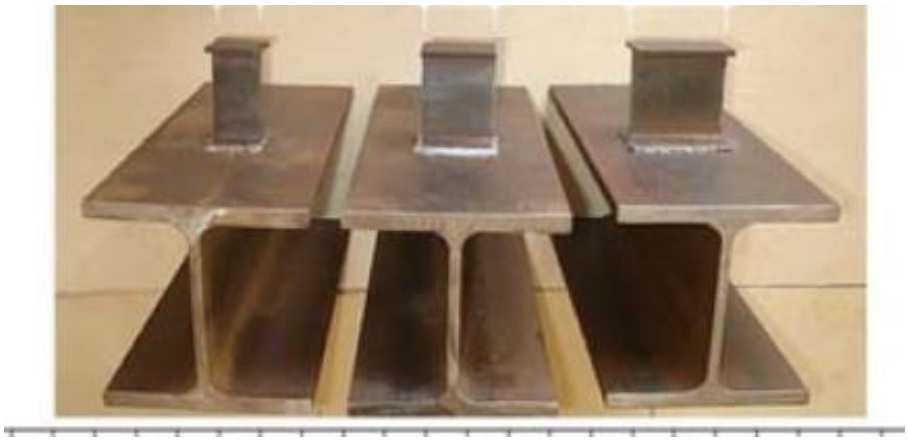

Figure 2.5 I-Shape Shear Connectors

2.5. T-Connectors

This connector is a section of a standard T-section welded to the H or I section with two fillet welds (Figure 2.6).T-connectors evolved from the observation by Oguejiofor (1997) that a large part of the bearing capacity of a perfobond strip was the result of the direct bearing of the concrete at the front end of the (discontinuous) perfobond strip. Therefore, a T section, which has a larger cross section than a single strip, and by its shape could prevent vertical separation between the steel-section and the concrete, seemed a good alternative. The behavior of the T-connector is very favorable. The beating stress on the front of the T is very high, as a result of the relatively small area. Local concrete crushing occurs, which results in a quasi-plastic performance (Zingoni, 2001). The load capacity for T-connectors is similar to that of the oscillating perfobondstrip, however, the ductility of these connectors is much larger (Rodera, 2008). When used in concrete with fibres, lightweight concrete or a higher strength concrete, there is a notable increase in the load capacity and ductility of this type of connector. In the case of the T-shape connectors, the strength of the connector itself is vital and the concrete is no longer decisive. Disregarding the perfobond strip, the resistance characteristic of the T-shape connectors is considered the highest and its failure mode varies according to different concrete strengths.

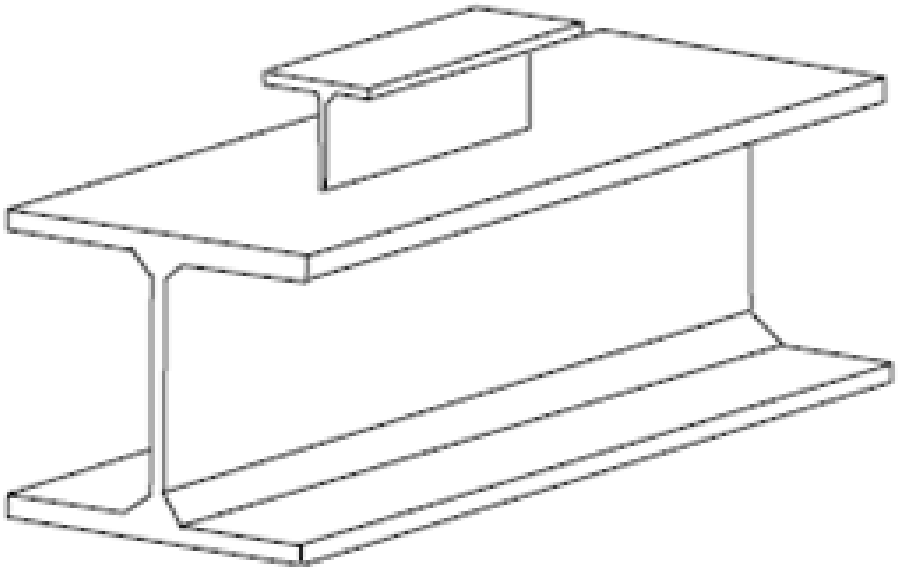

Figure 2.6 T- Shear Connector.

2.6. Perfobond Ribs

In the late 1980s, the office of Leonhardt, Andrå and Partners developed a new type of connector called the perfobondrib (Leonhardt et al., 1987a), which was introduced in recognition of the unsatisfactory behaviour of shear studs resulting from fatigue problems caused by live loads on composite bridges. Developed in Germany, this connector includes a welded steel plate, with a number of holes (Figure 2.7) (Ahn et al., 2010). The flow of concrete through the rib holes formed dowels that provide resistance in both the vertical and horizontal directions. This shear connector is a viable alternative to the headed stud connector, as signified in the experimental studies conducted previously (Ahn et al., 2010) and recently (Kisa 2011 and Jumaat et al., 2011). This connector was initially used in building structures (Ferreira et al., 1998). The fact that it not only ensures the concrete steel bond, but also enables a better anchorage of the internal columns hogging moment has encouraged its adoption.

By passing these through the perfobond web holes or simply by being superimposed to the transverse reinforcing bars that are generally used on them will allow these bars to be anchored. A study done by Zellner (1987) indicated that a one metre length of perfobond connector is comparable to eighteen 22 mm diameter studs disposed in two lines or twenty-four 19 mm diameter studs disposed in three lines.

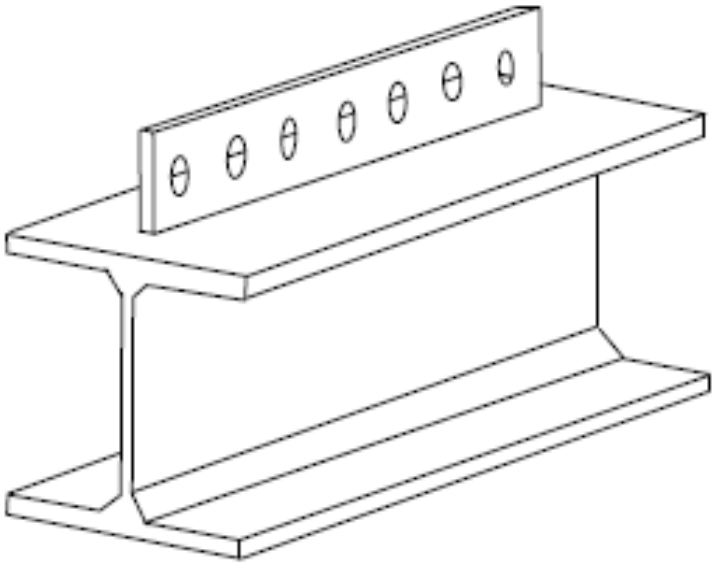

Figure 2.7 Perfobond Ribs Shear Connector

As compared to the headed studs and T-shape connectors, this type of connector has larger load capacity. However, due to the fast drop of the load capacity after the peak, the performance of this connector in the case of ordinary strength and normal weight concrete is rather disappointing. Nonetheless, the absence of such behaviour when they are in use in lightweight concrete, concrete with fibres or high strength concrete allows the oscillating perfobond strips con-nectors (Figure 2.8) to perform well (Rodera, 2008). The difference in the failure modes for lower and higher concrete strength for oscillating perfobond strip connectors should be taken into consideration. The addition of steel fibres to the concrete reported a very positive effect.

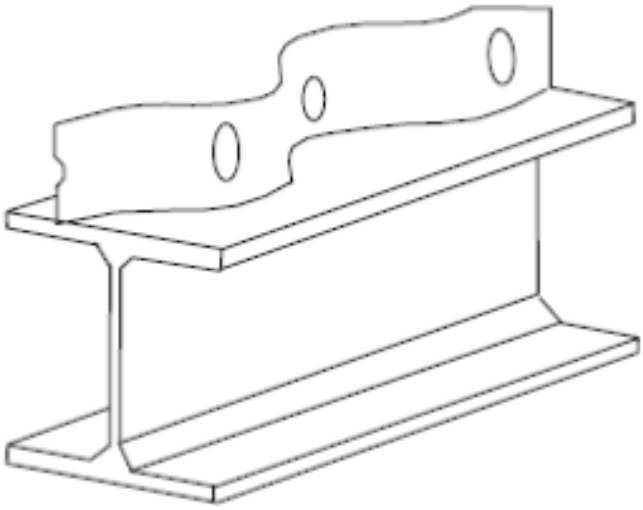

Figure 2.8 Oscillating-Perfobondstrip Shear Connector

2.8. Waveform Strips

The objective of the curved form is to improve the transfer of force between the steel and the surrounding concrete as opposed to a straight connector. It is however recognized that it would be more difficult to weld using conventional automated welding equipment. The strips are welded to the HE-section with two fillet welds of 5 *mm* waveform strip with a width of 50 *mm*, a thickness of 6 *mm* and bend in 2 waves with amplitude 110 *mm*; Figure 2.9. Although the strip is meant to be welded using point weld equipment, such equipment with sufficient capacity is very scarce, and it is even doubtful whether the connector could be successfully welded using this equipment (Galjaard et al., 2001).

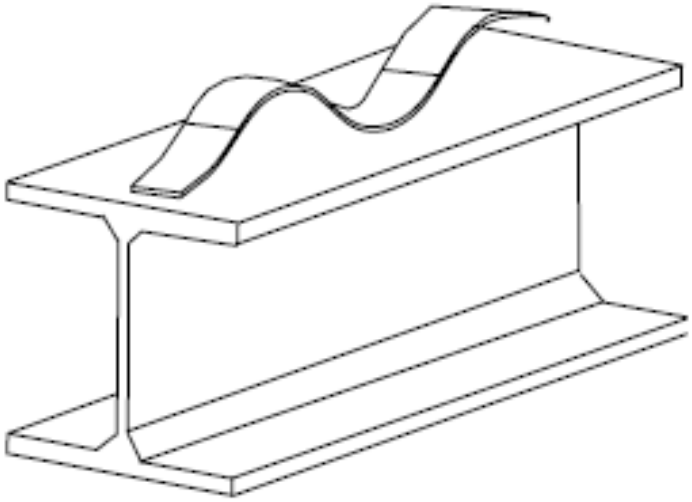

Figure 2.9 Waveform-Strip Shear Connector

2.9 Non-Welded Connectors

Non-welded shear connectors, which are fixed by fastening pins using a powder-actuated tool, were developed following the difficulties of welding shear studs through profiled sheeting on site. Composite beams and push-out specimens, with and without profiled sheeting, were used in testing non-welded connectors (Crisinel, 1990) cold-formed from mild steel. This new connector (Figure 2.10) is L-shaped and two hardened steel fastening pins, which are driven through the connector and into the flange of the steel beam using a powder-actuated tool were used to fix the foot of the connector to the flange of the steel beam (Crisinel, 1990). The behaviour of these connectors is ductile and resembles that of the stud shear connector, as found in the studies conducted on them based on push-out tests and beam tests with and without profiled sheeting.

Providing the connectors are positioned correctly, the strength reduction of the non-welded connectors caused by the presence of profiled sheeting can be estimated with the same formula that has been developed for the shear studs (Crisinel, 1990). This device has been specially designed to diminish and redistribute the bearing stresses transmitted to the concrete and to sustain non-linear deformations without inducing heavy damage on the steel-concrete connection.

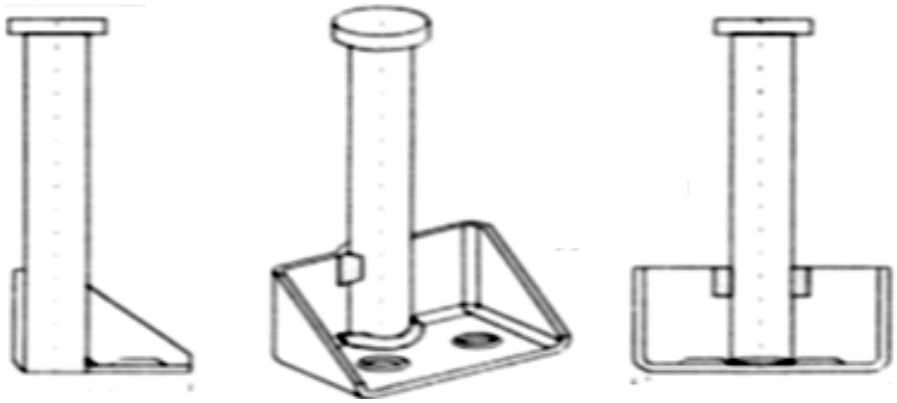

Figure 2.10 Non-welded shear connector

2.10. Pyramidal Shear Connectors

Sufficient bending strength and flexural rigidity for loads during and after construction is expected from a steel plate-concrete composite slab with pyramidal shear connectors (Figure 2.11). A TSC composite slab, which is composed of a bottom steel deck and concrete through pyramidal shear connectors could also be one of them (Lee and Han, 1998). The fatigue problem should play a significant role in design when such a TSC composite slab is applied to a bridge deck subjected to traffic loads. In particular, the fatigue strength of the thin bottom plate may be reduced through the welding of shear connectors (Matsui, 1984).

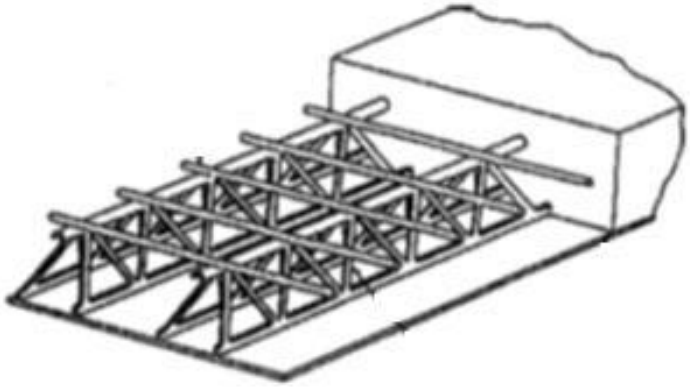

Figure 2.11 Pyramidal Shear Connector

2.11. Insa Hilti Shear Connector

This shear connector is developed for wood concrete mixed structures (Mungwa et al., 1999). This shear connector possesses higher rigidity, ductility and ultimate strength,as indicated in the test results. The INSA Hilti shear connector (Figure2. 12) is the innovative feature of the new shear connector. When subjected to alternating loads, the mechanism of shear transfer at the wood concrete interface for traditional dowel-type connectors, such as nails and screws, are notorious for shearing the wood along the grain fibres. Whereas failure of the wood in front of the connector causes the failure of non-dowel-type connectors, such as rigid ring connec-tors. The failure pattern is very much ductile despite the fact that the new connector is tubular. The connector was subjected to a push-out test, which is normally referred to as a local test (Mungwa et al., 1999) [8].

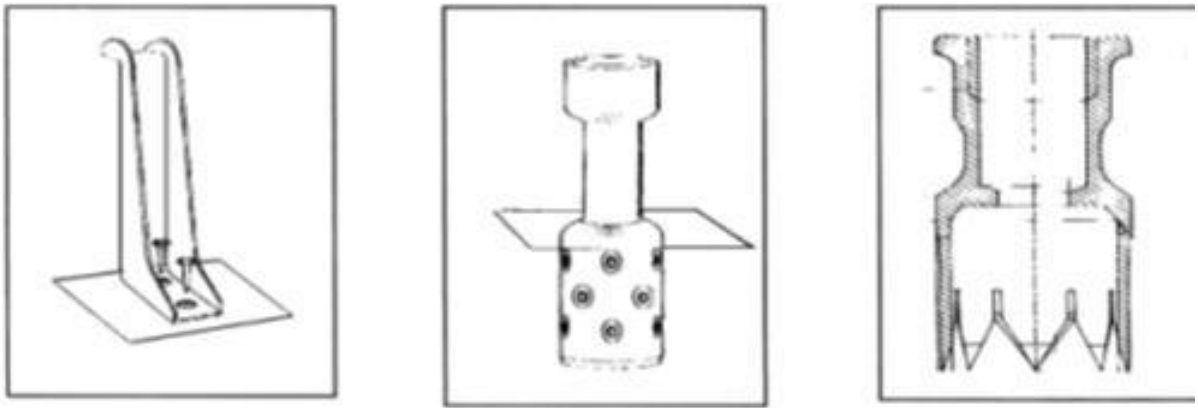

Figure 2.12 Insa Hilti Shear Connector.

CHAPTER III: *MODELLING OF CONCRETE BEHAVIOR*

1. Introduction

Different materials possess different properties in varying degree and therefore behave in different ways under given conditions. These properties include Mechanical properties, Electrical properties, Thermal properties, Chemical properties, Magnetic properties and Physical properties.

A design engineer is interested in the behaviour of materials under load which is mechanical in nature, for the design of machines and structures. Any material subjected to a load either deforms, yield, or break, depending upon the magnitude of the load. Those characteristics of the materials which describe their behaviour under external loads are known as Mechanical Properties. The most important and useful mechanical properties are:

1) Strength

It is the resistance offered by a material when subjected to external loading. So, stronger the material the greater the load it can withstand. Depending upon the type of load applied the strength can be tensile, compressive, shear or torsional. The maximum stress that any material will withstand before destruction is called its ultimate strength.

2) Elasticity

Elasticity of a material is its power of coming back to its original position after deformation when the stress or load is removed. Elasticity is a tensile property of its material. The greatest stress that a material can endure without taking up some permanent strain is called the elastic limit.

3) Stiffness (Rigidity)

The resistance of a material to deflection is called stiffness or rigidity. Stiffness is measured by Young's modulus E. The higher the value of the Young's modulus, the stiffer the material. E is the ratio of stress over strain and is given by the slope of line σ-ε.

4) Plasticity

The plasticity of a material is its ability to undergo some degree of permanent deformation without failure. Plastic deformation will take place only after the elastic range has been exceeded, Plasticity is an important property and widely used in several mechanical processes like forming, shaping, extruding and many other hot and cold working processes. In general, plasticity increases with increasing temperature and is a favorable property of material for secondary forming processes.

Due to these properties various metals can be transformed into different products of required shape and size. This conversion into desired shape and size is affected either by the application of pressure, heat or both.

5) Ductility

Ductility of a material enables it to draw out into thin wire on application of the load. Mild steel is a ductile material. The wires of gold, silver, copper, aluminium, etc. are drawn by extrusion or by pulling through a hole in a die due to the ductile property. The ductility decreases with increase of temperature. The per cent elongation and the reduction in area in tension are often used as empirical measures of ductility.

2. Steel

III.2.1 Modelling of steel

Different stress (σ)–strain (ε) models have been used for the steel material by different researchers, including elastic-perfectly plastic model, and elastic-plastic model with linear hardening or multi-linear hardening.

A σ-ε model was proposed by Tao et al. [9] for structural steel with a validity range of fy from 200 *MPa* to 800 *MPa*. This model is expressed as follows:

$$\sigma = \begin{cases} \text{Es}\varepsilon & 0 \le \varepsilon < \varepsilon y \\ \text{fy} & \varepsilon y \le \varepsilon < \varepsilon p \\ \text{fu} - (\text{fu} - \text{fy}).\left(\frac{\varepsilon u - \varepsilon}{\varepsilon u - \varepsilon p}\right)^{p} & \varepsilon p \le \varepsilon < \varepsilon u \\ \text{fu} & \varepsilon \ge \varepsilon u \end{cases} \quad (1)$$

In which fu is the ultimate strength; εy is the yield strain, $\varepsilon y = fy/Es$; εp is the strain at the onset of strain hardening; εu is the ultimate strain corresponding to the ultimate strength; p is the strain-hardening exponent, which can be determined by:

$$p = Ep.\left(\frac{\varepsilon u - \varepsilon p}{\text{fu} - \text{fy}}\right) \quad (2)$$

Which Ep is the initial modulus of elasticity at the onset of strain-hardening, and can be taken as $0.02Es$. εp and εu are determined using Eqs. (3) and (4), respectively

$$\varepsilon p = \begin{cases} 15\varepsilon y & \text{fy} \le 300\text{Mpa} \\ [15 - 0.018(\text{fy} - 300)] & 300\text{Mpa} < \text{fy} \le 800\text{Mpa} \end{cases} \quad (3)$$

$$\varepsilon p = \begin{cases} 100\varepsilon y & \text{fy} \leq 300\text{Mpa} \\ [100 - 0.15(\text{fy} - 300)]\varepsilon y & 300\text{Mpa} < \text{fy} \leq 800\text{Mpa} \end{cases} \quad (4)$$

A schematic diagram of this model is shown in Figure.3.1, where only three parameters, i.e. yield strength (fy), ultimate strength (fu) and modulus of elasticity (Es), are required to determine the full-range stress–strain curve. The value of Es is taken as 200,000 MPa in the modeling. Likewise, the following equation proposed by Tao et al. [9] was used to determine fu from fy if fu was not available.

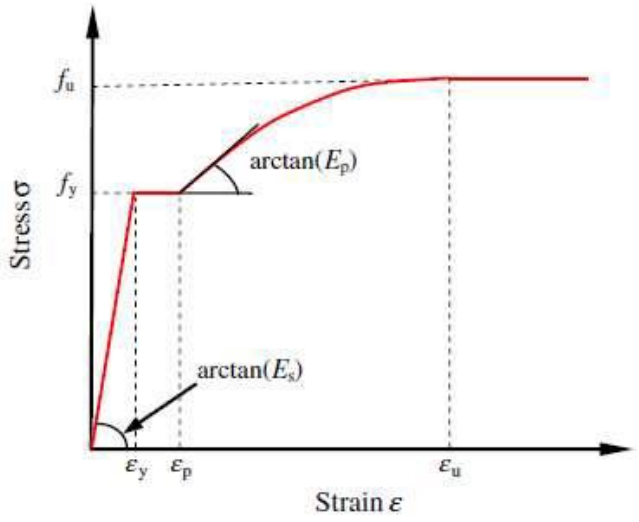

Figure.3.1 Σ–E Model Proposed by Tao Et Al. [9] For Structural Steel

$$fu = \begin{cases} [1.6 - 2 \times 10 - 3(\text{fy} & 200\text{Mpa} \leq \text{fy} \leq 400\text{Mpa} \\ [1.2 - 3.75 \times 10 - 4(\text{fy} - 200)]\text{fy} & 400\text{Mpa} < \text{fy} \leq 800\text{Mpa} \end{cases} \quad (5)$$

3. Concrete

3.1. Material Modeling of Concrete

The FE method is particularly advantageous in the modeling of concrete as it is capable of capturing complex stress variations in the concrete. Reliable FE modeling of concrete requires the use of an accurate constitutive model for the concrete. Many different constitutive models have been proposed for the analytical and FE modeling of concrete. These constitutive models include plasticity models (e.g. [10.11]) and plastic-damage models (e.g. [12.13]). Although some of the models [12.13] include damaged elasticity, a concrete plasticity model is common to all these constitutive models.

FE results are in good agreement with test results in terms of overall responses such as axial stress-strain curves, such good agreement provides only the necessary but not sufficient evidence for the accuracy and reliability of a constitutive model. A plasticity hardening/softening rule and the flow rule, which all affect its performance in predicting the behavior of concrete.

Concrete strength determined in simple states of stress (uniaxial compression or tension) radically differs from the one determined in complex states of stress. For example, the same concrete under biaxial compression reaches strength of between ten and twenty per cent higher than in the uniaxial state while in the hydro-static state (uniform triaxial compression) its strength is theoretically unlimited. In order to describe strength with the equation for triaxial stress, its plane should be presented in a three-dimensional stress space (since concrete is considered to be an isotropic material in a wide range of stress). The states of stress corresponding to material failure are on this surface while the states of safe behaviour are inside. Also, the so-called plastic potential surface is located inside this space. After the plasticity surface is crossed, two situations arise:

- an increase in strain with no change in stress (ideal plasticity),
- material weakening (rupture).

3.2. Plasticity Models:

Concrete plasticity models are generally based on the same framework of plasticity theory for metals, but with necessary modifications to include the unique properties of concrete. The key aspects of a plasticity model include the yield surface (including the initial and subsequent yield surfaces), the flow rule, and the hardening/softening rule. The initial yield surface determines when plastic deformation begins; the flow rule determines the direction of plastic deformation; and the hardening/softening rule defines how the yield surface evolves with plastic deformation.

Many yield functions have been proposed for concrete. The number of parameters included in these functions' ranges from one (e.g. Von Mises criterion originally developed for metals) to five [14]. Among these yield functions, the Drucker-Prager (D_P) criterion has been widely adopted for the modelling of confined concrete (e.g. [15.16.17]) because of its simplicity (involving only two parameters) and its capability to capture shear strength increases as a result of hydrostatic pressure increases, which is a unique property of concrete under confinement. The difference between the D_P yield criterion and pressure-insensitive criteria (e.g. Von Mises criterion) [14] is obvious in the $I1$-$\sqrt{J}2$ plane of the stress space (Figure.3.2). The latter is a line parallel to the abscissa while the former is an inclined line.

All D_P type models adopted for concrete are within the theoretical framework of the Extended Drucker-Prager Model of ABAQUS.

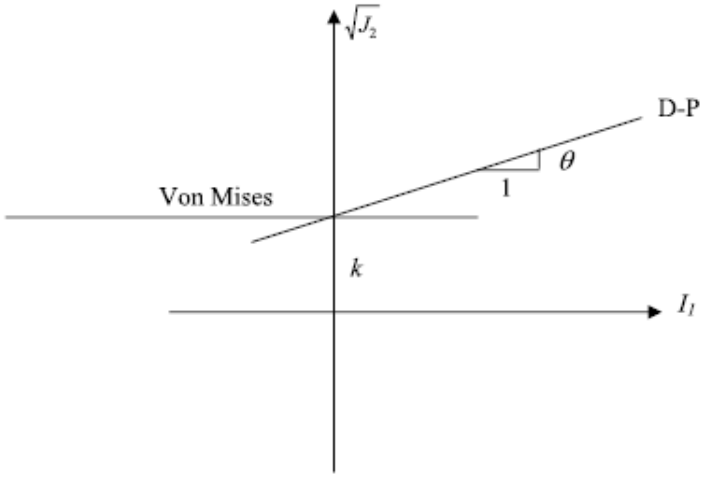

Figure.3.2. Drucker-Prager Yield Surface in I1 − $\sqrt{J2}$

3.3. Drucker-Prager Model

One of the strength hypotheses most often applied to concrete is the Drucker Prager hypothesis (1952). The Drucker-Prager yield criterion is a smooth approximation of the Mohr-Coulomb surface and expressed as a simple modification of the von Mises yield criterion (Chen, 2007) [18]. This yield criterion is capable of capturing the shear strength increase as a result of the hydrostatic pressure increases, which is a unique property of the confined concrete (Yu et al., 2010) [19]. Hence, this has meant that the Drucker-Prager model has been widely used for finite element simulation of confined concrete in many research studies (Ellobody and Young [20], 2006, Mirmiran et al., 2000 [20], Hu et al., 2003 [21], Yu et al., 2010 [18]). In this investigation, the concrete is confined by the steel tube and the failure of the concrete is dominated by the compressive failure surface expanding with increasing hydrostatic pressure. The Drucker-Prager model, therefore, is a reasonable choice for finite element simulation of confined concrete of CFST columns (Hu et al., 2003) [22].

Three types of yield surface associated with the Drucker-Prager model are available in ABAQUS, those being linear, hyperbolic, or general exponent. Figure 3.3 shows these three yield surfaces. Selection of one of these models depends on several factors such as the availability of the experimental data for calibration, type of analysis, the kind of material, and the range of stress values that the material would experience. For instance, for the cases where the stresses are mostly compressive, the linear model would be a better choice.

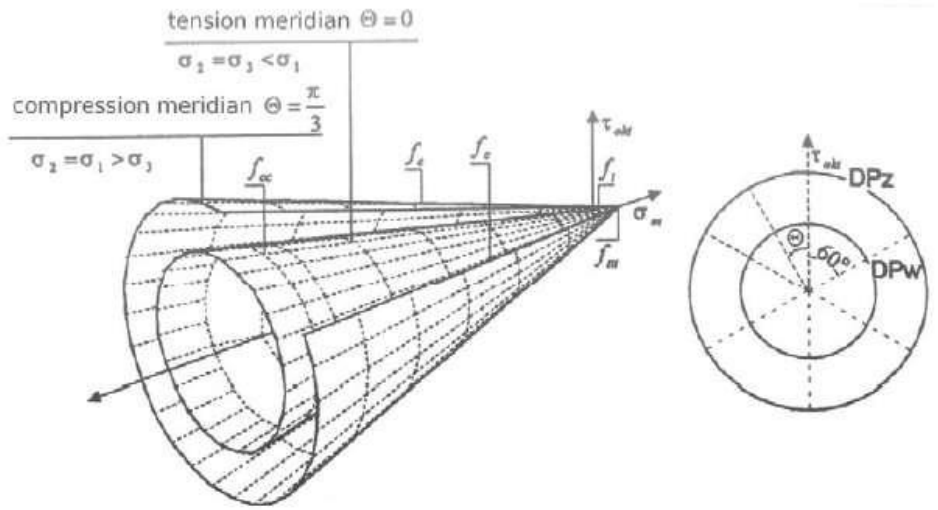

Figure.3.3 Drucker–Prager Boundary Surface: A) View, B) Deviatory Cross Section.

The Drucker-Prager hyperbolic function is accepted in the form:

$$G = \sqrt{(\mathrm{fc} - \mathrm{m.ft}\,.\tan\beta)^2 + \bar{\mathrm{q}}^2} - \bar{\mathrm{p}}.\tan\beta - \sigma \qquad (6)$$

Where ft and fc are the uniaxial tensile and compressive strengths of concrete, respectively. β is the dilation angle measured in the *p-q* plane at high confining pressure, while *m* is an eccentricity of the plastic potential surface. The flow potential surface is defined in the *p-q* plane, where $\bar{p} = -\frac{1}{3}\bar{\sigma}$. *I* is the effective.

Hydrostatic stress and $\bar{q} = \sqrt{\frac{3}{2}\bar{S}.\bar{S}}$ is the Misses equivalent effective stress, while $\bar{S}$ is the deviatoric part of the effective stress tensor $\bar{\sigma}$.

The no associative flow rule, which is used here, requires a loading surface definition. The plastic-damage concrete model uses a yield condition based on the loading function (7) proposed by Lubliner in [23] in the form:

$$F = \frac{1}{1-\alpha}(\bar{q} - 3.\alpha.\bar{p} + (\tilde{\varepsilon})\langle\bar{\sigma}max\rangle - \gamma\langle-\bar{\sigma}max\rangle) - \bar{\sigma}c\,(\tilde{\varepsilon}^{pl}) \qquad (7)$$

The shape of loading surface in the deviatoric plane is determined by parameter $\boldsymbol{\gamma}$, while the parameter α is calculated based on Kupfer's curve. $\bar{\sigma}max$ is the algebraically maximum eigenvalue of $\bar{\sigma}$. The Macauley bracket is defined by

$\langle x \rangle = \frac{1}{2}(|x| + x)$.

The function $\theta\ (\varepsilon\tilde{p}\ l)$ is given as:

$$\theta\ (\varepsilon\tilde{p}\ l) = \frac{\bar{\sigma}c(\tilde{\varepsilon}c^{pl})}{\bar{\sigma}t((\varepsilon\tilde{}t^{pl})}(1\ -\ \alpha)\ -\ (1\ +\ \alpha) \tag{8}$$

Where $\bar{\sigma c}$ and $\bar{\sigma t}$ are the effective tensile and compressive cohesion stresses, respectively. It is necessary to definite the parameter:

$$\alpha = \frac{(\mathrm{fb0}/\mathrm{fc})-1}{2(\mathrm{fb0}/\mathrm{fc})-1} \tag{9}$$

The compressive strength under biaxial loading of concrete is denoted by $fb0$. The parameter $\boldsymbol{\gamma}$ should be defined based on the full triaxle tests of concrete. Identification of that parameter is possible only if the full triaxle compression tests of concrete are done. In accordance to [23] the parameter $\boldsymbol{\gamma}$ is prescribed in the form:

$$\gamma = \frac{3(1-\rho)}{2\rho+3} \tag{10}$$

where the coefficient:

$$\rho = \frac{(\sqrt{J2}\,)\mathrm{TM}}{(\sqrt{J2})TC} \tag{11}$$

is defined at a given state p.

$J2$ is the second invariant of stress deviator for *TM* and *CM* subscribes.

3.4. Concrete Damaged Plasticity Model

The CDP (Concrete Damaged Plasticity) model used in the ABAQUS software is a modification of the Drucker–Prager strength hypothesis. In recent years the latter has been further modified by Lubliner, Lee and Fenves. According to the modifications, the failure surface in the deviatoric cross section needs not to be a circle and it is governed by parameter *Kc*.

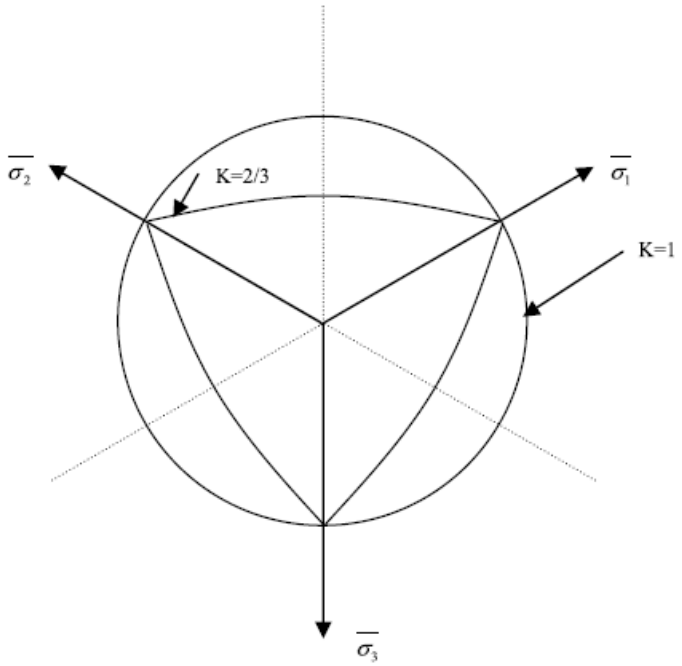

Figure.3.4. Failure Surfaces in The Deviatoric Plane.

Physically, parameter *Kc* is interpreted as a ratio of the distances between the hydrostatic axis and respectively the compression meridian and the tension meridian in the deviatoric cross section. This ratio is always higher than 0.5 and when it assumes the value of 1, the deviatoric cross section of the failure surface becomes a circle (as in the classic Drucker–Prager strength hypothesis). Majewski reports that according to experimental results this value for mean normal stress equal to zero amounts to 0.6 and slowly increases with decreasing mean stress. The CDP model recommends to assume *Kc* = 2/3.

It is a theoretical-experimental criterion based on triaxle stress test results. Similarly, the shape of the plane's meridians in the stress space changes. Experimental results indicate that the meridians are curves. In the CDP model the plastic potential surface in the meridional plane assumes the form of a hyperbola. The shape is adjusted through eccentricity (plastic potential eccentricity). It is a small positive value which expresses the rate of approach of the plastic potential hyperbola to its asymptote. In other words, it is the length (measured along the hydrostatic axis) of the segment between the vertex of the hyperbola and the intersection of the asymptotes of this hyperbola (the centre of the hyperbola). Parameter *eccentricity* can be calculated as a ratio of tensile strength to compressive strength [24]. The CDP model recommends to assume $\boldsymbol{\varepsilon} = 0.1$. When $\boldsymbol{\varepsilon} = 0$, the surface in the meridional plane becomes a straight line (the classic Drucker-Prager hypothesis).

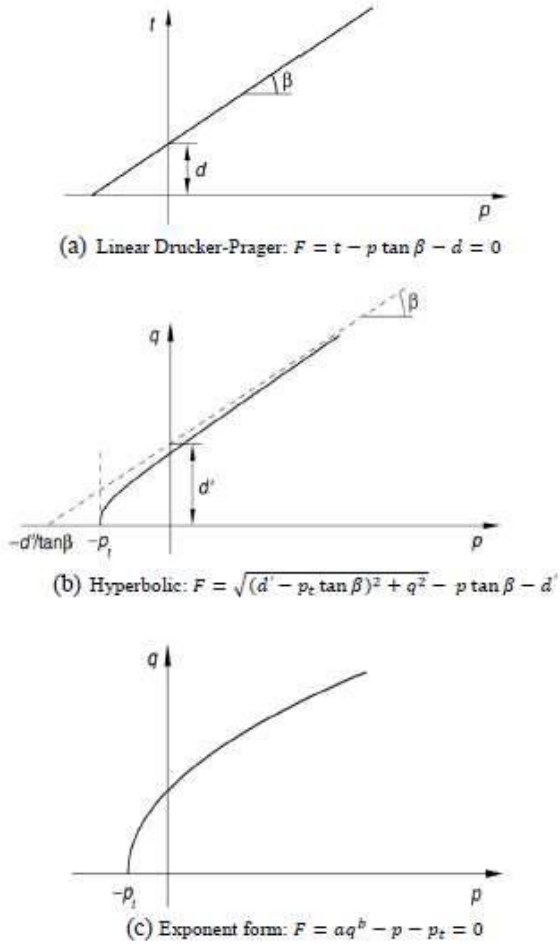

Figure 3.5 Yield Surfaces in the Meridional Plane of Drucker-Prager Model (ABAQUS, 2012).

Another parameter describing the state of the material is the point in which the concrete undergoes failure under biaxial compression. *σb0/σc0 (fb0 / fc0)* is a ratio of the strength in the biaxial state to the strength in the uniaxial state. After their approximation with the elliptic equation, uniform biaxial compression strength fcc *is* equal to 1.16248 *fc0*. The ABAQUS user's manual specifies default

σb0/σc0 = 1.16.

The last parameter characterizing the performance of concrete under compound stress is dilation angle, i.e. the angle of inclination of the failure surface towards the hydrostatic axis, measured in the meridional plane. Physically, dilation angle ψ is interpreted as a concrete internal friction angle. In simulations usually

ψ = 36° or ψ = 40° 0 is assumed.

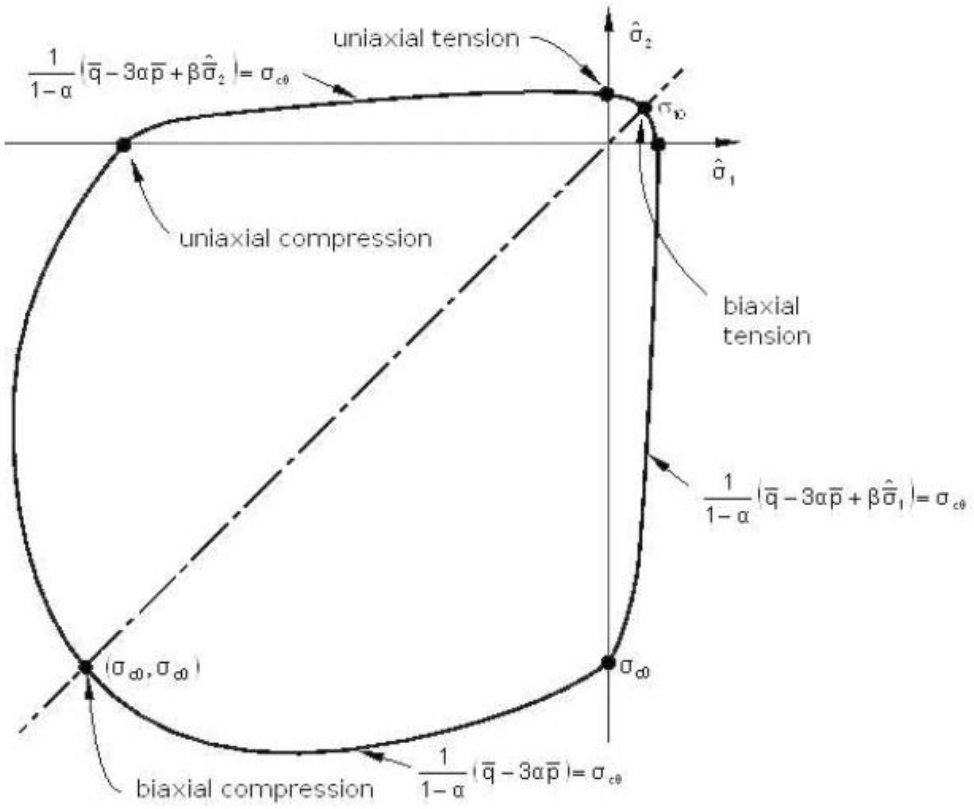

Figure.3.6 Strength of Concrete Under Biaxial Stress in CDP Model

Parameter name	Value
Dilatation angle	36
Eccentricity	0.1
f_{bo}/f_{co}	1.16
κ	0.667
Viscosity parameter	0

Table 3.1 Default Parameters of CDP Model Under Compound Stress

The unquestionable advantage of the CDP model is the fact that it is based on parameters having an explicit physical interpretation. The exact role of the above parameters and the mathematical methods used to describe the development of the boundary surface in the three-dimensional space of stresses are explained in the ABAQUS user's manual. The other parameters describing the performance of concrete are determined for uniaxial stress. Table 3.1 shows the model's parameters characterizing its performance under compound stress.

4. Stress-Strain Curves of Concrete

4.1. Stress-Strain Curve for Uniaxial Compression

The stress-strain relation for a given concrete can be most accurately described on the basis of uniaxial compression tests carried out on it. Having obtained a graph from laboratory tests one should transform the variables. Inelastic strains $\tilde{\varepsilon}c^{in}$ are used in the CDP model. In order to determine them one should deduct the elastic part (corresponding to the undamaged material) from the total strains registered in the uniaxial compression test:

$$\tilde{\varepsilon}c^{in} = \varepsilon c - \varepsilon 0c^{el} \tag{12}$$

$$\varepsilon 0c^{el} = \frac{\sigma c}{E0} \tag{13}$$

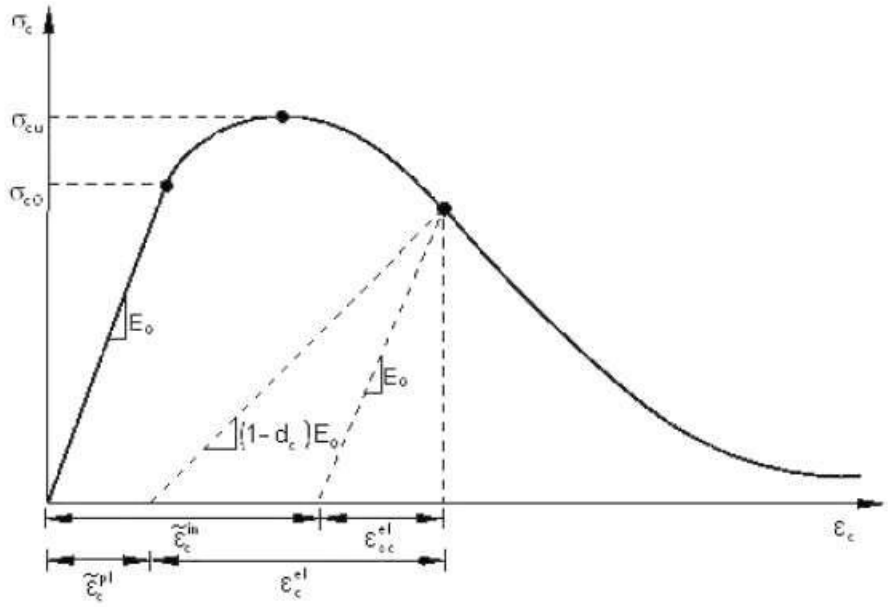

Figure 3.7 Definition of Inelastic Strains.

When transforming strains, one should consider from what moment the material should be defined as nonlinearly elastic. Although uniaxial tests show that such behaviour occurs almost from the beginning of the compression process, for most numerical analyses it can be neglected in the initial stage. According to Majewski [25], a linear elasticity limit should increase with concrete strength and it should be rather assumed than experimentally determined. He calculated it as a percentage of stress to concrete strength from this formula:

$$elim = 1 - exp\left(\frac{-fc}{80}\right) \tag{14}$$

This ceiling can be simply arbitrarily assumed as 0.4 *fcm*. Eurocode 2 [26] specifies the modulus of elasticity for concrete to be secant in a range of 0-0.4 *fcm*. Since the basic definition of the material already covers the shear modulus and the longitudinal modulus of concrete, at this stage it is good to assume such an inelastic phase threshold that the initial value of Young's modulus and the secant value determined according to the standard will be convergent. In most numerical analyses it is rather not the initial behaviour of the material, but the stage in which it reaches its yield strength which is investigated. Thanks to the level of 0.4·*fcm* there are fewer problems with solution convergence.

Having defined the yield stress-inelastic strain pair of variables, one needs to define now degradation variable *dc*. It ranges from zero for an undamaged material to one for the total loss of load-bearing capacity. These values can also be obtained from uniaxial compression tests, by calculating the ratio of the stress for the declining part of the curve to the compressive strength of the concrete. Thanks to the above definition the CDP model allows one to calculate plastic strain from the formula:

$$\tilde{\varepsilon}c^{pl} = \tilde{\varepsilon}c^{pl} - \frac{\mathrm{dc}}{(1-\mathrm{dc})}\frac{\sigma\mathrm{c}}{\mathrm{E0}} \tag{15}$$

Where *E0* stands for the initial modulus of elasticity for the undamaged material. Knowing the plastic strain and having determined the flow and failure surface area one can calculate stress $\boldsymbol{\sigma}$c for uniaxial compression and its effective stress$\bar{\sigma}c$:

$$\sigma c = (1 - \ )0(\varepsilon c - \tilde{\varepsilon}c^{pl}) \tag{16}$$

$$\bar{\sigma}\mathrm{c} = \frac{\sigma\mathrm{c}}{(1-\mathrm{dc})} = \mathrm{E0}(\varepsilon\mathrm{c} - \tilde{\varepsilon}c^{pl}) \tag{17}$$

4.2. Plotting Stress-Strain Curve Without Detailed Laboratory Test Results

On the basis of uniaxial compression test results one can accurately determine the way in which the material behaved. However, often the only available quantity is the average compressive strength (fcm) of the concrete. Another quantity which must be known in order to begin an analysis of the stress-strain curve is the longitudinal modulus of elasticity (Ecm) of the concrete. Its value can be calculated using the relations available in the literature:

$$Ecm = 22(0.01fcm)^{0.3} \quad (18)$$

Where:

fcm [MPa], Ecm [GPa].

Other values defining the location of characteristic points on the graph are strain $\boldsymbol{\varepsilon}$cl at average compressive strength and ultimate strain $\boldsymbol{\varepsilon}$cu:

$$\varepsilon cl = 0.7(fcm)^{0.31} \quad (19)$$

$$\varepsilon cu = 3.5\%0 \quad (20)$$

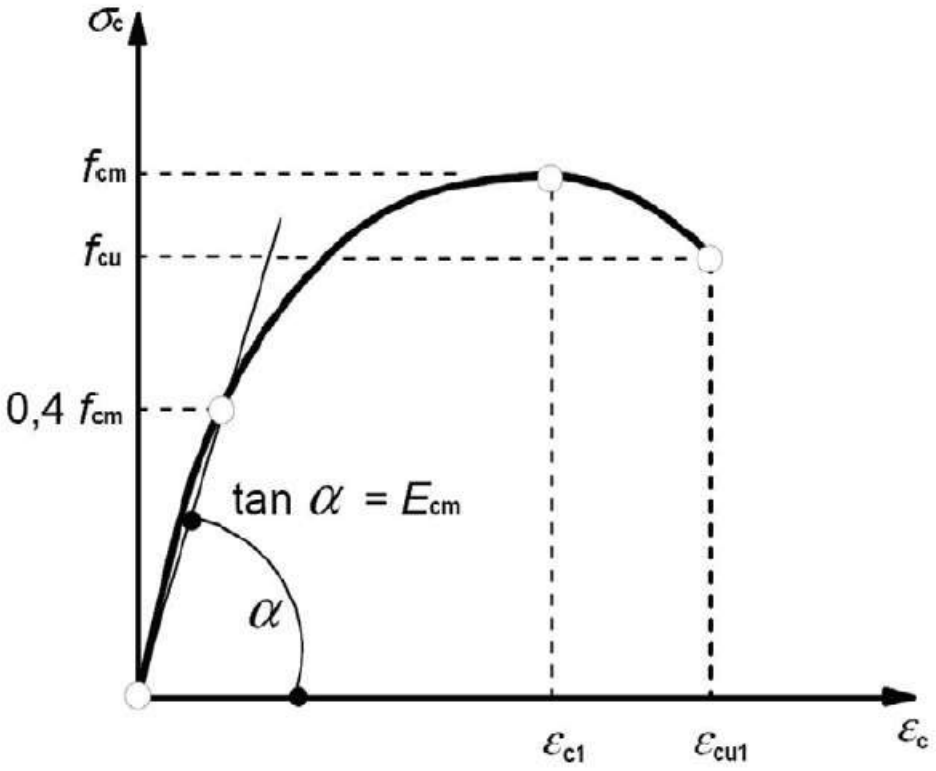

Figure 3.8 Stress-Strain Diagram for Analysis of Structures, According to Eurocode 2

The curve can be also plotted on the basis of the literature. The most popular formulas are presented in Table 3.2. The original symbols have been replaced with the uniform denotations used in Eurocode 2 [26].

Choosing a proper formula form to describe relation $\boldsymbol{\sigma}$c-$\boldsymbol{\varepsilon}$c one should note whether the longitudinal modulus of elasticity represents initial value *Ec* (at stress $\boldsymbol{\sigma}c$= 0) or that of secant modulus *Ecm*. Most of the formulas use initial modulus *Ec* which is neither experimentally determined nor taken from the standards. Another important factor is the functional dependence itself. Even though the Madrid parabola has been recognized as a good relation by CEB (Comité

Euro-International du Béton), this function is not flexible enough to correctly describe the performance of concrete.

Formula name/ source	Formula form	Variables
Madrid parabola	$\sigma_c = E_c\varepsilon_c\left[1-\frac{1}{2}\left(\frac{\varepsilon_c}{\varepsilon_{c1}}\right)\right]$	$\sigma_c = f(E_c, \varepsilon_{c1})$
Desay & Krishnan formula	$\sigma_c = \frac{E_c\varepsilon_c}{1+\left(\frac{\varepsilon_c}{\varepsilon_{c1}}\right)^2}$	$\sigma_c = f(E_c, \varepsilon_{c1})$
EN 1992-1-1	$\sigma_c = f_{cm}\frac{k\eta-\eta^2}{1+(k-2)\eta}$ $k = 1.05E_{cm}\frac{\varepsilon_{c1}}{f_{cm}}, \quad \eta = \frac{\varepsilon_c}{\varepsilon_{c1}}$	$\sigma_c = f(E_{cm}, f_{cm}, \varepsilon_{c1})$
Majewski formula	$\sigma_c = E_c\varepsilon_c$ if $\sigma_c \le e_{lim}f_{cm}$ $\sigma_c = f_{cm}\frac{(e_{lim}-2)^2}{4(e_{lim}-1)}\left(\frac{\varepsilon_c}{\varepsilon_{c1}}\right)^2 + -f_{cm}\frac{(e_{lim}-2)^2}{2(e_{lim}-1)}\left(\frac{\varepsilon_c}{\varepsilon_{c1}}\right)+f_{cm}\frac{e_{lim}^2}{4(e_{lim}-1)}$ $E_c = \frac{f_{cm}}{\varepsilon_c}(2-e_{lim})$, if $\sigma_c > e_{lim}f_{cm}$ e_{lim} in formula (3)	$\sigma_c = f(E_c, f_{cm}, \varepsilon_{c1})$
Wang & Hsu formula	$\sigma_c = \zeta f_{cm}\left[2\left(\frac{\varepsilon_c}{\zeta\varepsilon_{c1}}\right)-\left(\frac{\varepsilon_c}{\zeta\varepsilon_{c1}}\right)^2\right]$ if $\frac{\varepsilon_c}{\zeta\varepsilon_{c1}} \le 1$ $\sigma_c = \zeta f_{cm}\left[1-\left(\frac{\varepsilon_c/\zeta\varepsilon_{c1}-1}{2/\zeta-1}\right)^2\right]$ if $\frac{\varepsilon_c}{\zeta\varepsilon_{c1}} > 1$	$\sigma_c = f(f_{cm}, \varepsilon_{c1})$
Sáenz formula	$\sigma_c = \frac{\varepsilon_c}{A+B\varepsilon_c+C\varepsilon_c^2+D\varepsilon_c^3}$ symbols in formula (12)	$\sigma_c = f\begin{pmatrix}E_c, f_{cm}, f_{cu},\\ \varepsilon_{c1}, \varepsilon_{cu1}\end{pmatrix}$

Table 3.2 Stress-Strain Relation for Nonlinear Behaviour of Structure

4.3. Stress-Strain Curve for Uniaxial Tension

The tensile strength of concrete under uniaxial stress is seldom determined through a direct tension test because of the difficulties involved in its execution and the large scatter of the results. Indirect methods, such as sample splitting or beam bending, tend to be used [26]:

$$fcm = 0.30fck^{(2/3)} \tag{21}$$

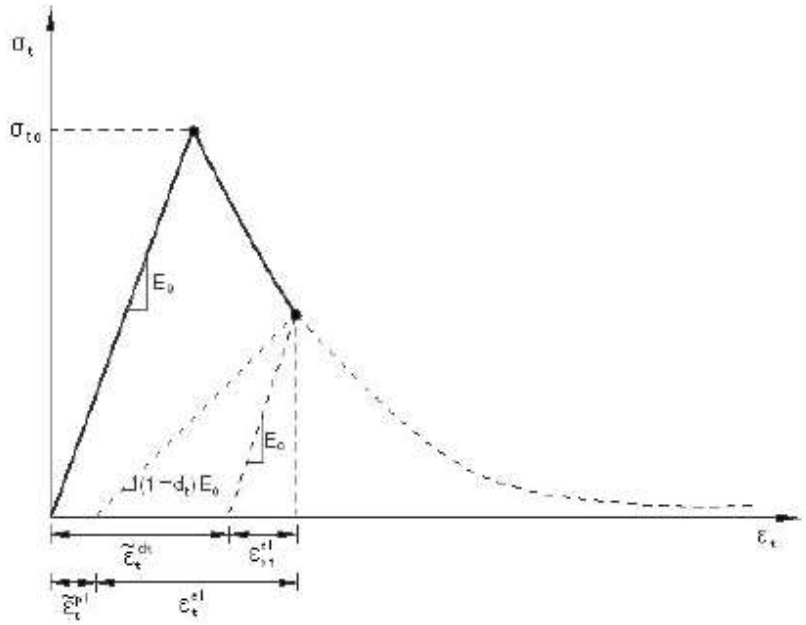

Figure 3.9 Definition of Strain After Cracking – Tension Stiffening

The term cracking strain $\tilde{\varepsilon}t^{\mathbf{ck}}$ is used in CDP model numerical analyses. The aim is to take into account the phenomenon called tension stiffening. Concrete under tension is not regarded as a brittle elastic body and such phenomena as aggregate interlocking in a crack and concrete-to-steel adhesion between cracks are taken into account. This assumption is valid when the pattern of cracks is fuzzy. Then stress in the tensioned zone does not decrease sharply but gradually. The strain after cracking is defined as the difference between the total strain and the elastic strain for the undamaged material:

$$\varepsilon t^{ck} = \varepsilon t - \varepsilon 0 t^{el} \tag{22}$$

$$\varepsilon 0 t^{el} = \frac{\varepsilon t}{\mathrm{Ec}} \tag{23}$$

Plastic strain εt^{pl} is calculated similarly as in the case of compression after defining degradation parameter dt.

In order to plot curve $\boldsymbol{\sigma}$t-$\boldsymbol{\varepsilon}$t one should define the form of the weakening function.

According to the ABAQUS user's manual, stress can be linearly reduced to zero, starting from the moment of reaching the tensile strength for the total strain ten times higher than at the moment of reaching *f*ctm. But to accurately describe this function the model needs to be calibrated with the results predicted for a specific analysed case.

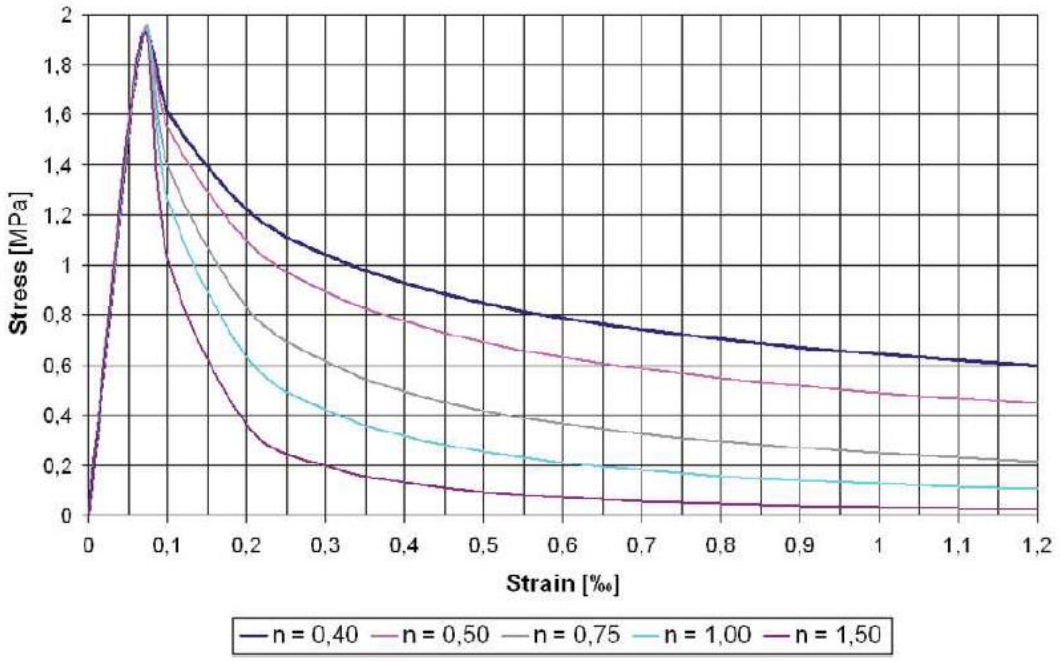

Figure 3.10 Modified Wang & Hsu Formula for Weakening Function at Tension Stiffening for Concrete C16/20.

The proper relation was proposed by, among others, Wang and Hsu [27]:

$$\sigma t = Ec * \varepsilon t \text{ if } \varepsilon t \leq \varepsilon cr$$
$$\sigma t = fcm * (\frac{\varepsilon cr}{\varepsilon t})^{0.4} \text{ if } \boldsymbol{\varepsilon} t > \boldsymbol{\varepsilon} cr \quad (24)$$

Where εcr stands for strain at concrete cracking. Since tension stiffening may considerably affect the results of the analysis and the relation needs calibrating for a given simulation, it is proposed to use the modified Wang & Hsu [19] formula for the weakening function:

$$\sigma t = fcm\ (\frac{\varepsilon cr}{\varepsilon t})^{n} \quad (25)$$

Where n represents the rate of weakening.

CHAPTER IV : FE MODELING

1. Introduction

The finite element method (FEM) is the most widely used method for solving problems of engineering and mathematical models. Typical problem areas of interest include the traditional fields of structural analysis, heat transfer, fluid flow, mass transport, and electromagnetic potential. The FEM is a particular numerical method for solving partial differential equations in two or three space variables (i.e., some boundary value problems). To solve a problem, the FEM subdivides a large system into smaller, simpler parts that are called finite elements. This is achieved by a particular space discretisation in the space dimensions, which is implemented by the construction of a mesh of the object: the numerical domain for the solution, which has a finite number of points. The finite element method formulation of a boundary value problem finally results in a system of algebraic equations. The method approximates the unknown function over the domain. The simple equations that model these finite elements are then assembled into a larger system of equations that models the entire problem. The FEM then uses variational methods from the calculus of variations to approximate a solution by minimizing an associated error function.

2. Finite Element Modelling

2.1. Introduction to Abaqus

The multipurpose finite element software package ABAQUS is a software application for finite element analysis and computer-aided engineering, originally released in 1978. It is a powerful engineering simulation program, based on the finite element method, which can solve problems ranging from relatively simple linear analyses to the most challenging nonlinear simulations. ABAQUS contains an extensive library of elements that can model virtually any geometry. Furthermore, it is a program that having the ability to consider geometric, material and contact nonlinearities in a given model, and merging these nonlinearities together in the same analysis.

ABAQUS has also an extensive list of material models that can simulate the behavior of most typical engineering materials including metals, rubber, polymers, composites, reinforced concrete, crushable and resilient foams, and geotechnical materials such as soils and rock. Designed as a general-purpose simulation tool, ABAQUS can be used to study more than just structural (stress/displacement) problems. It can simulate problems in such diverse areas as heat transfer, mass diffusion, thermal management of electrical components (coupled thermal-electrical analyses), acoustics, soil mechanics (coupled pore fluid-stress analyses), and piezoelectric analysis.

ABAQUS is simple to use and offers the user a wide range of capabilities to visualize results. Even the most complicated analyses can be modelled easily. It has the ability to treat

advanced analysis that may rise in a given structural system: the geometric and material non linearity, cycling loadings, dynamic analysis etc. For example, problems with multiple components are modelled by associating the geometry defining each component with the appropriate material models. In most simulations, including highly nonlinear ones, the user need only provide the engineering data such as the geometry of the structure, its material behavior, its boundary conditions, and the loads applied to it.

In a nonlinear analysis ABAQUS automatically chooses appropriate load increments and convergence tolerances. Not only does it choose the values for these parameters, it also continually adjusts them during the analysis to ensure that an accurate solution is obtained efficiently. The user rarely has to define parameters for controlling the numerical solution of the problem.

The commercial multipurpose finite element software package ABAQUS standard (Version-6.14-1) [28] is employed in this research.

2.2. Abaqus Applications Capabilities

• ABAQUS/Standard is a general-purpose, finite element module: ABAQUS/Standard employs solution technology ideal for static and low-speed dynamic events where highly accurate stress solutions are critically important. Within a single simulation, it is possible to analyses a model both in the time and frequency domain.

• ABAQUS/Explicit is an explicit dynamics finite element module: it is a finite element analysis product that is particularly well-suited to simulate brief transient dynamic events such as consumer electronics drop testing, automotive crashworthiness, and ballistic impact. The ability of ABAQUS/Explicit to effectively handle severely nonlinear behaviour such as contact makes it very attractive for the simulation of many quasi-static events.

2.3. Organization of Abaqus

1) Abaqus Modules Part Module:

This module allows the user to create the geometry required for the problem. To create a 3-D geometry the user first creates a 2-D profile and then manipulate it to obtain the solid geometry.

• PROPERTY MODULE: In this module the user defines the material properties for the analysis and assign those properties to the available parts.

• Assembly Module: This module allows to assemble together parts that have created. Even if the model has a single part, one need to include it in your assembly.

• INTERACTION MODULE: This module allows to relay different part by Tie, embedded region, Rigid body… etc.

• STEP MODULE: This module allows the user to select the kind of analysis to perform and define the parameters associated with it. One can also select which variables to include in the output files in this module. To apply a sequence of loads, one must create several steps and define the loads for each of them.

• LOAD MODULE: The Load Module is where the user defines the loads and boundary conditions for the model for a particular step. One can even define loads and boundary conditions as fields like electric potential, acoustic pressure, etc.

• MESH MODULE: The mesh module controls how to mesh the model: the type of element, their size… etc.

• JOB MODULE: This module allows to submit the model for analysis.

• VISUALIZATION MODULE: This module allows to look at the model after deformation. One can also plot values of stress, displacement, reaction forces… etc as contours on the model surface or as vectors or tensors.

2) Element Type in Abaqus

There are various kinds of element types in ABAQUS. Each element can be differed by family, number of nodes, and Degrees of freedom.

• Family: solid (Continuum), shell, membrane, rigid, beam, truss elements, etc.

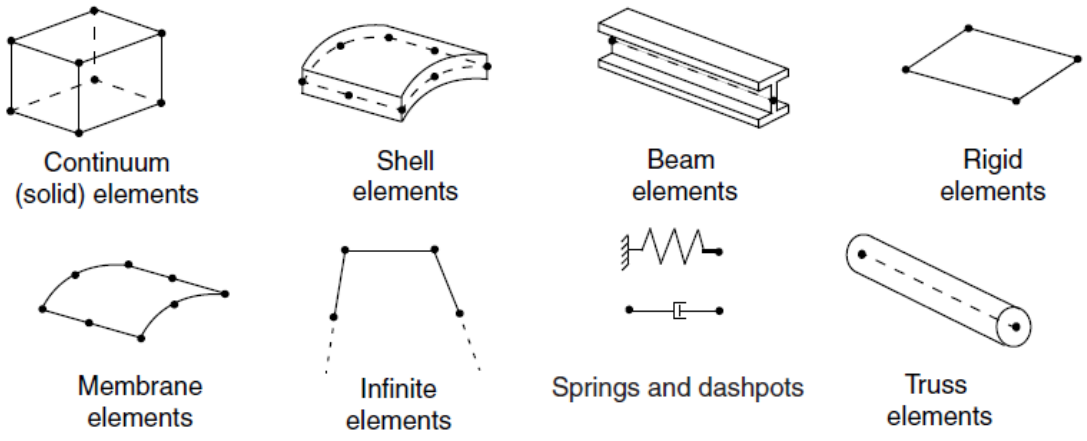

Figure 4.1 Family of Element in ABAQUS

• Number of nodes—order of interpolation

Displacements, rotations, temperatures, and the other degrees of freedom mentioned in the previous section is calculated only at the nodes of the element. At any other point in the element,

the displacements are obtained by interpolating from the nodal displacements. Usually the interpolation order is determined by the number of nodes used in the element.

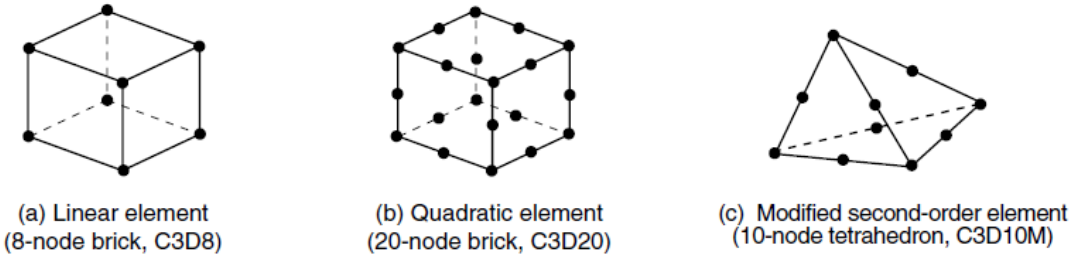

Figure 4.2 Linear Brick, Quadratic Brick, and Modified Tetrahedral Elements.

• Degrees of freedom

1 Translation towards 1

2 Translations towards 2

3 Translation directions 3

4 rotations around the axis 1

5 rotations around the axis 2

6 rotations around the axis 3

7 buckling in beams elements to open profile

8 Sound pressure, pore pressure, or hydrostatic pressure

9 Electrical potential

10 Temperatures

Directions 1, 2 and 3 correspond to the global directions 1, 2 and 3, respectively; unless a local coordinate system has been defined at the nodes.

Axisymmetric elements exceptionally, the degrees of freedom of movement along and rotation:

1 Translation direction r

2 Translation in the z direction

6 Rotation around the r-z plane

r directions (radial) and z (axial) correspond to the global directions 1 and 2, respectively, unless a local coordinate system has been defined at the nodes.

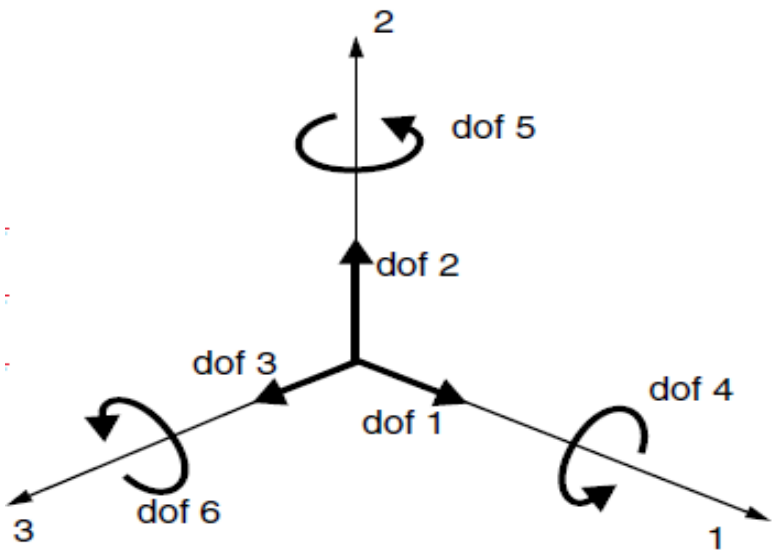

Figure 4.3 Displacement and Rotational Degrees of Freedom

2.4. Element Shapes in Abaqus

There are various kinds of element shapes in ABAQUS:

• Quad: Use exclusively quadrilateral elements.

• Quad-dominated: Use primarily quadrilateral elements, but allow triangles in transition regions. This setting is the default.

• Tri: Use exclusively triangular elements.

• Hex: Use exclusively hexahedral elements. This setting is the default.

• Hex-dominated: Use primarily hexahedral elements, but allow some triangular prisms (wedges) in transition regions.

• Tet: Use exclusively tetrahedral elements.

• Wedge: Use exclusively wedges elements.

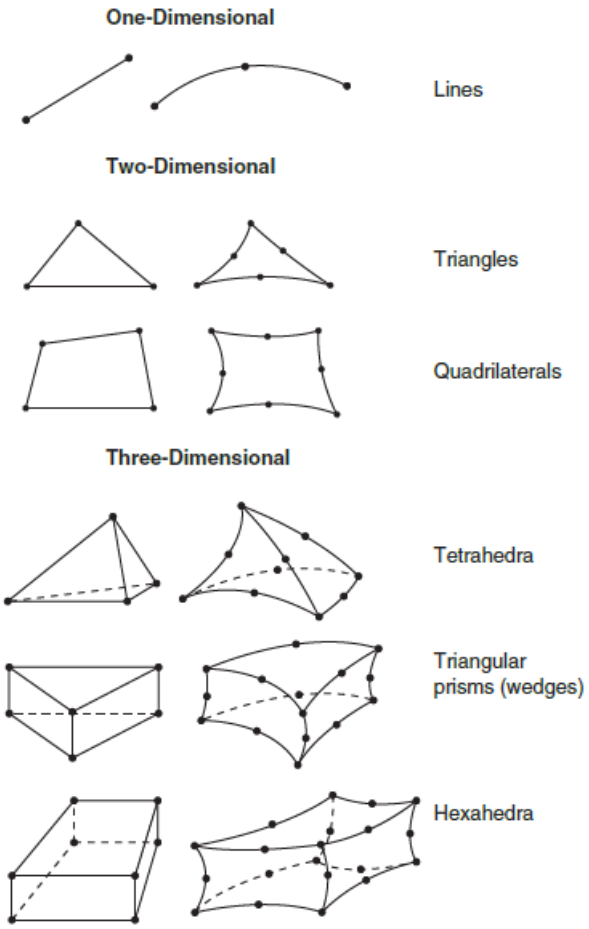

Figure 4.4 Element Shapes in ABAQUS.

3. Finite Element Modeling

This section shows the details of the finite element modeling using ABAQUS standard (Version-6.14-1) [28] to simulate the behavior of push out test.

3.1. Description of Specimens

1) Study on Channel Shear

Push-out specimens consist of a rolled steel IPB270 profile with two channel shear connectors attached to each flange. These channel shear connectors are embedded in 150 thickness for each slab. 250wide,300mm long, concrete blocks. The channel connector with 100mm depth and a web and flange thickness of 6 and 8.5 mm, respectively. Each specimen was reinforced longitudinally and transversely with four 10 mm diameter bars positioned in two layers for each concrete slab.

2) **Study on I-Shape Connector**

A push-out specimen consists of two small concrete slabs held in the vertical position, and attached to the flanges of a short IPB 270 steel beam of 360 mm long, by means of welded

I-shape shear connectors. The dimensions of concrete slabs were 360 mm long, 320 mm wide, and 120 mm thickness for each slab. The I shear connector with 80 mm depth and a web and flange thickness of 8 and 3.8mm, respectively. Each specimen was reinforced longitudinally and transversely with four 10 mm diameter bars positioned in two layers for each concrete slab.

3.2. Parts of the Model

a) Shear connector

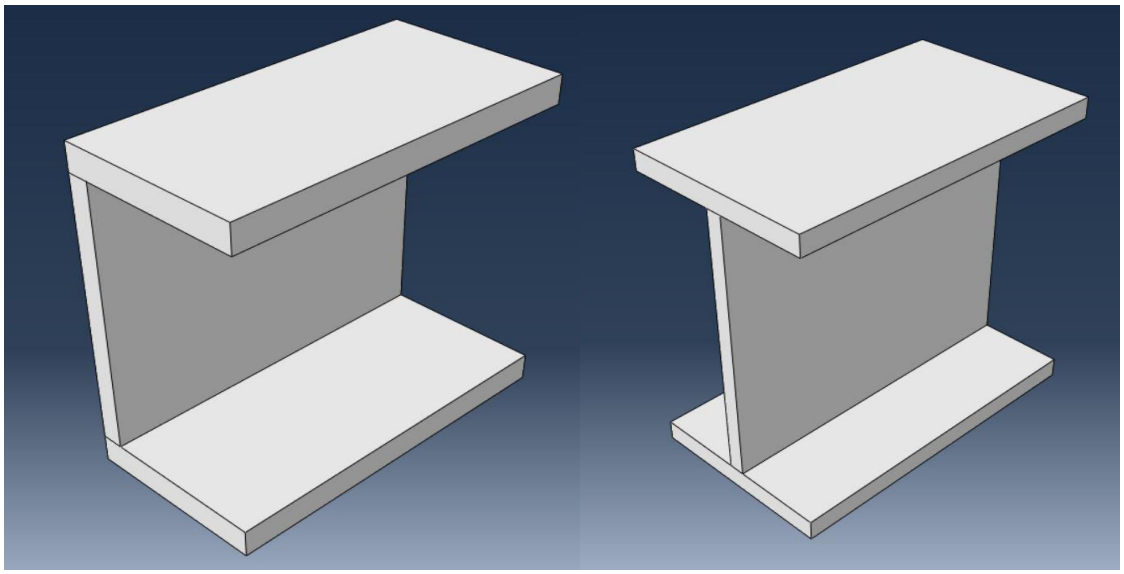

Figure 4.5 The Geometrical Shape of Shear Connector.

b) Concrete fill

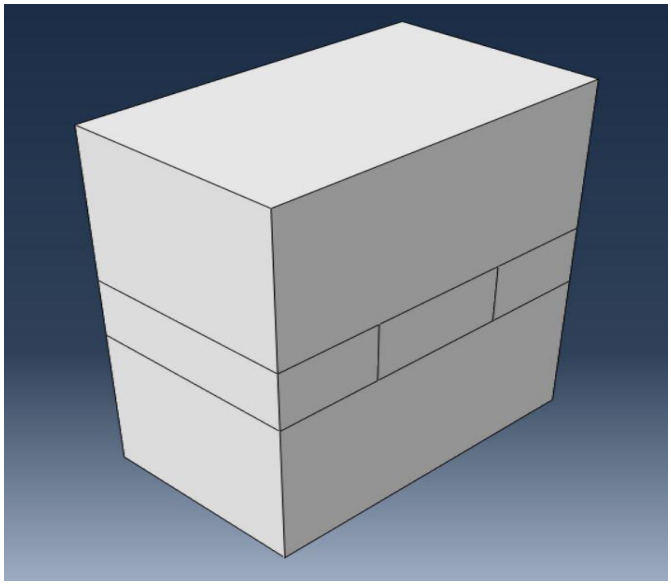

Figure 4.6 The Geometrical Shape of Concrete Filled.

c) Steel beam

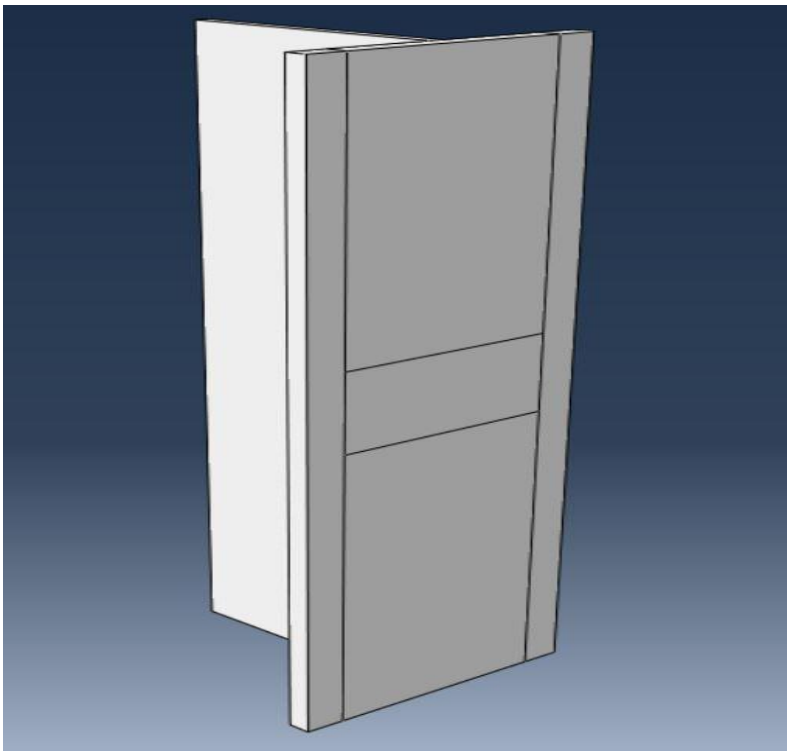

Figure 4.7 The Geometrical Shape of Steel Beam.

d) Rigid plate

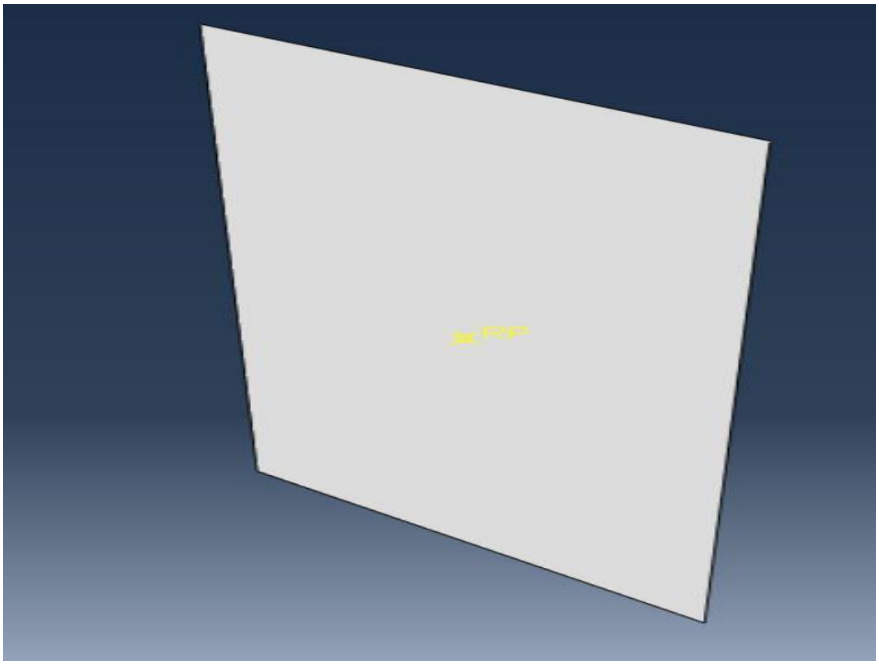

Figure 4.8 The Geometrical Shape of the Plate that's Placed at the End of the Concrete.

e) Bars

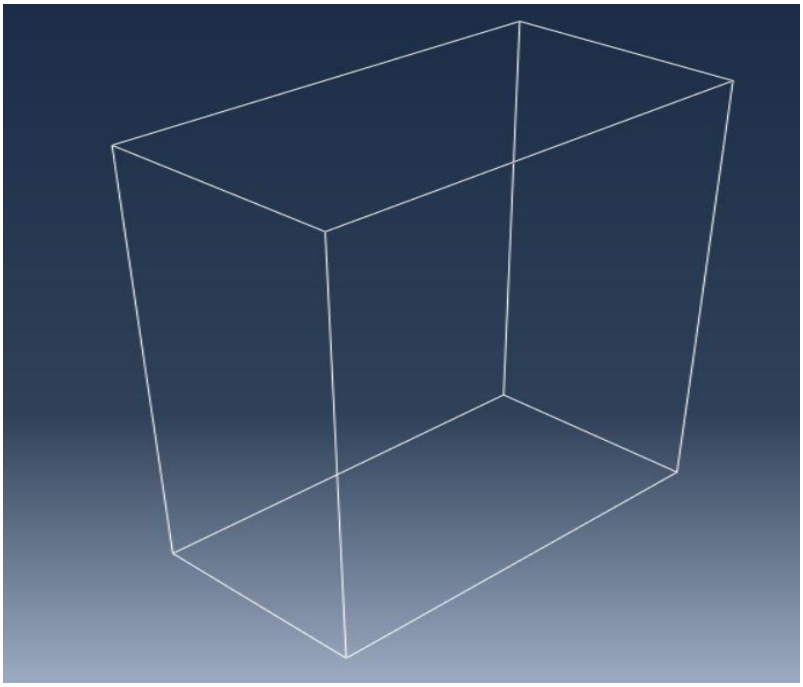

Figure 4.9 The Geometrical Shape of the Bars.

3.3. Materials properties

The materials properties of steel and concrete are used throughout this research project. For the purpose of linear elastic analysis, the Young's modulus for steel Es =210000 MPa and the Poisson's ratio υ = 0, 3 value have been used respectively as recommended by Eurocode part 3 [29]. For the non-linear plastic analysis, the yield strength fy = 235 N mm2 is added to the material properties, The Young's modulus for concrete are Ec =20000 MPa and the Poisson's ratio υ = 0.18. For the non-linear concrete damaged plasticity analysis These specimens were similar in every respect (plasticity and Tensile Behavior) except that Compressive Behavior and Compression damage they are mentioned in chapter specimens' curves results by ABAQUS.

Plasticity	**Dilation angle**	13
	Eccentricity	0.1
	***fb*0 / *fc*0**	1.16
	K	0.7
	Viscosity parameter	0.0001

Table 4.1 Properties of the Plasticity.

	Yield stress	Cracking strain
Tensile Behavior	2.76217039	0
	0.54082976	0.00150835
	0.21415593	0.00261451
	0.21415593	0.00421048
	0.21415593	0.00586105
	0.21415593	0.00751162
	0.21415593	0.0091622

Table 4.2 Properties of the Tensile Behavior

3.4. Meshing

3.4.1 Element Types

The push out specimen components are modeled using a combination of 3-D solid element (C3D8R): An 8-node linear brick, reduced integration, hourglass control. for concrete, and steel section, shear connector, transverse reinforcing bars using a combination of (T3D2): A 2-node linear 3-D truss.

a) Shear connector

Meshing divides the three-dimensional model into the shell elements. For the mesh density the division of the flange is set at 17 elements and the division of the web is set at 14 elements.

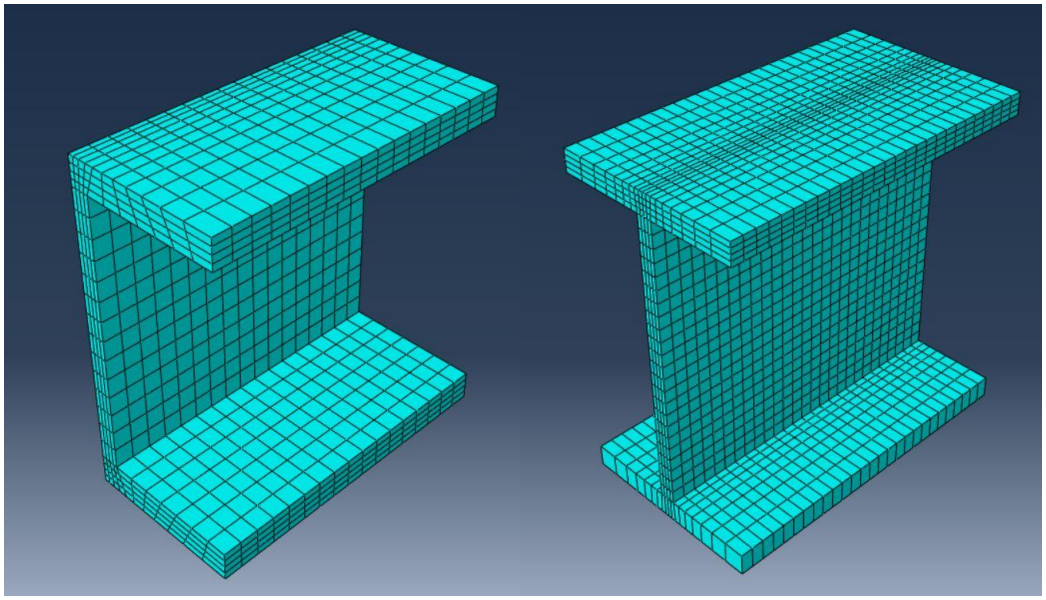

Figure 4.10 Mesh Density of Shear Connector.

b) Concrete fill

Based on our mesh convergence tests, the division of the length 22 elements and width 15 elements and height 17 elements.

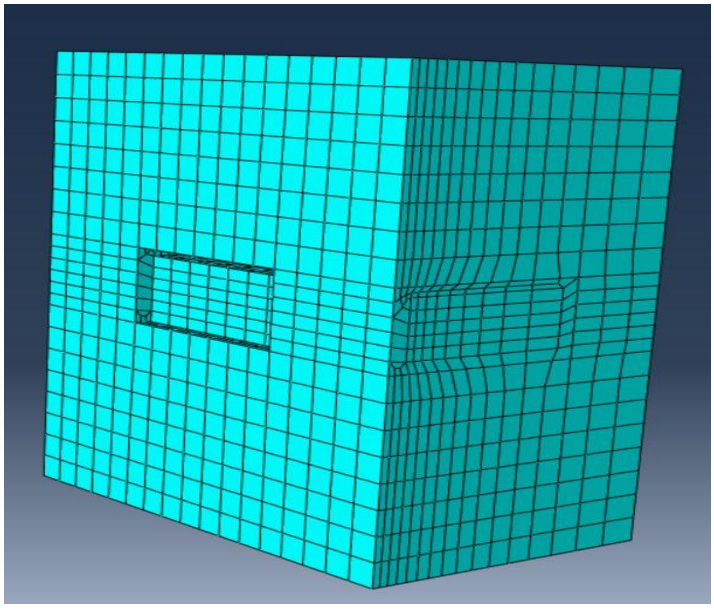

Figure 4.11 Mesh Density of Concrete Fill.

c) steel beam

The division of 20 elements.

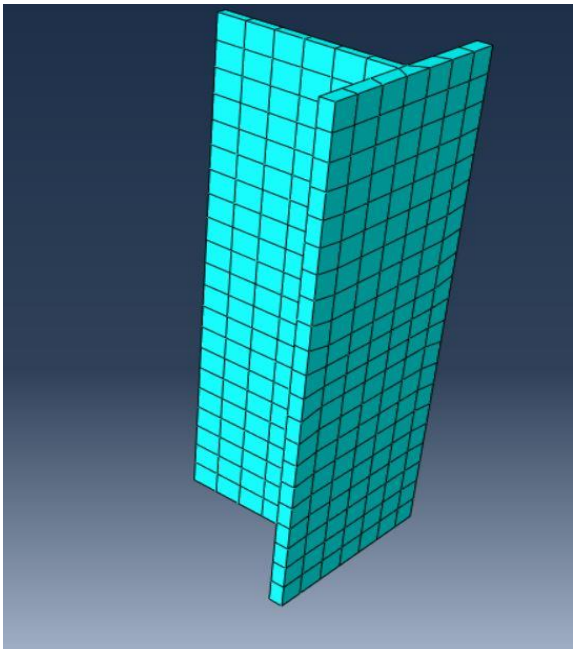

Figure 4.12 Mesh Density of Beam Steel.

d) Rigid plate

The division of 10 elements.

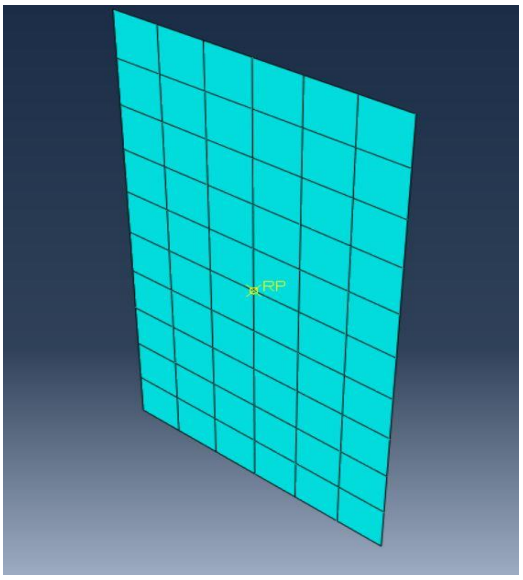

Figure 4.13 Mesh Density of Rigid Plates.

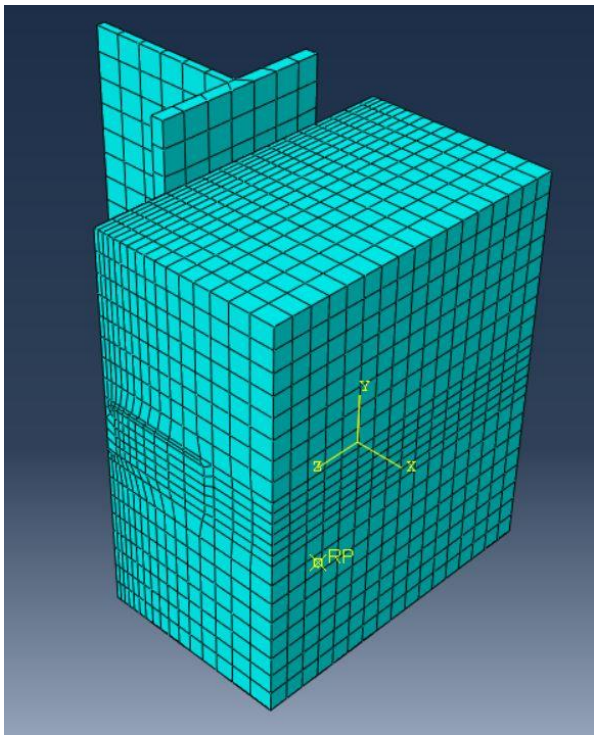

Figure 4.14 Mesh Density of FEM Model.

3.5. Contact

Surface-to-surface contact is usually used for the interaction simulation of the steel and concrete and shear connector.

A contact surface pair comprised of the outer surface of the steel and the outer surface of concrete, the inner surface of concrete and the outer surface of the shear connector , the outer surface of the steel and the outer surface of the shear connector, the outer surface of concrete and the outer surface of Rigid plates. Embedded region contact was used between concrete and reinforced bars.

Tangential contact can be simulated by using the Coulomb friction model. A coefficient of was taken as 0.25.

3.6. Boundary Conditions

The displacement was applied to the upper surfs of the beam steel in the direction Y.

The nodes on the are prevented from displacing in both X and Z directions, the displacement in the Y-direction of the beam steel and shear connector because of the connection between them.

Has been put Rigid plate under concrete for non-displacement in the direction Y.

The analysis type used is the static general analysis including the nonlinear geometric effect.

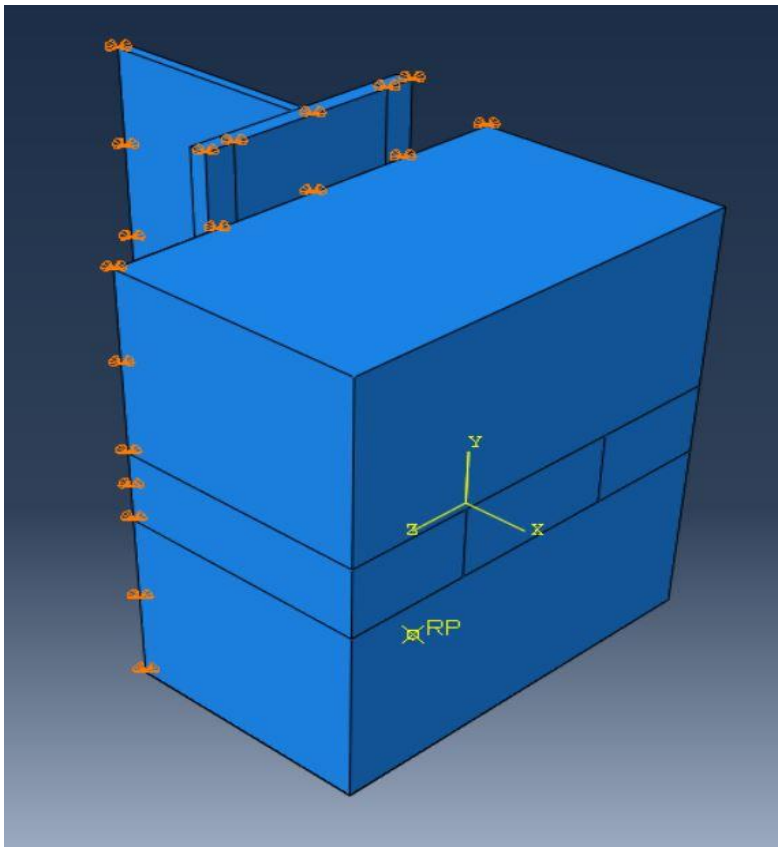

Figure 4.15 Type of Boundary Condition.

CHAPTER V: *SPECIMENS CURVES RESULTS BY ABAQUS*

1. INTRODUCTION

The shear connectors are placed at the interface between steel beam and concrete slab, and they are responsible for transferring the horizontal shear forces that are formed due to flexural action.

A third component of a composite "steel-concrete" beam is the shear connector at the interface between the steel section and the concrete slab. The shear connector provides the connection that allow the transfer of forces from the concrete to the steel and vice versa, and also resists vertical uplift forces at the interface. The shear connectors are usually welded to the top flange of the steel beam before the slab is cast in. These connectors ensure that the two different materials act as a single unit. A variety of shapes and devices have been used as shear connectors and the economic considerations continue to motivate the development of new systems.

The structural behavior of shear connectors has been investigated by a number of researchers through experimental and numerical investigations. Studies have shown that the structural response of shear connectors is affected mainly by geometrical characteristics, such as the number, height, length, and thickness of the connectors, compressive strength of the concrete, and percentage of the transverse steel reinforcement presented in the concrete slab. The need for mechanical shear connectors also arises to transfer earthquake forces between concrete slab and steel beams that are part of the lateral load resisting system of the structure. Besides, these elements function under axial loads to resist vertical upward forces and prevent the premature separation of steel beams and concrete slab in the vertical direction.

2. Tests on Shear Connectors According to Eurocode 4

2.1. Generalities

The resistance to loading, other than fatigue, may be determined by push tests in accordance with the requirements in this EN 1994-1-1:2004 [30]:

(1) The design should be based on experimental tests carried out in a way that provides information on the properties of the shear connection required for design in accordance with the standards.

(2) The variables to be investigated include the geometry and the mechanical properties of the concrete slab, the shear connectors and the reinforcement.

2.2. Testing Arrangements According to EN 1994-1-1:2004

1) Where the shear connectors are used in T-beam with a concrete slab of uniform thickness, standard push tests may be used. In other cases, specific push tests should be used.

2) For standard push tests the dimensions of the test specimen, the steel section and the reinforcement should be as given in Figure 5.1. The recess in the concrete slabs is optional.

3) Specific push tests should be carried out such that the slabs and the reinforcement are suitably dimensioned in comparison with the beam for which the test is designed. In particular:

a) the length *I* of each slab should be related to the longitudinal spacing of the connectors in the composite structure;

b) the width *b* of each slab should not exceed the effective width of the slab of the beam;

c) the thickness *h* of each slab should not exceed the minimum thickness of the slab in the beam

d) the slabs of the push specimen should have the same haunch and reinforcen1ent as the beam.;

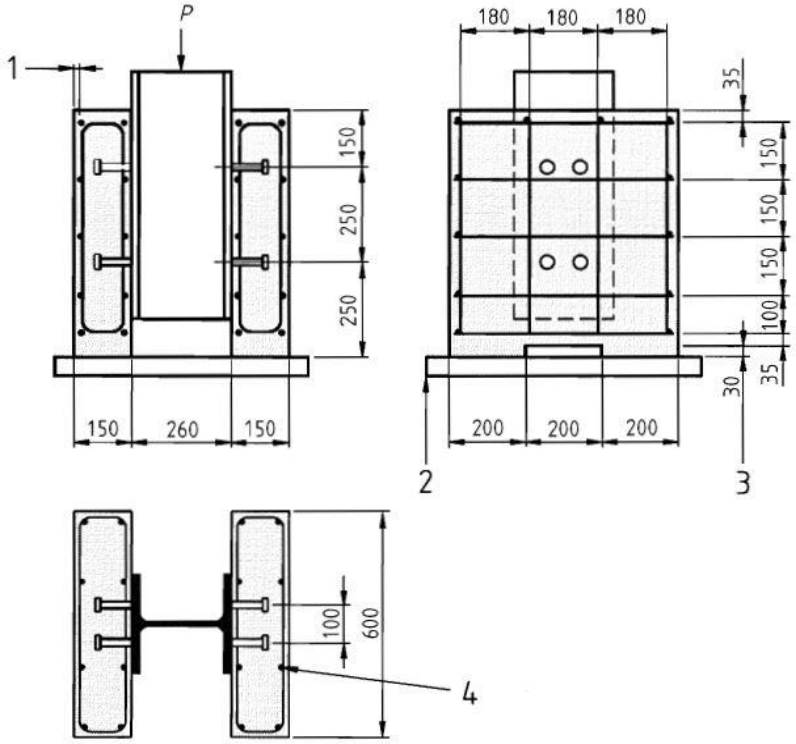

1) cover 15 *mm*

2) bedded in mortar or gypsum

3) recess optional

4) reinforcement: ribbed bars Ø 10 *mm* resulting in a high bond with 450 < fsk < 550 N/mm^2, steel section: HE 260 B or 254 x 254 x 89 kg. UC

Figure 5.1: Test Specimen for Standard Push Test according to the Eurocode 4

2.3. Preparation of Specimens

-Each of both concrete slabs should be cast in the horizontal position, as is done for composite beams in practice.

-Bond at the interface between flanges of the steel beam and the concrete should be prevented by greasing the flange or by other suitable means.

-The push specimens should be air-cured.

- For each mix a minimum of four concrete specimens (cylinders or cubes) for the determination of the cylinder strength should be prepared at the time of casting the push specin1ens. These concrete specimens should be cured alongside the push specimens. The concrete strength fcm should be taken as the mean value.

-The compressive strength fcm of the concrete at the time of testing should be 70 % ± 10% of the specified strength of the concrete fck of the beams for which the test is designed. This requirement can be met by using concrete of the specified grade, but testing earlier than 28 days after casting of the specimens.

-The yield strength, the tensile strength and the maximum elongation of a representative sample of the shear connector material should be determined.

-If profiled steel sheeting is used for the slabs, the tensile strength and the yield strength of the profiled steel sheet should be obtained from coupon tests on specimens cut from the sheets as used in the push tests.

2.4. Testing Procedure

The load should first be applied in increments up to 40% of the expected failure load and then cycled 25 times between 5% and 40% of the expected failure load. Subsequent load increments should then be imposed such that failure does not occur in less than 15 minutes.

The longitudinal slip between each concrete slab and the steel section should be measured continuously during loading or at each load increment. The slip should be measured at least until the load has dropped to *20%* below the maximum load.

As close as possible to each group of connectors, the transverse separation between the steel section and each slab should be measured.

2.5 Test Evaluation

(1) If three tests on nominally identical specimens are carried out and the deviation of any individual test result from the mean value obtained from all tests does not exceed 10 %, the design resistance may be determined as follows:

-The characteristic resistance P_{RK} should be taken as the minimum failure load (divided by the number of connectors) reduced by 10 %;

-The design resistance P_{Rd} should be calculated from:

$$P_{\mathrm{Rd}} = \frac{f_{\mathrm{u}}}{f_{\mathrm{ut}}} \frac{P_{\mathrm{Rk}}}{\gamma_{\mathrm{V}}} \leq \frac{P_{\mathrm{Rk}}}{\gamma_{\mathrm{V}}} \tag{5.1}$$

where:

f_u: is the minimum specified ultimate strength of the connector material;

f_{ut}: is the actual ultimate strength of the connector material in the test specimen; and γ_V: is the partial safety factor for shear connection.

(2) If the deviation froll1 the mean exceeds 10%, at least three more tests of the same kind should be made. The test evaluation should then be carried out in accordance with EN 1990, Annex D [31].

(3) Where the connector is composed of two separate elements, one to resist longitudinal shear and the other to resist forces tending to separate the slab from the steel beam, the ties which resist separation shall be sufficiently stiff and strong so that separation in push tests, measured when the connectors are subjected to 80 % of their ultimate load, is less than half of the longitudinal movement of the slab relative to the beam.

(4) The slip capacity of a specimen $\delta_u$should be taken as the maximum slip measured at the characteristic load level, as shown in Figure 5.2. The characteristic slip capacity δ_{uK} should be taken as the minimum test value of δ_u reduced by 10% or determined by statistical evaluation from all the test results. In the latter case, the characteristic slip capacity should be determined in accordance with EN 1990, Annex D[31].

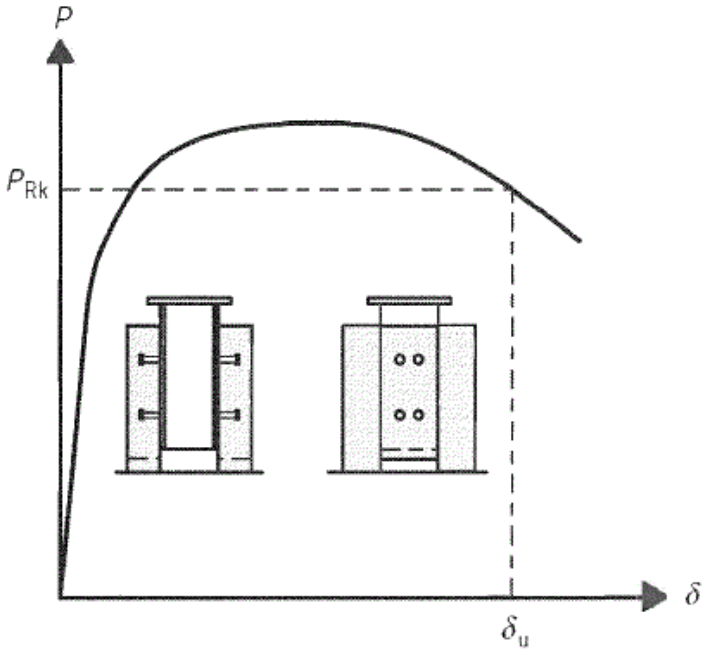

Figure 5.2: Determination of Slip Capacity δ_u

3. Description of Specimens

This study consisted of 19 push-out tests of channel and 3 I-Shape Connector.

3.1. Test on Channel Shear Connector

This study consisted of 19 push-out tests grouped in five series. Each series included five different specimens in Serie (A, B and C) and three specimens in Serie (D) and one in Serie (E). The test specimens were designed to study the effect of the following parameters on the ultimate load capacity: Height and length of connectors, and the Compressive Strength of concrete. Details of each push-out specimen are provided in Table 5.1.

Series	Specimens	Channel shear connector			Concrete slab		Profile of steel beam
		Length (mm)	Height (mm)	Depth (mm)	Compressive Strength *fck* (N/mm^2)	Transverse reinforcement	
A	A1	50	65	100	26.52	4 Ø 10	IEP (270)
	A2		80				
	A3		100				
	A4		120				
	A5		140				
B	B1	50	65	100	31.47	4 Ø 10	IEP (270)
	B2		80				
	B3		100				
	B4		120				
	B5		140				
C	C1	50	65	100	38.6	4 Ø 10	IEP (270)
	C2		80				
	C3		100				
	C4		120				
	C5		140				
D	D1	30	65	100	38.6	4 Ø 10	IEP (270)
	D2	30	80		31.47		
	D3	30	100		28.8		
	D4	30	120		26.52		

Table 5.1: Summary FEM of Channel Connector Specimens.

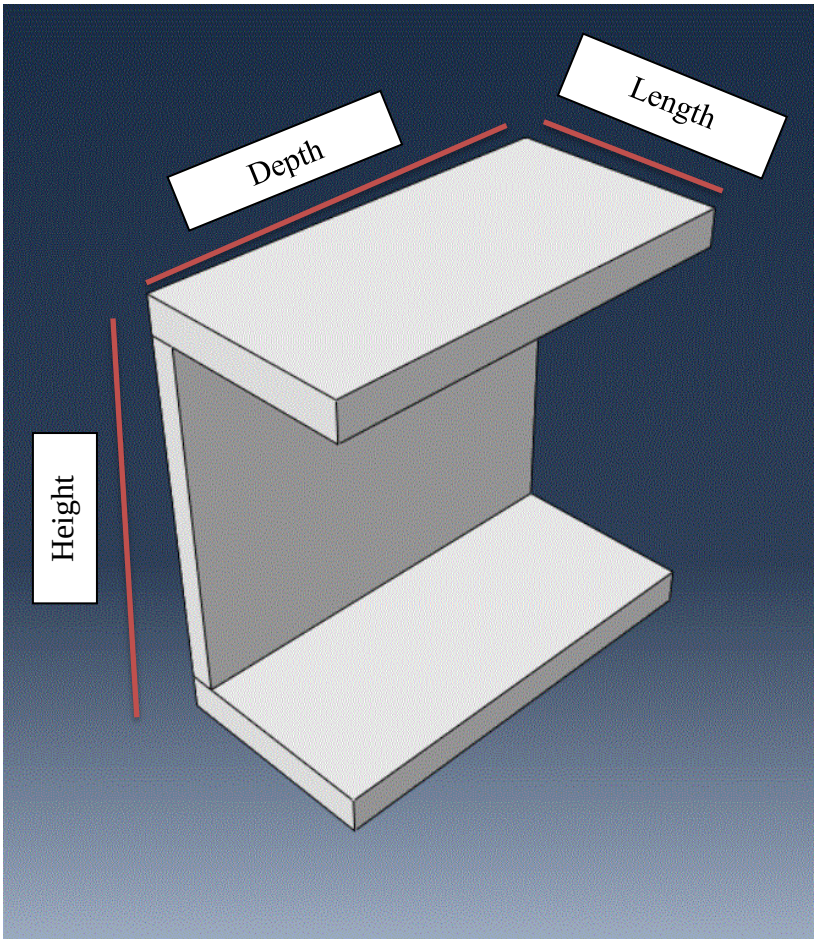

Figure 5.3: Channel Connector Specimen.

4. Push-Out Test Results

4.1. C3– Specimen

This test represents a Push-Out Specimens (Channel shear connector) with geometrical dimensions as follows:

Length 50

Height 100

Depth 100

4.1.1. Materials properties

	Yield stress	Inelastic strain
Compressive Behavior	15.44	0
	28.1547365	0.00054588
	35.9365995	0.00107991
	38.6	0.00161019
	12.524855	0.01376382
	4.13830604	0.02620876
	1.95573274	0.03847993

Table 5.2: Properties of The Compressive Behavior (Compressive Strength 38.6).

	Damage Parameter	Inelastic Strain
Compression Damage	0	0
	0.0166623	0.00054588
	0.03516844	0.00107991
	0.05520071	0.00161019
	0.55541182	0.01376382
	0.83065519	0.02620876
	0.93911179	0.03847993

Table 5.3: Properties of The Compression Damage (Compressive Strength 38.6).

A nonlinear finite element (FE) model of the push-out specimens is developed in the ABAQUS environment. The model is proved to predict the shear capacity close to the values obtained from tests. Therefore, by using this model the effects of various parameters such as height and length of channel shear connectors and different concrete properties could be effectively predicted.

At first, two models matching the properties of C3 and D1 specimens were built and the obtained results were compared to the push-out experimental tests results for specimen RC1 and RC2 taken from ref [32]. After adopting the appropriate material model, mesh sizing and interface

boundary conditions, the model is considered accurate enough to predict the shear capacity of channel connectors embedded in concrete. Figure 5.3 and Figure 5.6 present a comparison between the (load-slip) curves recorded experimentally (from ref [32]) and those obtained numerically by the finite element model. Based on these results of this comparison, more Series (A, B and C) were created as shown in the table 5.1.

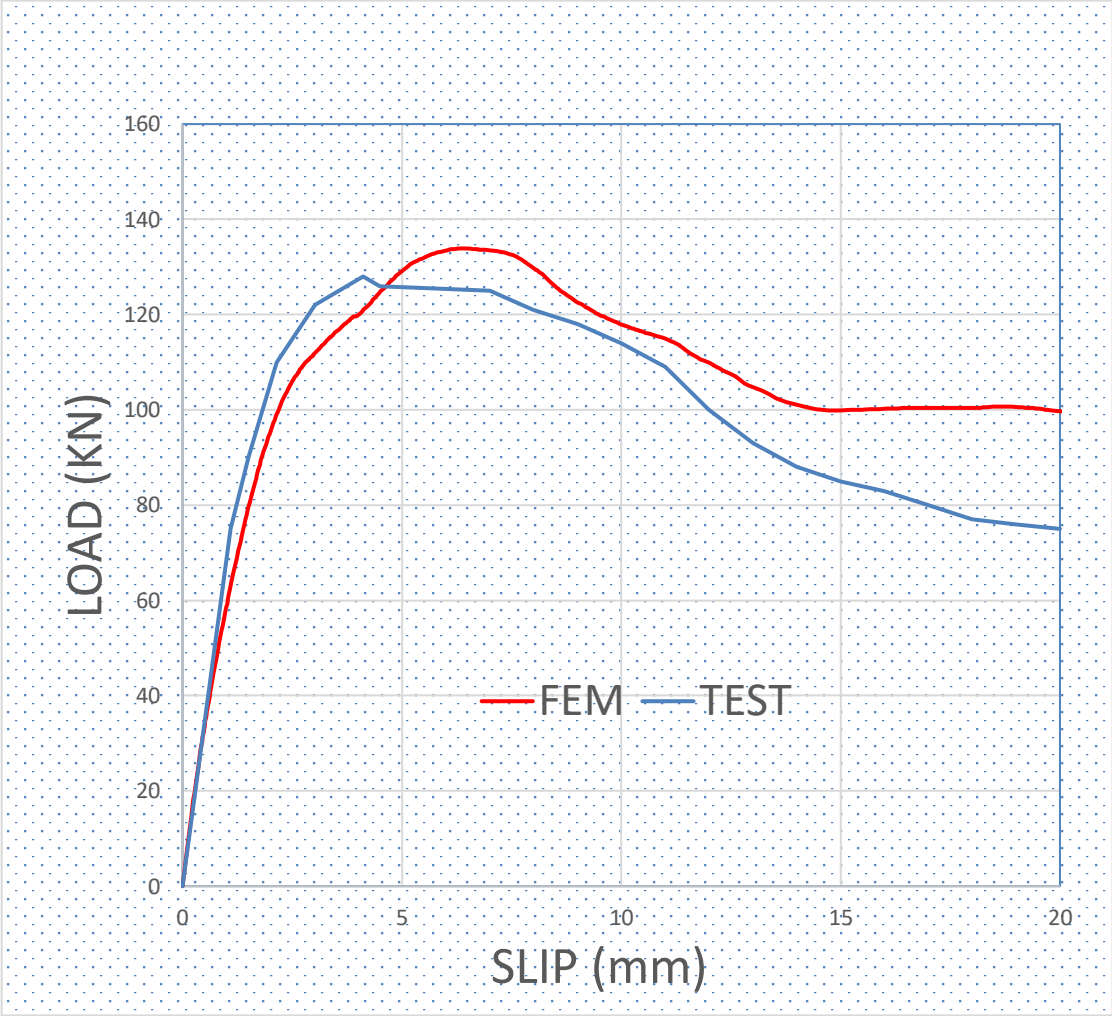

Figure 5.4: Comparison of Load–Slip Curves for Specimens C3 FEM and Experimental Test.

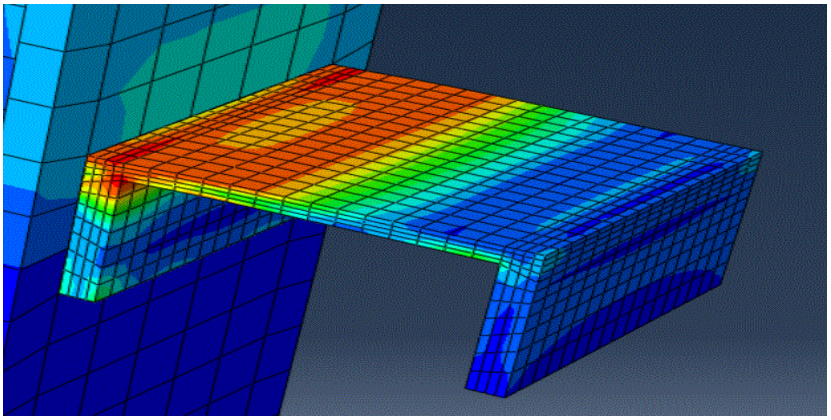

a

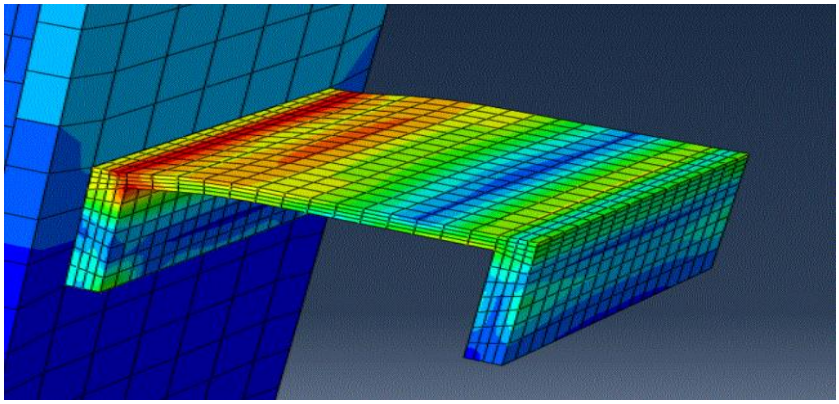

b

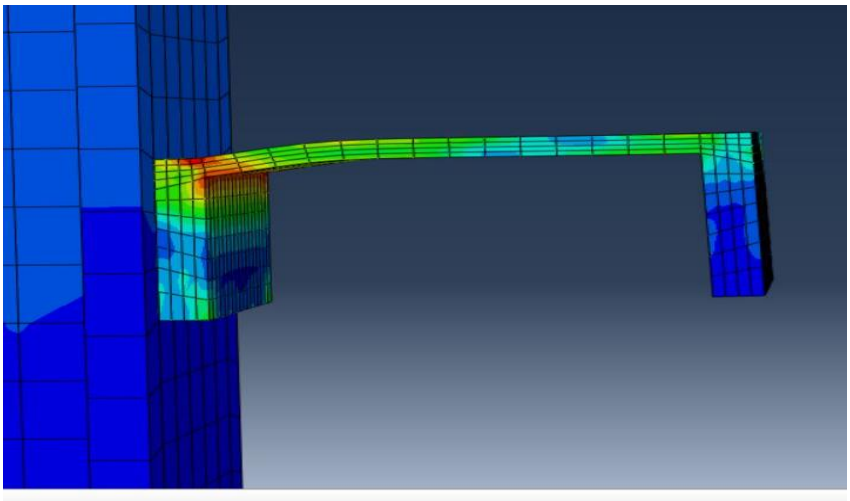

c

Figure 5.5: Distributions of Stress in the Channel Connector Specimen C3 at the Load Max =132.67 KN (a) and Load 100.6 KN (b) and at Last Increment (c).

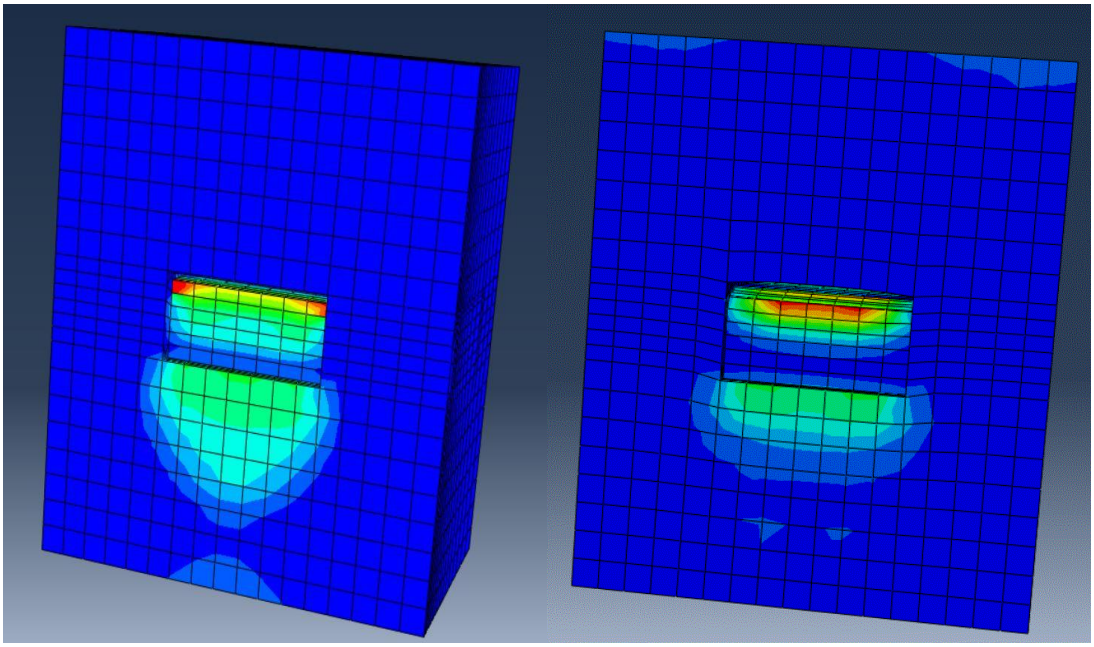

(a) (b)

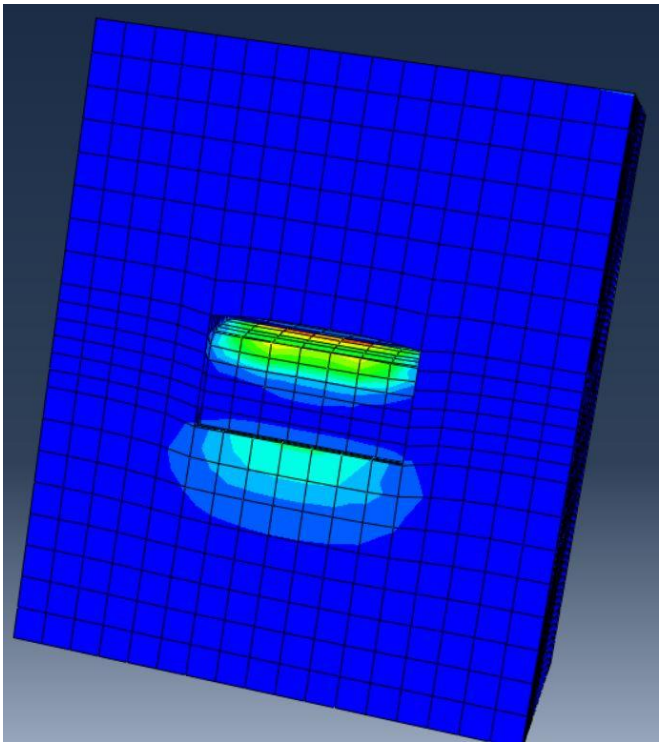

(c)

Figure 5.6: Distributions of Stress in the Concrete Specimen C3 at the Load Max =132.67 KN (a) and Load 100.6 KN(b) and at Last Increment (c).

4.2. D3– Specimen

This test represents a Push-Out Specimens (Channel shear connector) with geometrical dimensions represented as follows:

Length 30

Height 100

Depth 100

4.2.1. Materials properties

	Yield Stress	Inelastic Strain
Compressive Behavior	11.52	0
	21.6842159	0.00056733
	27.1510654	0.0011183
	28.8	0.00166336
	5.49493937	0.01384332
	1.60313997	0.02614053
	0.7352439	0.03782277

Table 5.4: Properties of The Compressive Behavior (Compressive Strength 28.8).

	Damage Parameter	Inelastic Strain
Compression Damage	0	0
	0.02533961	0.00056733
	0.05438281	0.0011183
	0.08618136	0.00166336
	0.71608099	0.01384332
	0.93176566	0.02614053
	0.98434765	0.03782277

Table 5.5: Properties of the Compression Damage (Compressive Strength 28.8).

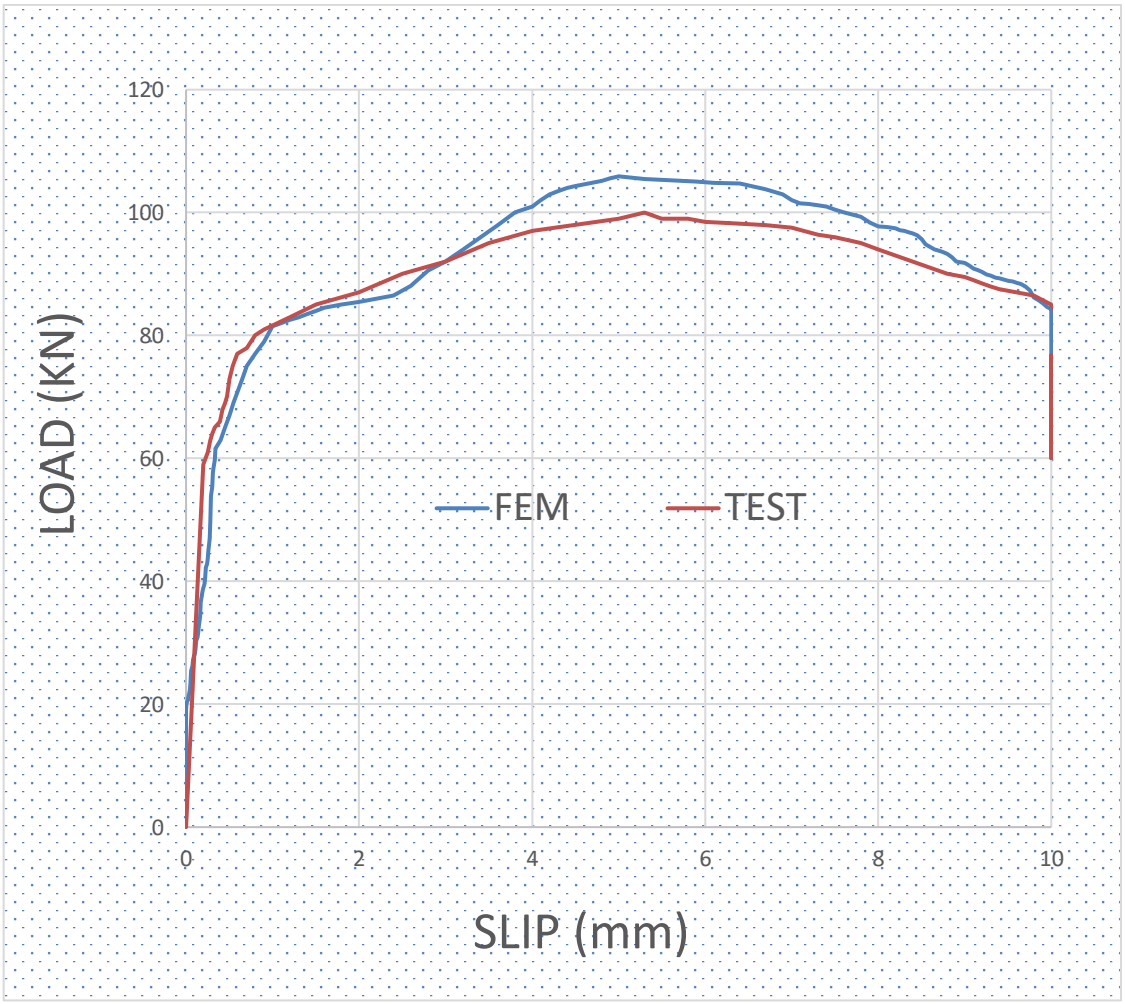

Figure 5.7: Comparison of Load–Slip Curves for Specimens D1 FEM and Experimental Test.

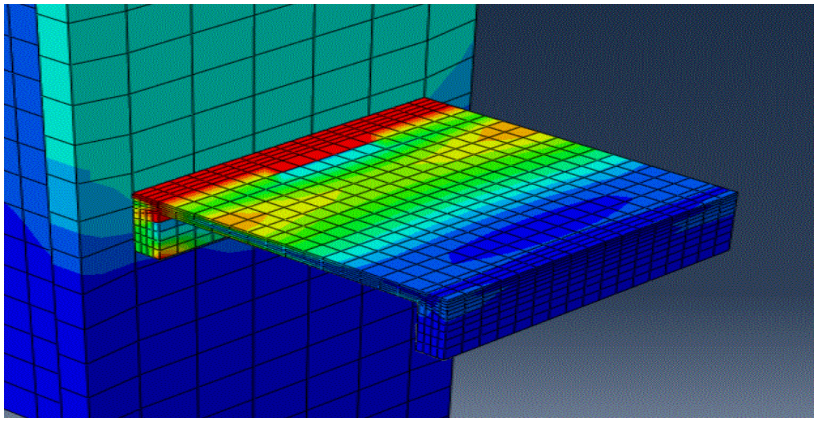

a

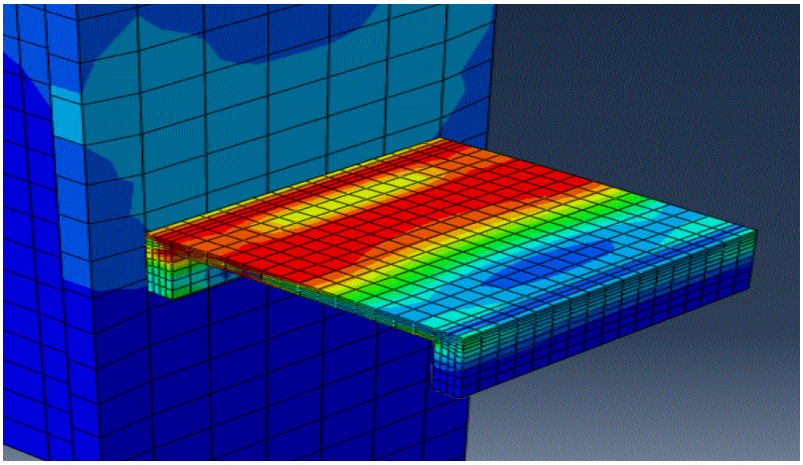

b

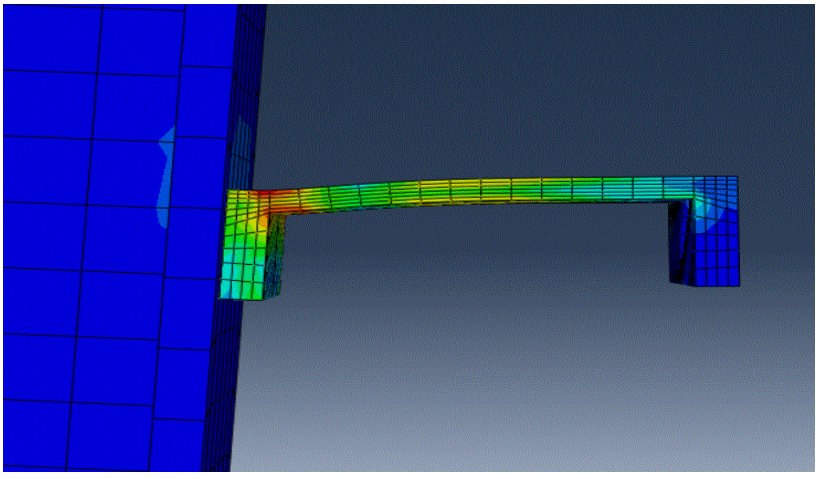

c

Figure 5.8: Distributions of Stress for Channel Connector Specimen C3 at the Load Max =108.44 KN (a) and Load 87.23 KN (b) and at Last Increment (c).

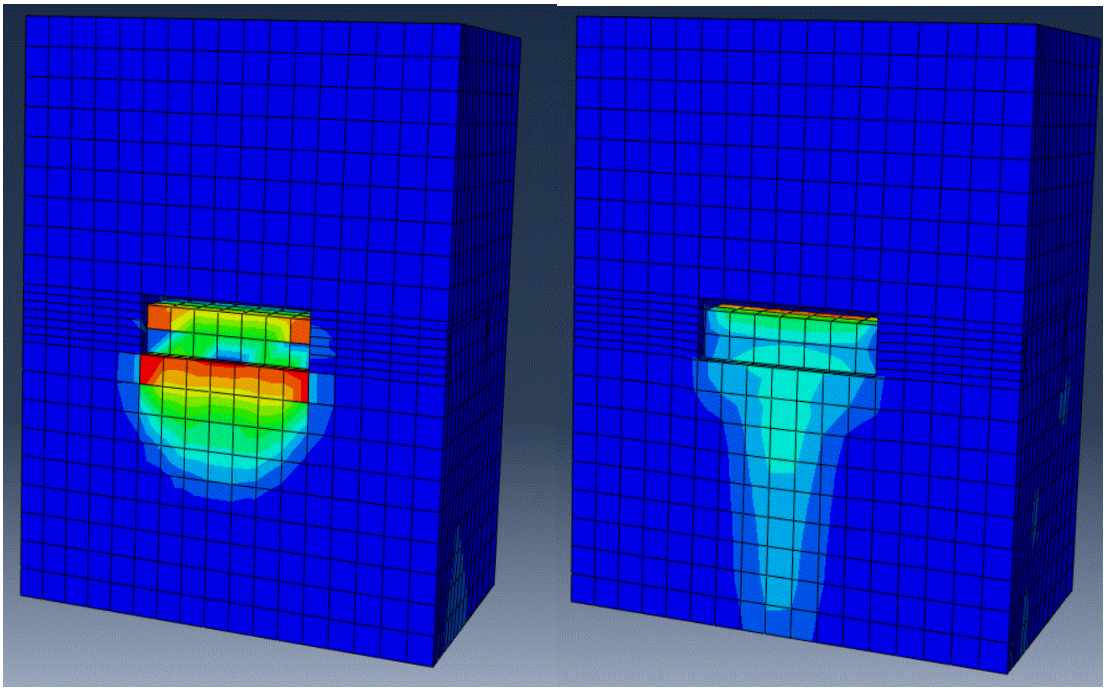

a b

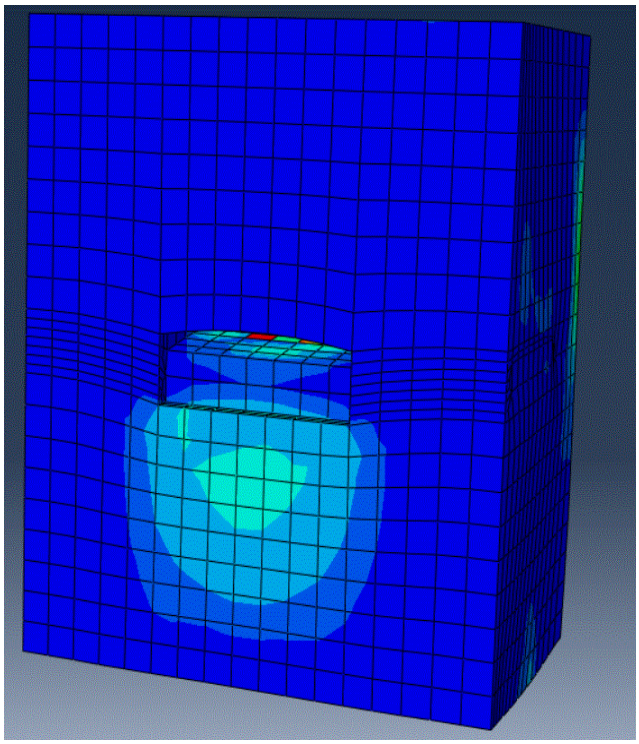

c

Figure 5.9: Distributions of Stress for the Concrete Specimen C3 at the Load Max =108.44 KN (a) and Load 87.23 KN(b) and at Last Increment (c).

4.3. Effect of the Height of channel Connector

4.3.1. Series A

This test represents a Push-Out Specimens in series A (Channel shear connector). Five specimens were similar in every aspect except the height of channel connectors as follows:

Series	Specimens	Channel shear connector			Concrete slab		Profile of steel beam
		Length (mm)	Height (mm)	Depth (mm)	Compressive Strength *fck* (N/mm^2)	Transverse reinforcement	
A	A1	50	65	100	26.52	4 Ø 10	IEP (270)
	A2		80				
	A3		100				
	A4		120				
	A5		140				

Table 5.6: Summary FEM of Channel Connector Specimens in series A.

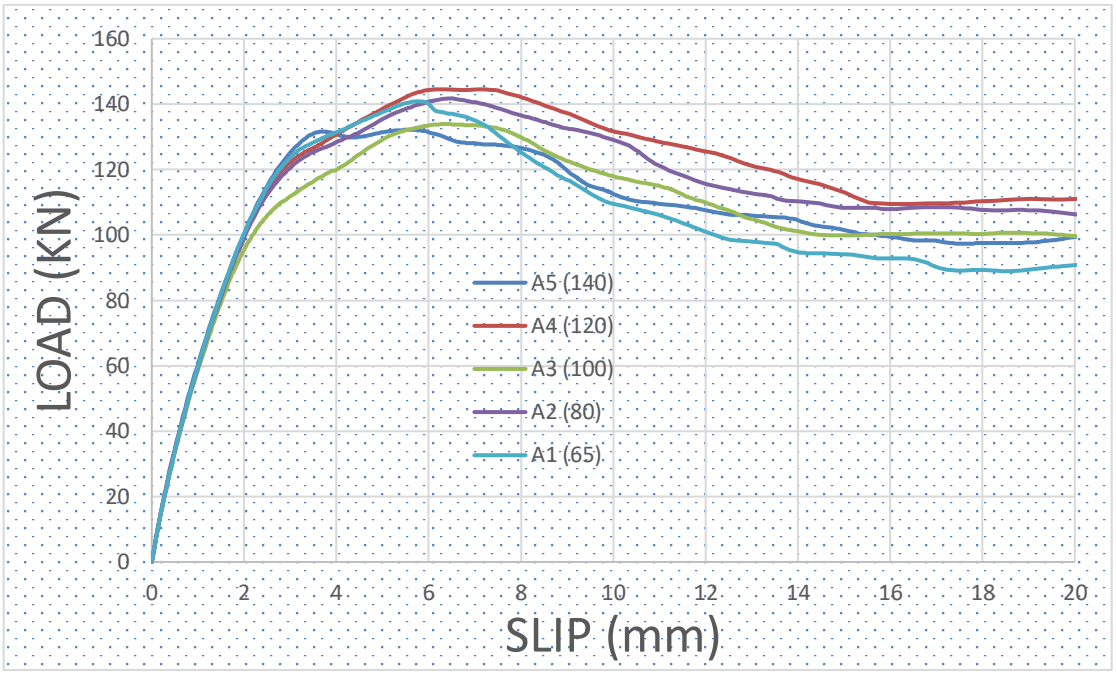

Figure 5.10: Comparison of Load–Slip Curves for Specimens A1, A2 and A3, A4 and A5.

4.3.2. Series B

This test represents a Push-Out Specimens in series B (Channel shear connector). Five specimens were similar in every aspect except the height of channel connectors as follows:

Series	Specimens	Channel shear connector			Concrete slab		Profile of steel beam
		Length (mm)	Height (mm)	Depth (mm)	Compressive Strength *fck* (N/mm^2)	Transverse reinforcement	
B	A1	50	65	100	31.47	4 Ø 10	IEP (270)
	A2		80				
	A3		100				
	A4		120				
	A5		140				

Table 5.7: Summary FEM of Channel Connector Specimens in series B.

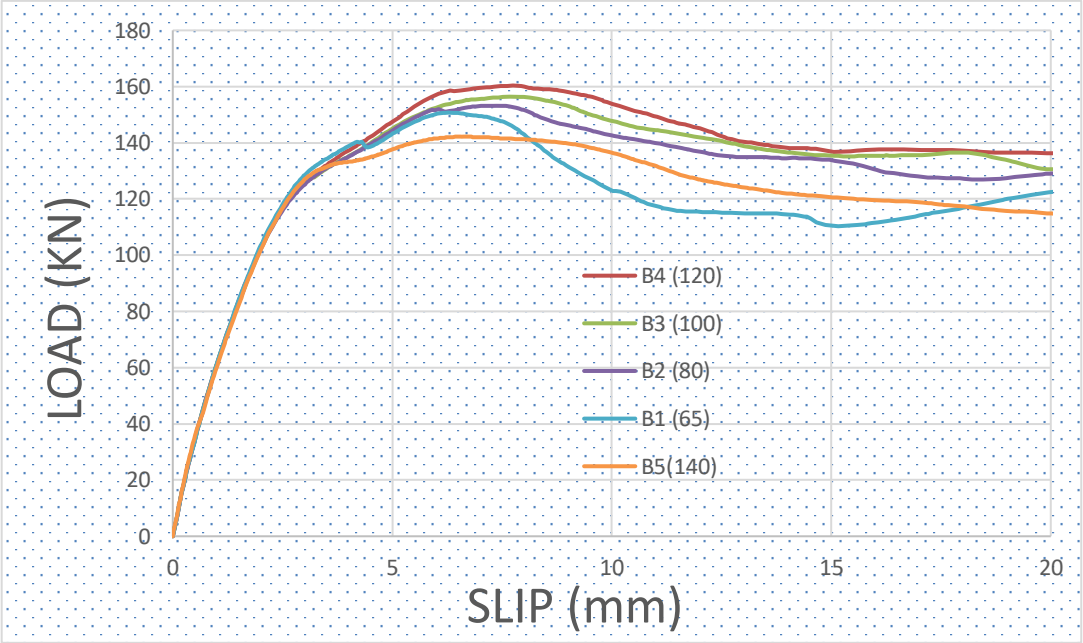

Figure 5.11: Comparison of Load–Slip Curves for Specimens B1, B2 and B3, B4 and B5.

4.3.3 Series C

This test represents a Push-Out Specimens in series C (Channel shear connector). Five specimens were similar in every aspect except the height of channel connectors as follows:

Series	Specimens	Channel shear connector			Concrete slab		Profile of steel beam
		Length (mm)	Height (mm)	Depth (mm)	Compressive Strength *fck* (N/mm^2)	Transverse reinforcement	
C	A1	50	65	100	38.6	4 Ø 10	IEP (270)
	A2		80				
	A3		100				
	A4		120				
	A5		140				

Table 5.8: Summary FEM of Channel Connector Specimens in series C.

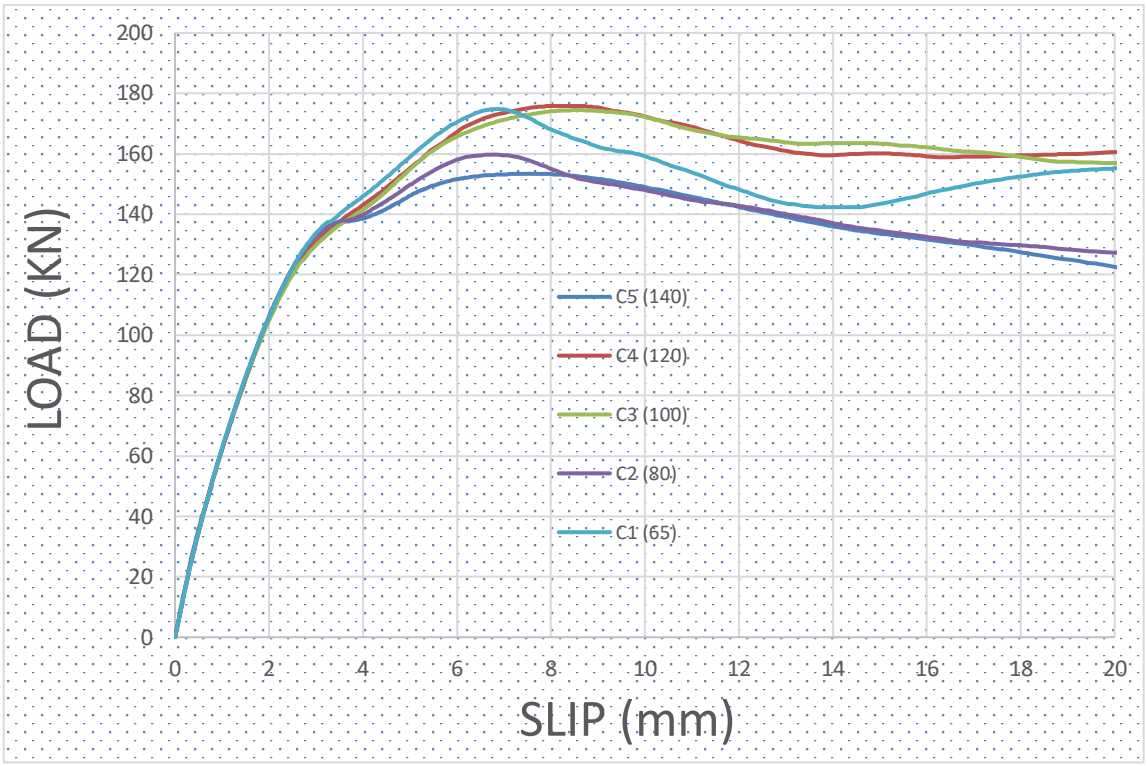

Figure 5.12: Comparison of Load–Slip Curves for Specimens C1, C2 and C3, C4 and C5.

4.3.4. Discussion

The load–slip curves for three series. five specimens were similar in every aspect except the height of the channel connector 65, 80, 100, 120 and 140 *mm* respectively. The compressive strength of concrete used in all three pair specimens was 26.52 ,31.47 and 38.6 *MPa*. As the load-slip curves indicate, the ultimate load capacity of channel connector increased slightly with the increase in the height of connector.

4.4. Effect of the Compressive Strength

4.4.1. Specimens with a Height of 65, 80, 100, 120- and 140-mm.

This test represents a Push-Out Specimens with a height of 65, 80, 100, 120- and 140-mm Channel shear connector. These specimens were similar in every aspect except the Compressive Strength of concrete as follows: 26.52, 31.47 and 38.6 *MPa*.

Specimens	Channel shear connector			Concrete slab		Profile of steel beam
	Length (mm)	Height (mm)	Depth (mm)	Compressive Strength f_{CK} (N/mm^2)	Transverse Reinforcement	
A1	50	65	100	26.52	4 Ø 10	IEP (270)
B1				31.47		
C1				38.6		
A2	50	80	100	26.52	4 Ø 10	IEP (270)
B2				31.47		
C2				38.6		
A3	50	100	100	26.52	4 Ø 10	IEP (270)
B3				31.47		
C3				38.6		
A4	50	120	100	26.52	4 Ø 10	IEP (270)
B4				31.47		
C4				38.6		
A5	50	140	100	26.52	4 Ø 10	IEP (270)
B5				31.47		
C5				38.6		

Table 5.9: Summary FEM of Channel Connector Specimens with a height of 65,85 and 100,120 and 140.

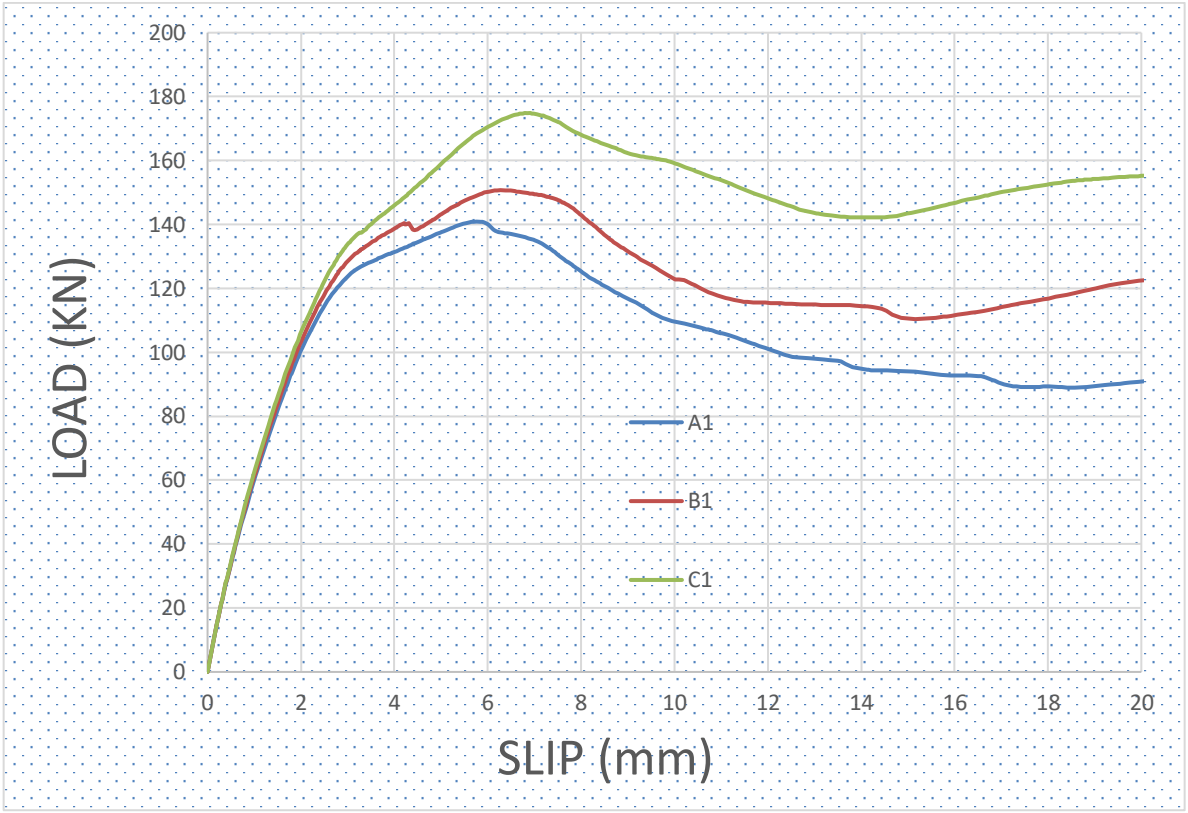

Figure 5.13: Comparison of Load–Slip Curves for Specimens A1, B1 and C1.

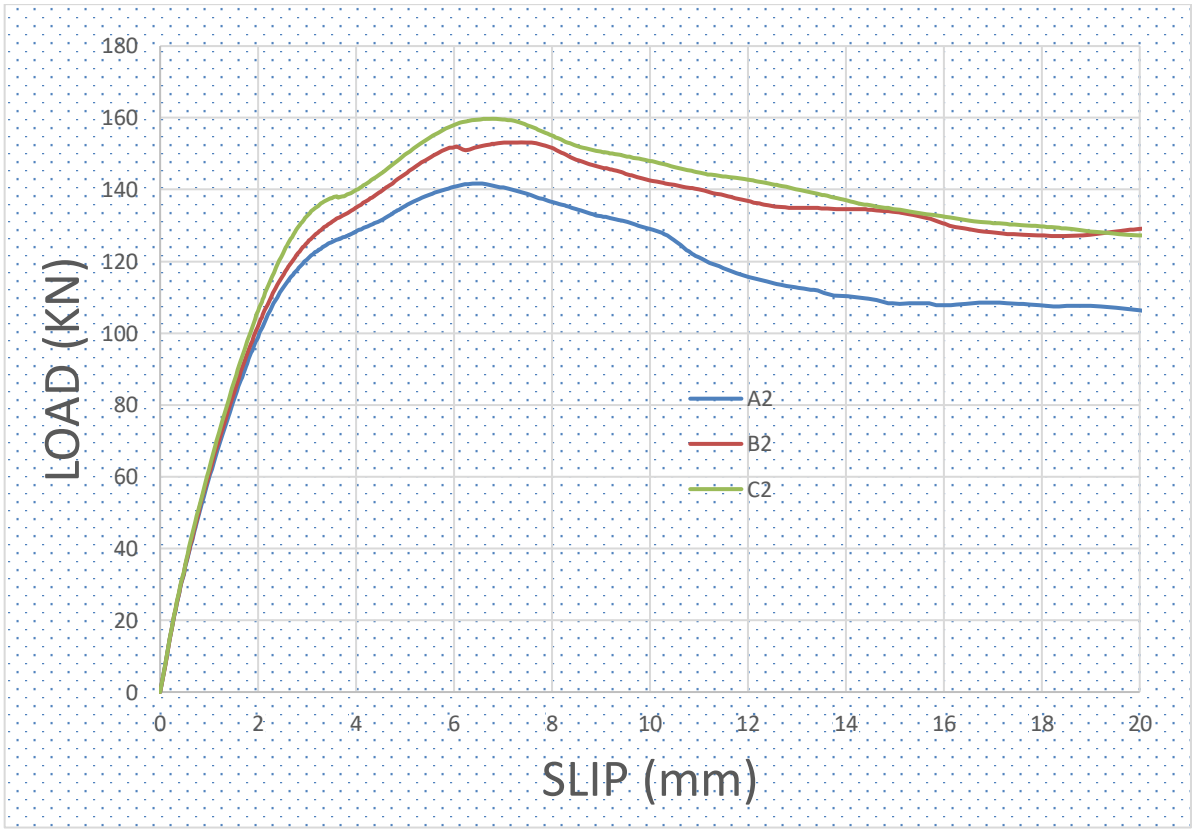

Figure 5.14: Comparison of Load–Slip Curves for Specimens A2, B2 and C2.

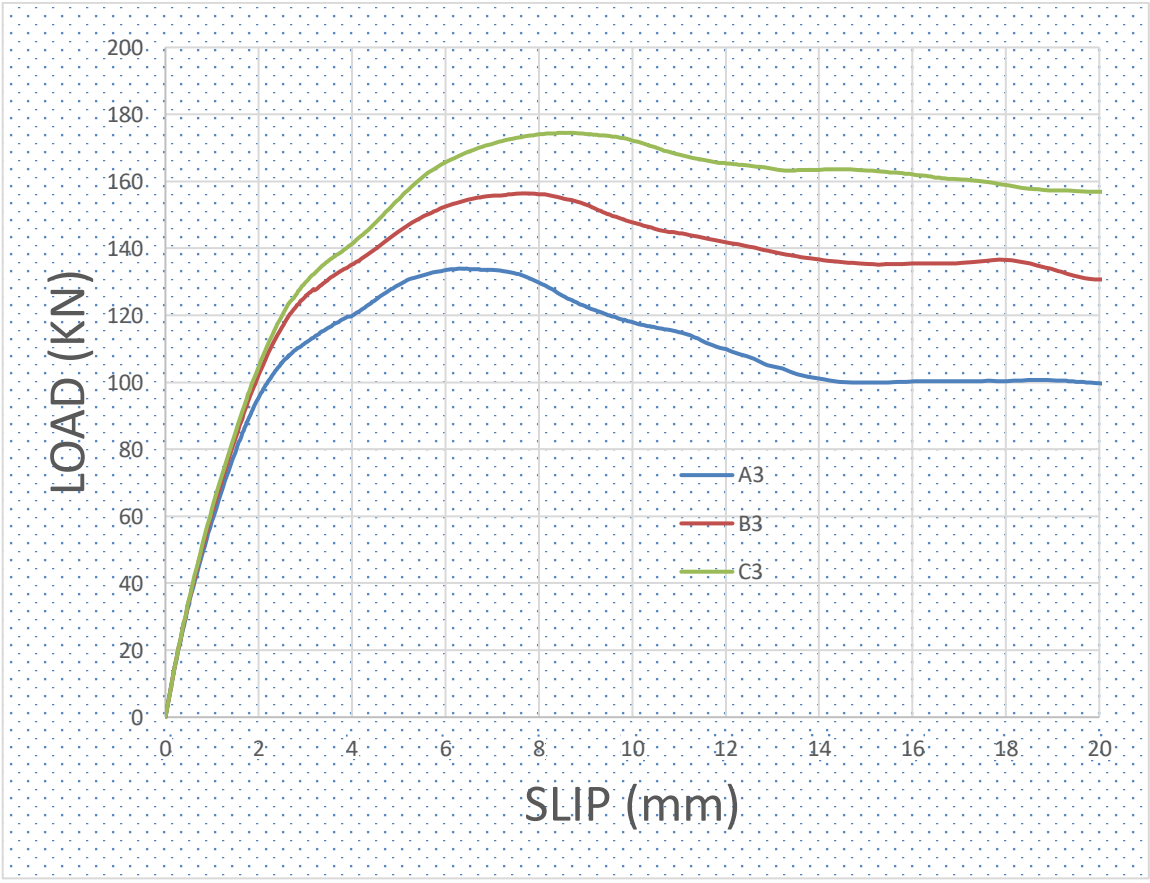

Figure 5.15: Comparison of Load–Slip Curves for Specimens A3, B3 and C3.

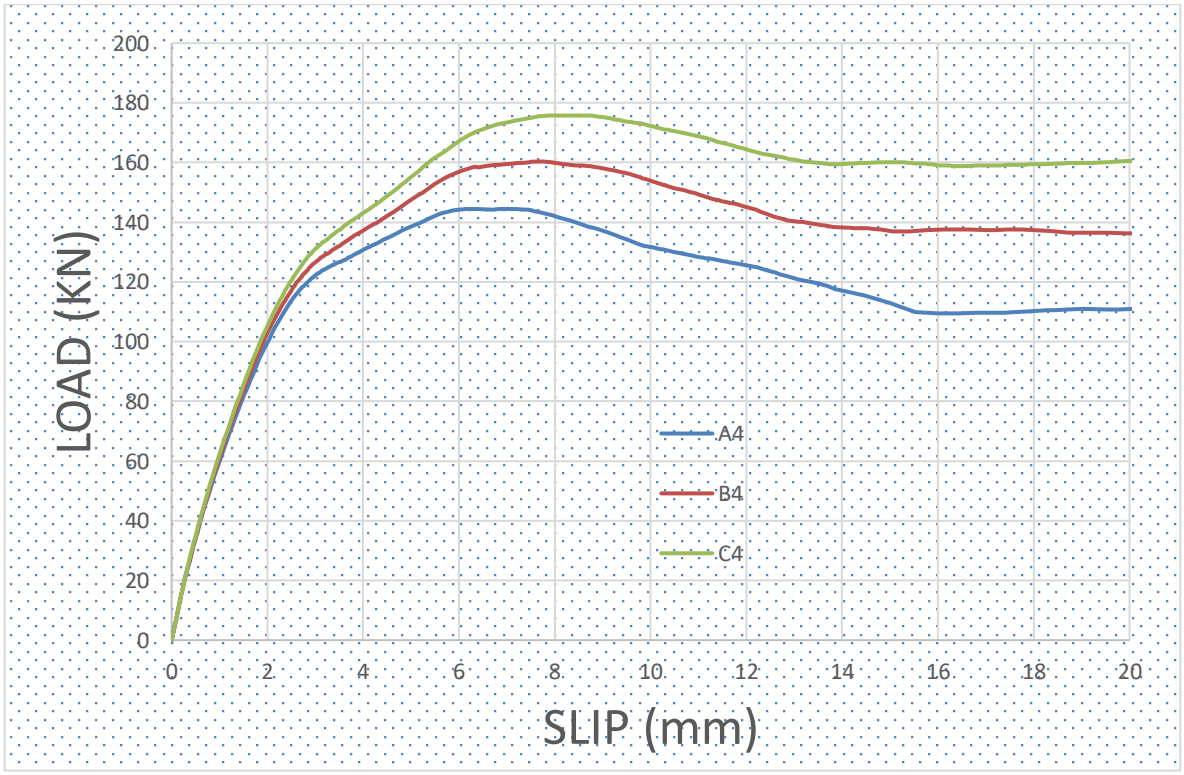

Figure 5.16: Comparison of Load–Slip Curves for Specimens A4, B4 and C4.

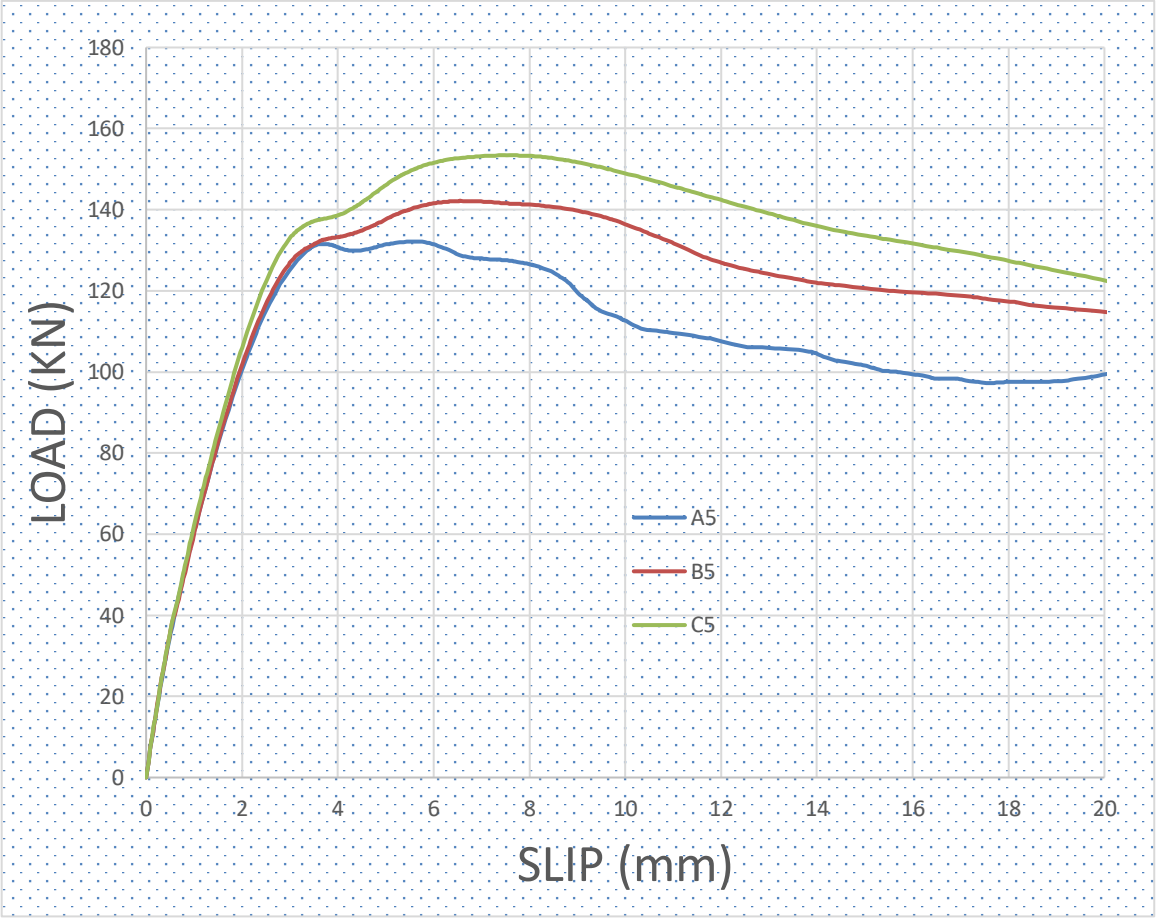

Figure 5.17: Comparison of Load–Slip Curves for Specimens A5, and B5 C5.

4.4.2. Discussion

The load-slip curves for three pair of specimens are shown in Figures 5.12, 5.13, 5.14, 5.15 and 5.16. These specimens were similar in every aspect except the Compressive Strength that was: 26.52, 31.47 and 38.6 *MPa* respectively. As the load-slip curves indicate, the ultimate load capacity is influenced by the compressive strength. Increasing Compressive Strength from 26.52 *MPa* to 31.47 *MPa* led to an increase in the ultimate load capacity of approximately 7.14%, as well as a further increase of Compressive Strength from 31.47 *MPa* to 38.6 *MPa* led to an increase in the ultimate load capacity of approximately 16.66%.

4.5. Effect of The Length of Channel Connector

This test represents a Push-Out Specimens (Channel shear connector) with different geometrical dimensions as follows:

4.5.1. D1 – Specimen

Length 50

Height 65

Depth 100

C1 – Specimen

Length 30

Height 65

Depth 100

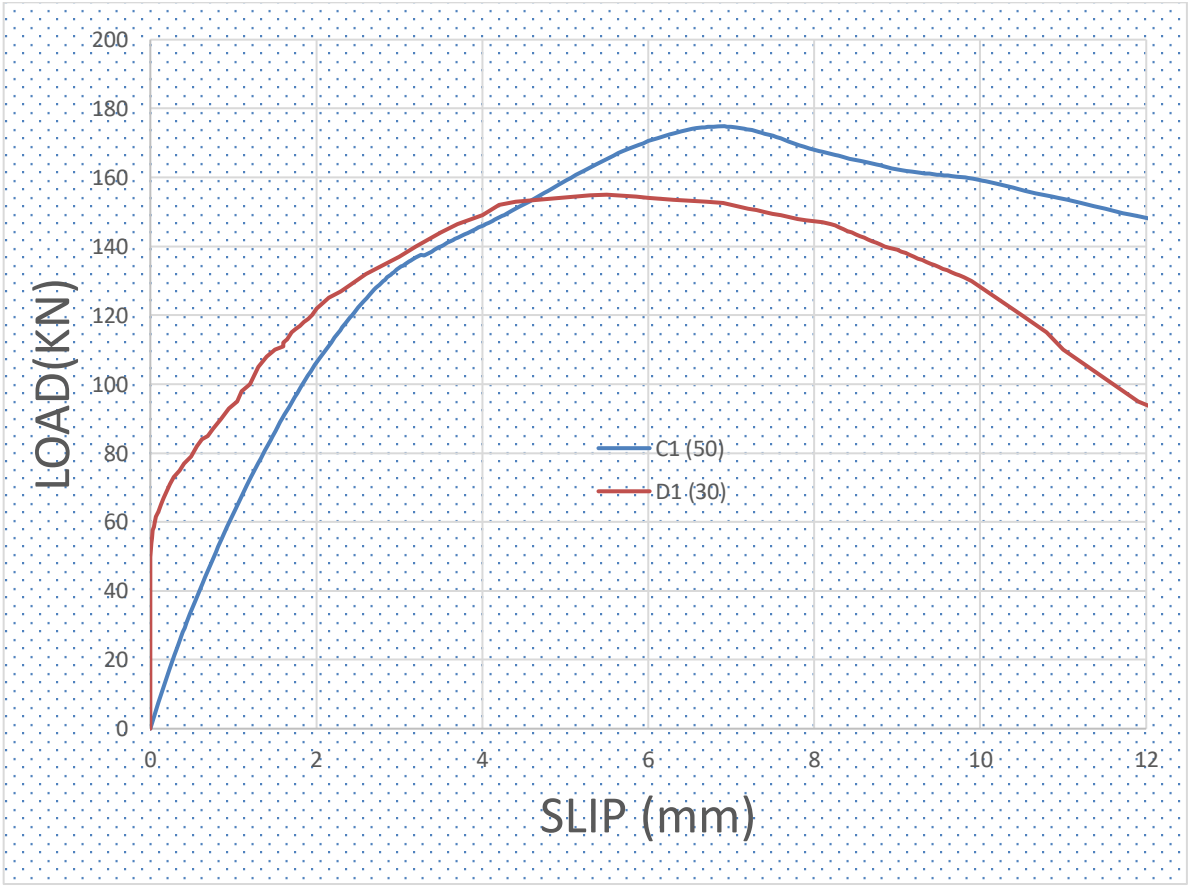

Figure 5.18: Comparison of Load–Slip Curves for Specimens D1 and C1.

This test represents a Push-Out Specimens (Channel shear connector) with different geometrical dimensions as follows:

4.5.2 D2 – Specimen

Length 50

Height 80

Depth 100

B2 – Specimen

Length 30

Height 80

Depth 100

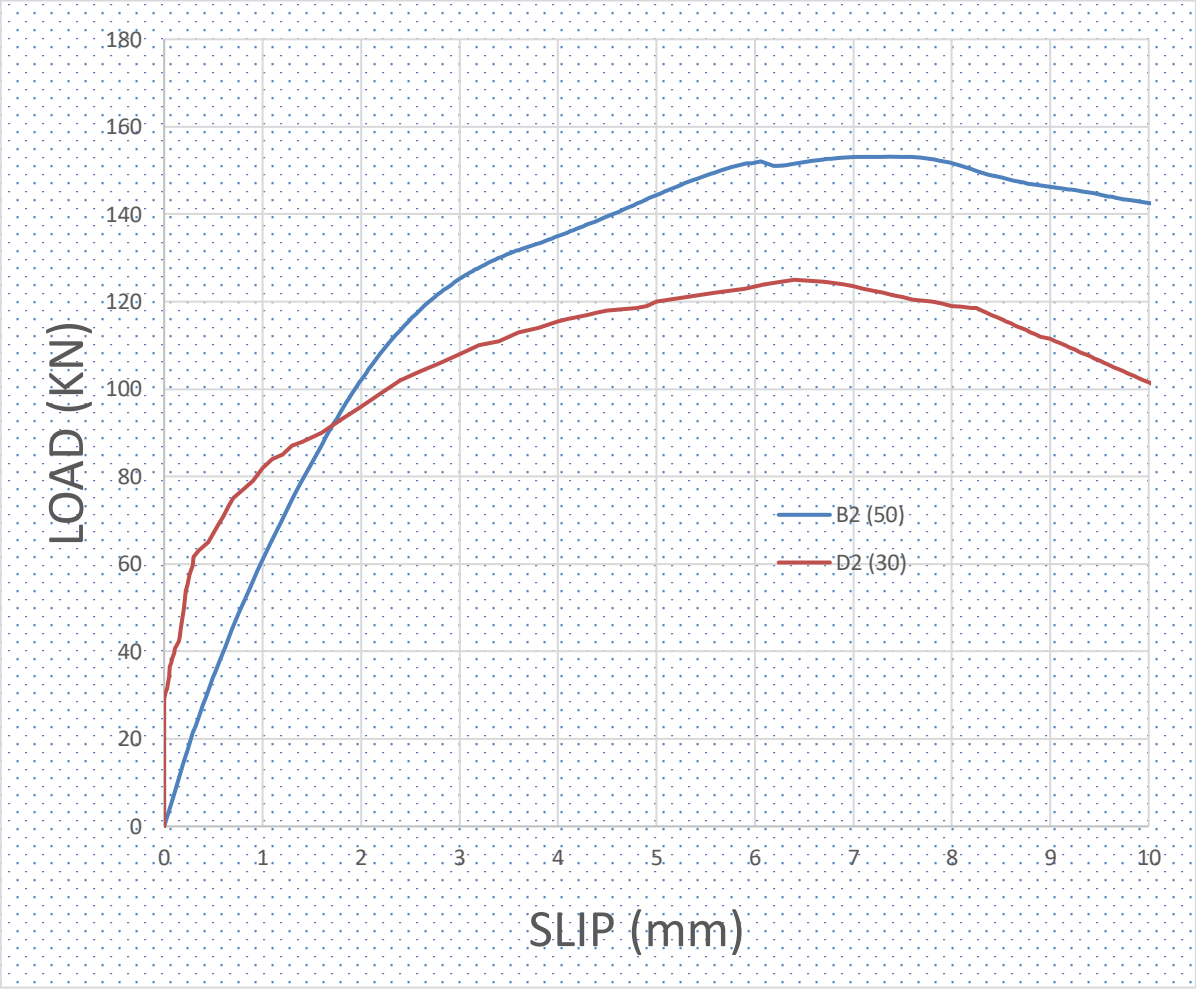

Figure 5.19: Comparison of Load–Slip Curves for Specimens D2 and B2.

This test represents a Push-Out Specimens (Channel shear connector) with different geometrical dimensions as follows:

4.5.3. D4 – Specimen

Length 50

Height 120

Depth 100

A4 – Specimen

Length 30

Height 120

Depth 100

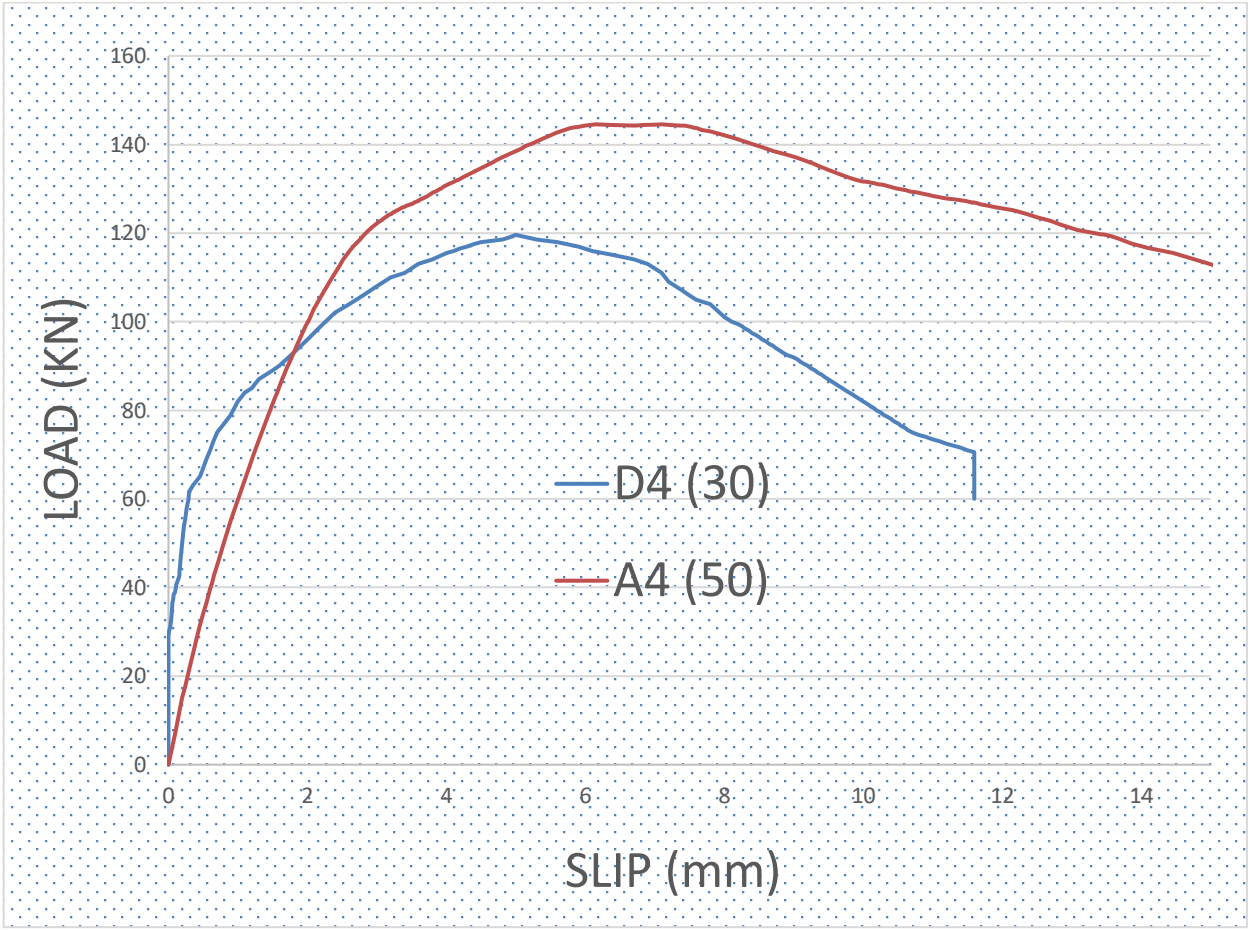

Figure 5.20: Comparison of Load–Slip Curves for Specimens D4 and A4.

4.5.4. Discussion

The load-slip curves for two pair of specimens are shown in Figures 5.17, 5.18 and 5.19. These specimens were similar in every aspect except the length of the channel connector in all pair of specimens. As the load-slip curves indicate, the ultimate load capacity is influenced significantly by the increase in connector length. On average, increasing the length of channel connector led to an increase in the ultimate load capacity of approximately 20.83%.

5. Test On I-Shape Connector

The FEM program consisted of 3 push-out tests. The test specimens were designed to study the effect of the shear connector type on the ultimate load capacity, Details of each push-out specimen are provided in Table 5.28.

Specimens	Channel shear connector			Concrete slab		Profile of steel beam
	Height (mm)	Length (mm)	Depth (mm)	Compressive Strength f_{KN} (N/mm^2)	Transverse reinforcement	
F	80	46	80	26.52	4 Ø 10	IEP (270)
G	80	46	80	38.6	4 Ø 10	IEP (270)
H	80	50	100	31.47	4 Ø 10	IEP (270)

Table 5.10 Summary FEM of I-Shape Connector Specimens.

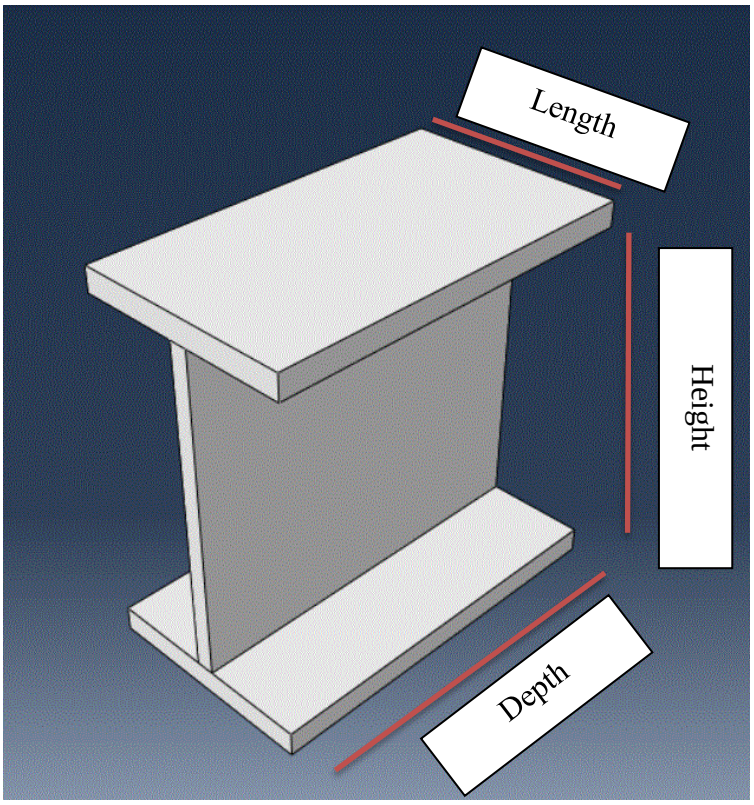

Figure 5.21: I-Shape Connector Specimen.

5.1. Push-Out Test Results

5.1.1. F– Specimen

This test represents a Push-Out Specimen (I-Shape shear Connector) with geometrical dimensions represented as follows:

Length 46

Height 80

Depth 80

Own model matching the properties of F specimen was built and the obtained results were compared to the push-out experimental test results for specimen B3a taken from ref [5]. After adopting the appropriate material model, mesh sizing, and interface boundary conditions, the model is considered accurate enough to predict the shear capacity of I-shape shear connectors embedded in concrete. Figure 5.22 presents a comparison between the (load-slip) curves recorded experimentally (from ref [5]) and those obtained numerically by the finite element model. Based on these results of this comparison, more Specimens (G.H) were created as shown in table 5.10.

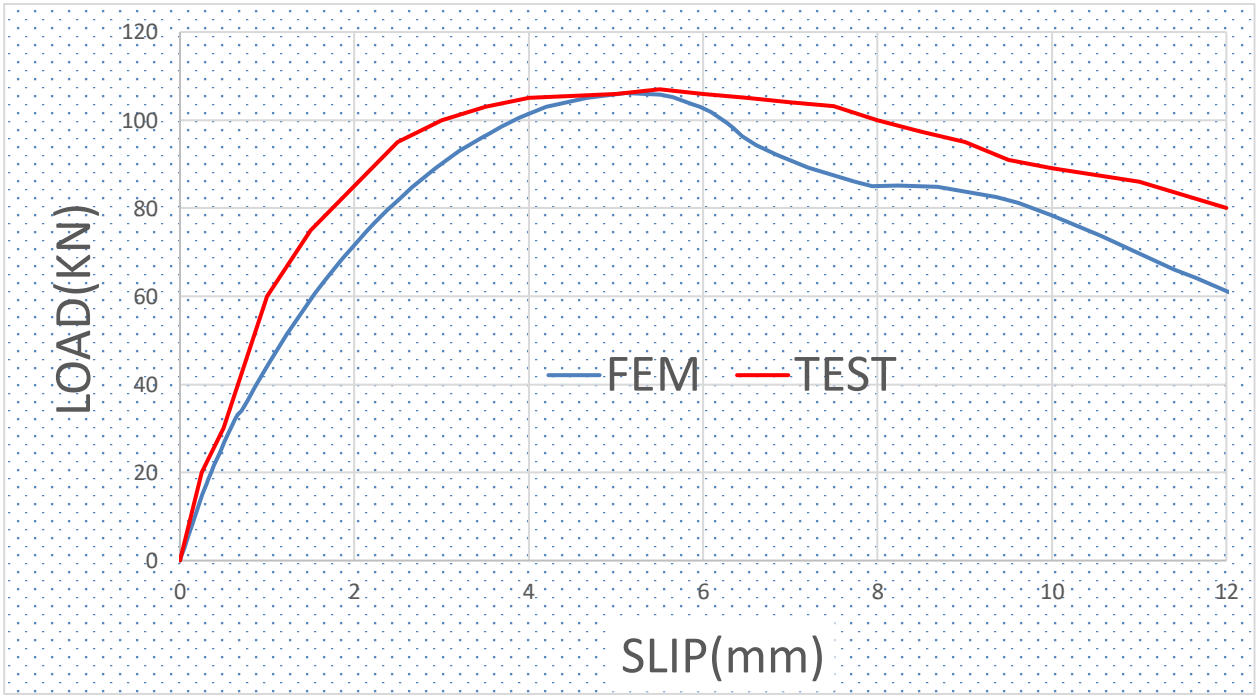

Figure 5.22: Comparison of load–slip Curves for Specimens F: FEM and TEST.

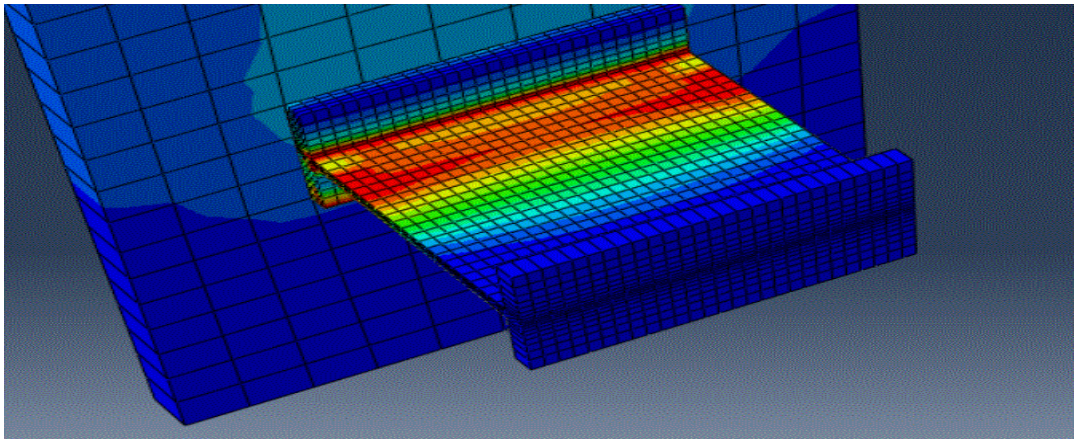

a

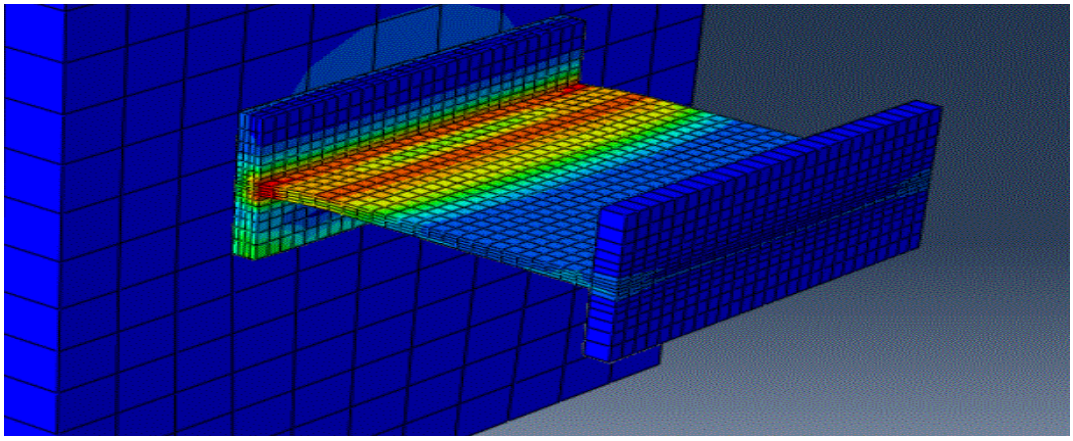

b

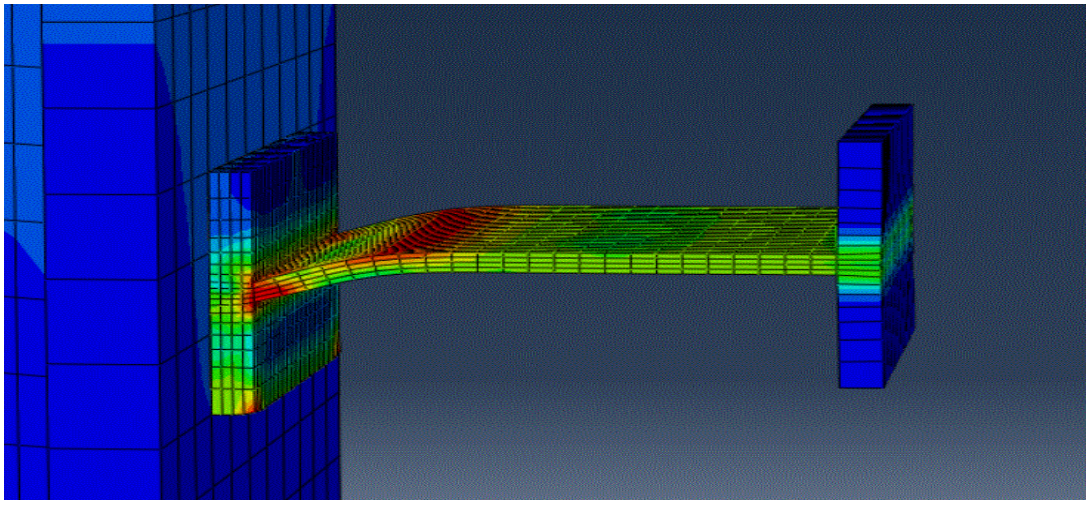

c

Figure 5.23: Distributions of Stress for I-Shape Connector Specimen F at the Load Max =106.15 KN (a) and Load 73.25 KN (b) and at Last Increment (c).

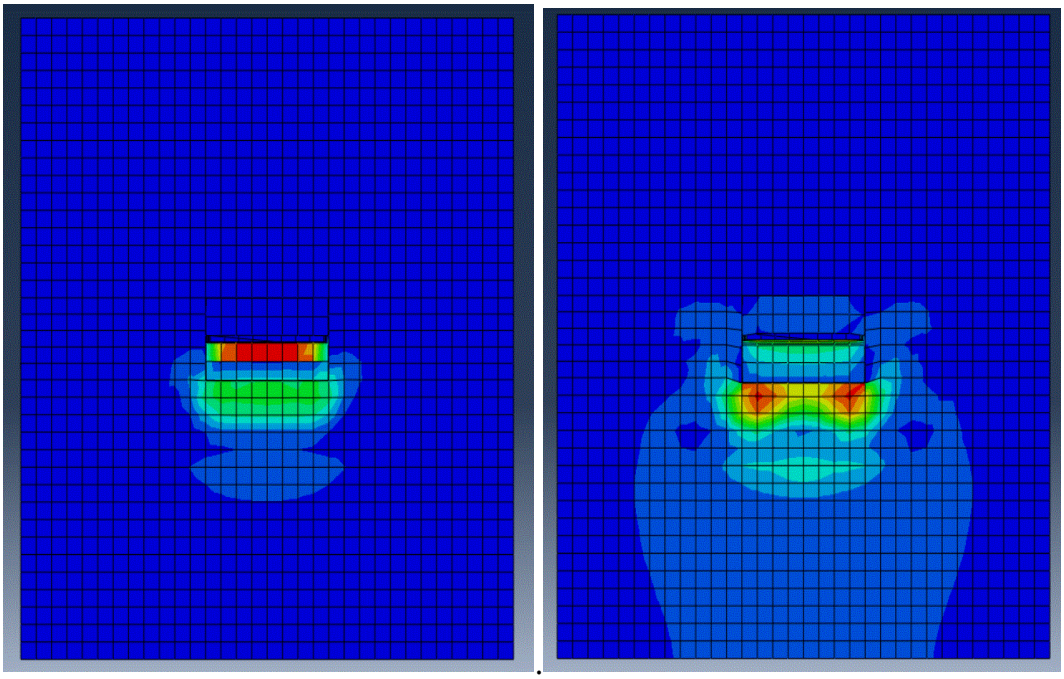

a b

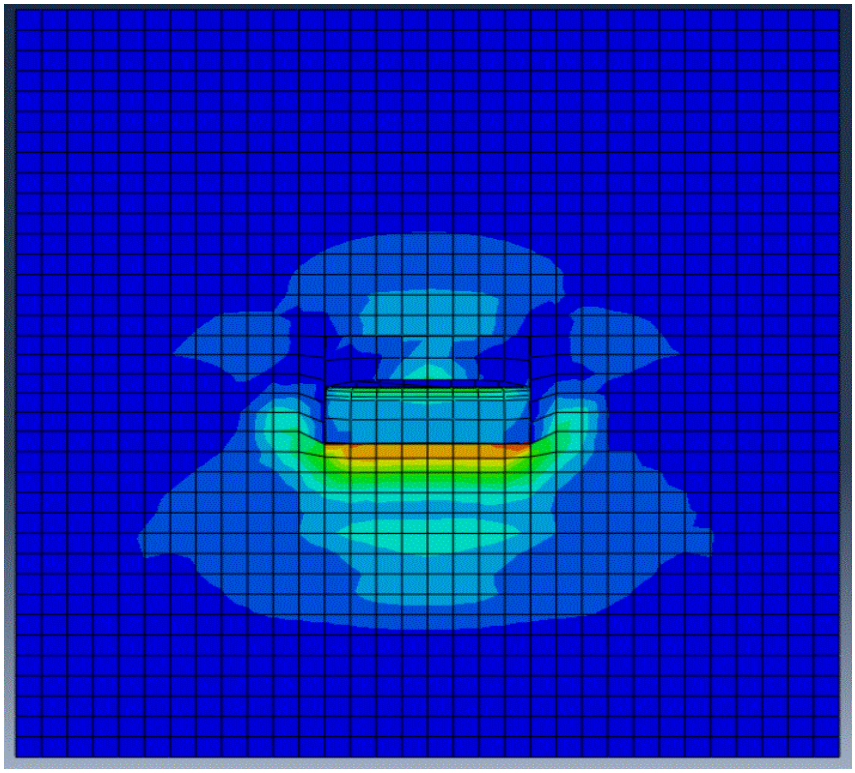

c

Figure 5.24: Distributions of Stress for I-Shape Connector Specimen F at the Load Max =106.15 KN (a) and Load 73.25 KN (b) and at Last Increment (c).

5.1.2. Modelling Comparison of the Push-out Specimens Channel Connector with I-shape connector.

This test represents a Push-Out Specimens (Channel shear connector B4) with geometrical dimensions different as follows:

Length 50

Height 120

Depth 100

This test represents a Push-Out Specimen (I-Shape shear Connector H) with geometrical dimensions represented as follows:

Length 50

Height 120

Depth 100

Figure 5.23 shows a comparison between the (load-slip) curves obtained from the finite element analysis for the two types of shear connectors. There is slight difference between the two curves for the two specimens. shows an increase in the ultimate load capacity of approximately 25.98%.

However, the load-slip curve of channel connector appears more rigid and higher than that of I-shape connector.

Specimens	FE analysis capacity (kN)
I-Shape Connector (H)	127.36
Channel Connector (B4)	160.59

Table 5.11: Type Specimens and FE Analysis Capacity.

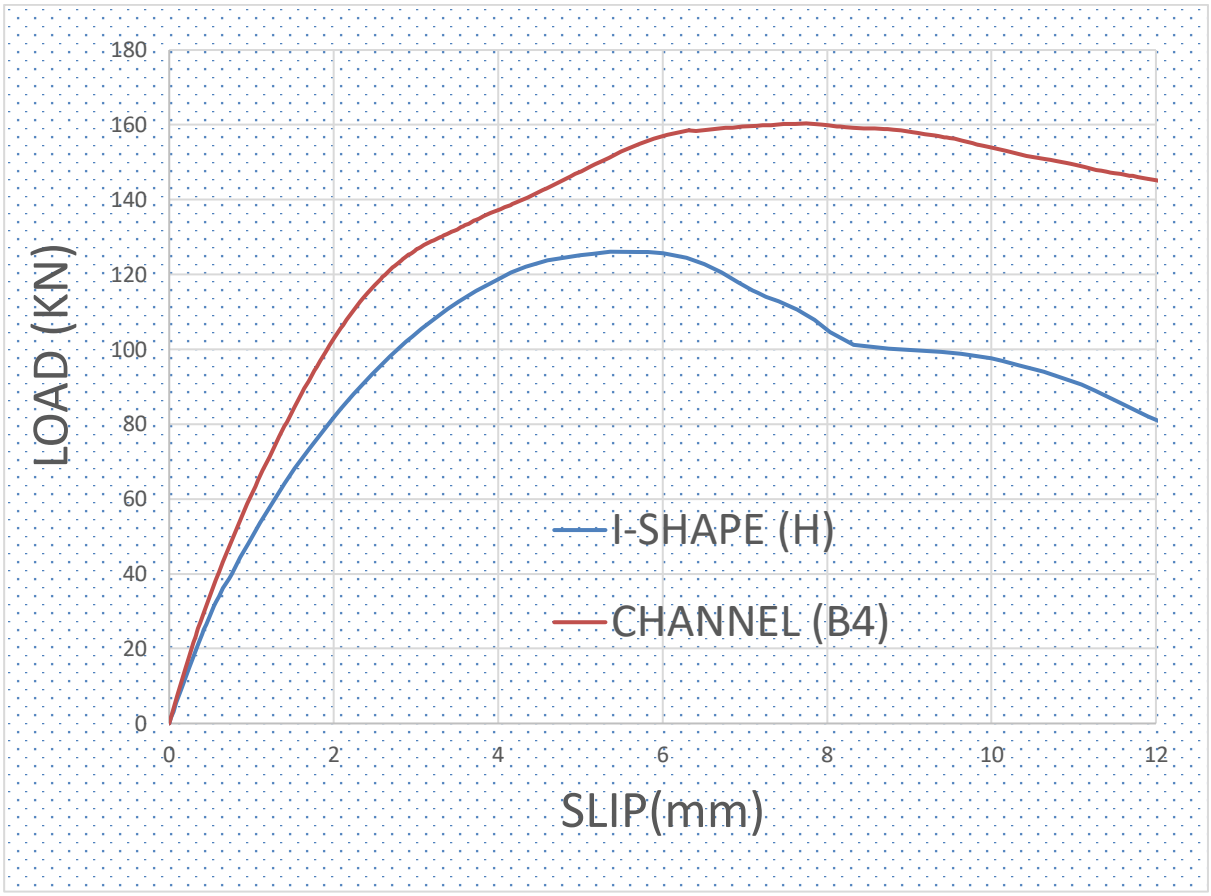

Figure 5.25: Comparison of Load–Slip Curves for Specimens (I-Shape Connector H) and (Channel Connector B2).

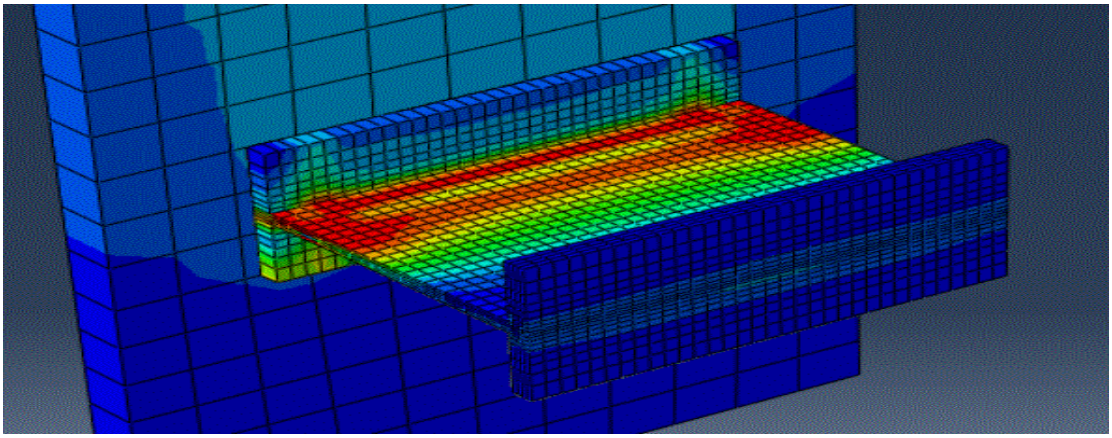

a

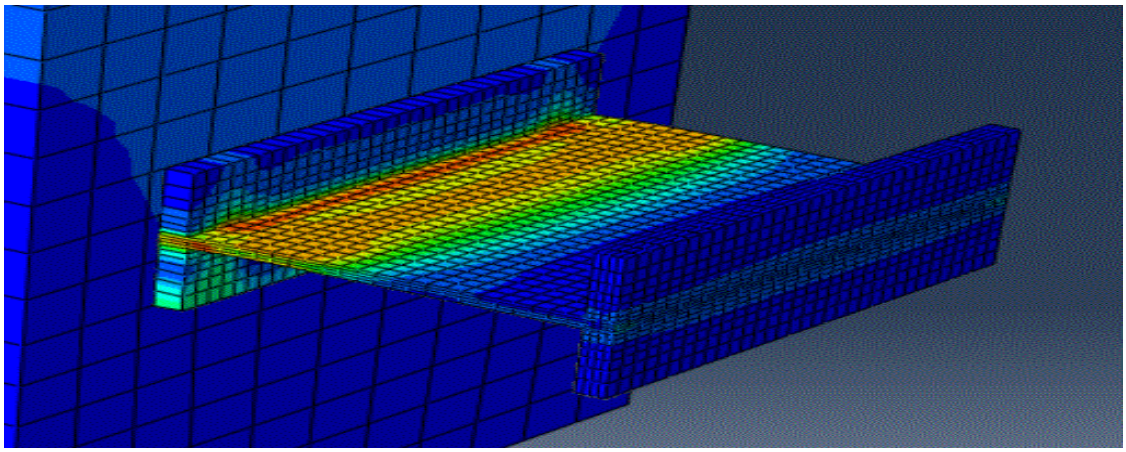

b

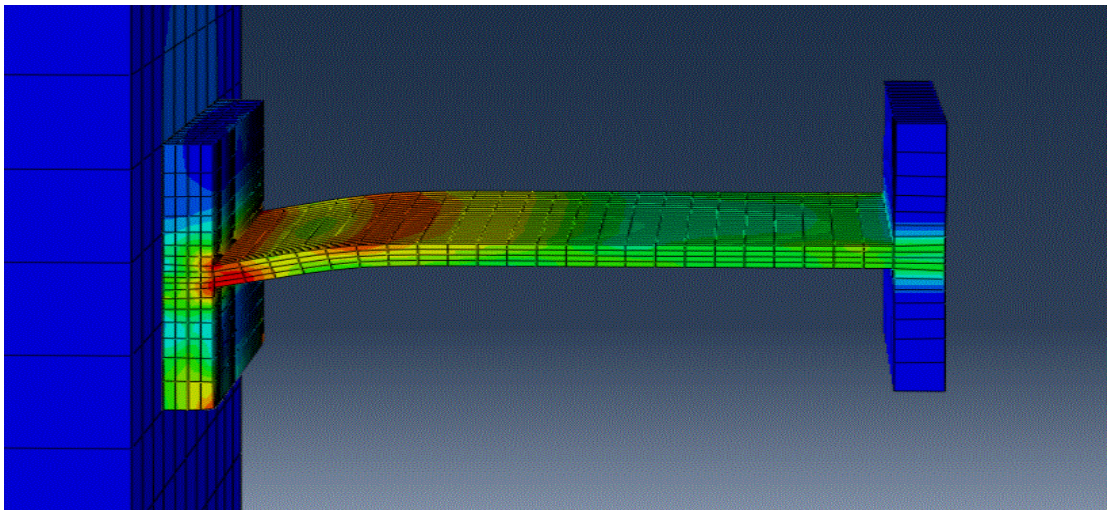

c

Figure 5.26: Distributions of Stress for I-Shape Connector Specimen F at the Load Max =127.36 KN (a) and Load 93.68 KN (b) and at Last Increment (c).

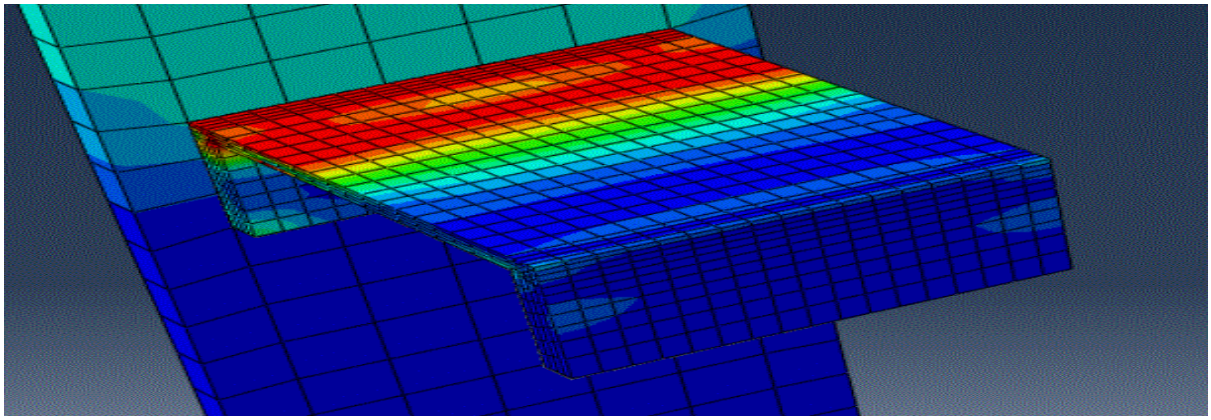

a

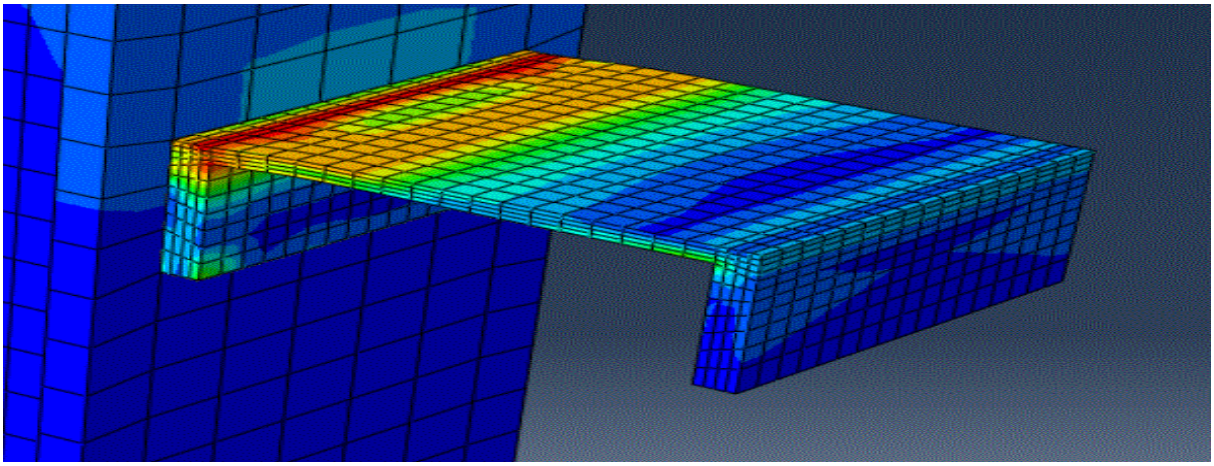

b

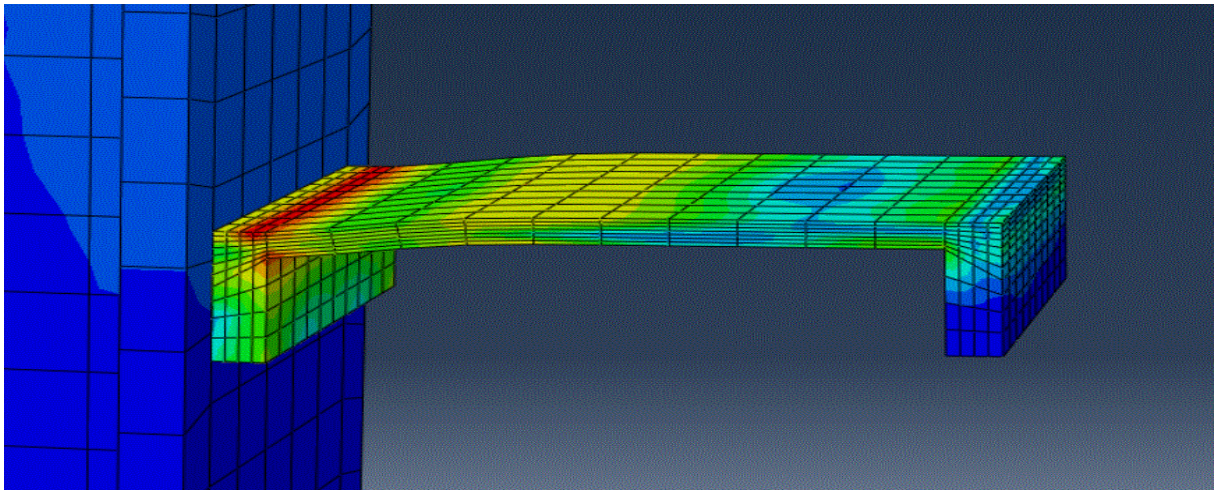

c

Figure 5.27: Distributions of Stress for Channel Connector Specimen C3 at the Load Max =160.59 KN (a) and Load 110.47 KN (b) and at Last Increment (c).

CONCLUSION

This work has presented details of numerical modelling and validation of a finite element simulation of the push-out tests carried out using ABAQUS software on 19 push-out specimens' type of channel shear connector and 3 specimens' type of I-shape shear connector. The obtained results are compared against the relevant tests presented in the literature.

Based on the extensive numerical studies the following conclusions can be drawn:

• A good agreement has been obtained between experimental results and finite element results which indicates that we can perform lots of push out tests with different varieties for extensive study, which will be more economic than the experimental work.

• The numerical model is able to investigate the failure modes, the ductility and the ultimate load capacity and stress distribution for the concrete and the shear connectors efficiently.

• The comparison between the I-shape connector and the channel connector by the finite element analysis confirms the similarity of their behaviour.

• For most push-out tests, the characteristic slip capacity was found greater than 6 mm. Therefore, the channel type and I type shear connectors can be considered as ductile according to Eurocode 4.

• The failure modes observed from the push-out tests can be generally classified into two types: Shearing of the connector and Crushing-cracking of the concrete slab.

• The test results showed that the ultimate load capacity of both the channel connector and I connector increases almost linearly with the increase in the connector Height.

• The test results showed that increasing the concrete strength increases the shearing capacity of the proposed shear connector.

• Crushing of the concrete adjacent to the channel web was the observed mode of failure in specimens when lower strength concrete was used.

• Shearing of the connector was occurred in smaller length connectors embedded in high strength concrete slabs.

• Finally, the connectors I-shape and channel can be effectively used in composite beams to transfer the longitudinal shear forces across the steel–concrete interface.

RECOMMENDATIONS FOR FUTURE WORK

Here are listed a few recommendations that we think is interesting for future investigations:

 Explore the effect of the other types, shapes and dimensions of shear connectors.

 Explore the effect of other grades and types of concrete. For instance, high strength concrete, fiber-reinforced concrete …etc.

 Incorporate the effect of material nonlinearity on the shear connectors behaviour.

 investigate the effect of time on the shear connectors behaviour.

REFERENCES

1.ELLOBODY. E. (2014), Finite Element Analysis and Design of Steel and Steel–Concrete Composite Bridges. Department of Structural Engineering, Faculty of Engineering, Tanta University, Egypt, First edition, pp. 82

2. SAMHAL.E. (2005), Composite Construction, SSEDTA (European Steel Computer Aided Learning, pp.7-15

3. PASHAN. A. (2006), Behaviour Of Channel Shear Connectors: Push-Out Tests. Master thesis OF University of Saskatchewan, pp.1-3

4. KOFI GAND A, SAIDANI M, ETA EKPO O and FOM P. Push-out experimental evaluation of pultruded FRP-concrete composites. Fifth International Conference on Sustainable Construction Materials and Technologies, Coventry university, Coventry, Uk PP. 01

5. MAZOZ1 A, BENANANE A and OUINAS D. (2016). Experimental Study and Finite Element Modelling of Push-Out Tests on A New Shear Connector Of I-Shape, Algeria, Advanced Steel Construction Vol. 12, pp. 488.

6. ZINGONI A (2001). Behaviour Of Different Types of Shear Connectors For Steel-Concrete Structures. In, 2001. Elsevier Science Ltd, PP. 385

7. MEL H and PASHAN A (2006), Channel Shear Connectors In Composite Beams: Push-Out Tests**,** Professor, Department Of Civil & Geological Engineering University Of Saskatchewan, 57 Campus Drive Saskatoon, Canada. PP 2-3

8. SHARIATI A, RAMLISULONG N, SUHATRIL M AND SHARIATI M, (2012), Various types of shear connectors in composite structures: A review International Journal of Physical Sciences Malaysia, Vol. 7(22), pp. 2876-2890

9.Tao Z, Wang XQ, Uy B. Stress–strain curves of structural and reinforcing steels after exposure to elevated temperatures. J Mater Civ Eng 2013; 25(9).

10. Karabinis AI, Kiousis PD. Effects of confinement on concrete columns:

Plasticity approach. J Struct Eng, ASCE 1994;120(9):2747_66.

11. Papanikolaou VK, Kappos AJ. Confinement-sensitive plasticity constitutive model for concrete in triaxial compression. Internat J Solids Structures 2007; 44(21):7021_48.

12. Cervenka J, Papanikolaou VK. Three-dimensional combined fracture-plastic material model for concrete. Int J Plasticity 2008 ;24(12):2192_220.

13. Yan Z, Pantelides CP. Fiber-reinforced polymer jacketed and shape-modified compression members-II: Model. ACI Struct J 2006; 103(6):894_903.

14. Chen WF. Plasticity in reinforced concrete. New York (NY): McGraw-Hill Book Company; 1982.

15. Karabinis AI, Kiousis PD. Effects of confinement on concrete columns: Plasticity approach. J Struct Eng, ASCE 1994;120(9):2747_66.

16. Oh B. A plasticity model for confined concrete under uniaxial loading, Ph.D. thesis. Lehigh University; 2002.

17. Rousakis TC, Karabinis AI, Kiousis PD. FRP-confined concrete members: Axial compression experiments and plasticity modeling. Eng Struct 2007; 29: 1343_53.

18. CHEN, W. F. 2007, *Plasticity in Reinforced Concrete*, J.Russ.

19. YU, T., TENG, J. G., WONG, Y. L. & DONG, S. L. 2010. Finite element modeling of confined concrete-I: Drucker–Prager type plasticity model. *Engineering Structures,* 32**,** 665-679.

20. ELLOBODY, E., YOUNG, B. & LAM, D. 2006. Behaviour of normal and high strength concrete-filled compact steel tube circular stub columns. *Journal of Constructional Steel Research,* 62**,** 706-715.

21. MIRMIRAN, A., ZAGERS, K. & YUAN, W. 2000. Nonlinear finite element modeling of concrete confined by fiber composites. *Finite Elements in Analysis Structures,* 32**,** 665-679.

22. HU, H. T., HUANG, C. S., WU, M. H. & WU, Y. M. 2003. Nonlinear analysis of axially loaded concrete-filled tube columns with confinement effect. *Journal of Structural Engineering,* 129**,** 1322-1329.

23. Lubliner J.J., Oliver S.O., Oñate E., A plastic-damage model for concrete, International Journal of Solids and Structures, 25, 3(1989)229-326.

24. Jankowiak I., K_kol W., Madaj A.: Identification of a continuous composite beam numerical model, based on experimental tests, 7th Conference on Composite Structures, Zielona Gó ra, 2005, pp. 163–178.

25. Majewski S.: *The mechanics of structural concrete in terms of elastoplasticity*, Silesian Polytechnic Publishing House, Gliwice, 2003.

26. *Eurocode 2: Design of concrete structures. Part 1-1: general rules and rules for buildings*, Brussels, 2004.

27. Wang T., Hsu T.T.C.: Nonlinear finite element analysis of concrete structures using new constitutive models, Computers and Structures, Vol. 79, Iss. 32, 2001, pp. 2781–2791.

28. ABAQUS Standard Analysis User's Manuel Version 6.14.

29. Euro code part 3 ,1993: Design of the steel structures

30. EN 1994-1-1:2004: Eurocode 4: Design of composite and concrete structures - Part 1-1: General Rules and Rules for Buildings, European Committee for Standardization.

31. EN1990: :2002: Eurocode: Basis of Design, Annex D: Design Assisted by Testing.

32. MALEKI. SH, MEHRDAD MAHOUTIAN.M, (2009), Experimental and analytical study on channel shear connectors in Fiber-reinforced concrete, Department of Civil Engineering, Sharif University of Technology, Azadi Ave., Tehran, Iran, pp 1787_1793.